DESIGN, SYNTHESIS, AND FABRICATION OF BIODEGRADABLE,

BIOACTIVE-BASED POLYMERS FOR CONTROLLED RELEASE

APPLICATIONS

by

MICHELLE AIMEE OUIMET

A Dissertation submitted to the

Graduate School-New Brunswick

Rutgers, The State University of New Jersey

in partial fulfillment of the requirements

for the degree of

Doctor of Philosophy

Graduate Program in Chemistry and Chemical Biology

written under the direction of

Dr. Kathryn E. Uhrich

and approved by

_____

_____

_____

_____

New Brunswick, New Jersey

[October, 2013]

ABSTRACT OF THE DISSERTATION

Design, synthesis, and fabrication of biodegradable, bioactive-based polymers

for controlled release applications

by MICHELLE AIMEE OUIMET

Dissertation Director:

Kathryn E. Uhrich

Novel, controlled release drug delivery systems have transformed therapeutics used in modern medicine but exhibit limitations for treating various diseases. Biodegradable polymers have been extensively studied to overcome such challenges. Through incorporating therapeutic bioactives into a polymer backbone via hydrolytically degradable bonds, high drug loading, improved delivery, and enhanced bioactive stability can be achieved. Polymers containing a non-steroidal anti-inflammatory drug, salicylic acid, and antioxidant molecules from the hydroxycinnamic acid class were synthesized into bioactive-based poly(anhydride-esters) as controlled release drug delivery systems.

Polymer properties have been tuned by changing the bioactive covalently incorporated into the monomer unit, altering the monomer's molecular structure, adding small molecules to the polymer matrix, and fabricating the polymer into different devices. Salicylic acid-based poly(anhydride-ester) (SAPAE) release

profiles were first tuned using small molecule admixtures at varying weight percentages to overcome a lag period (i.e., no drug release) for applications where immediate, constant drug release is desired. SAPAEs were also designed as microparticles, or microspheres, for short-term salicylic acid release. These polymers were prepared using monomers comprised of linear aliphatic or heteroatomic molecules with two salicylic acid units. Microsphere size and morphology was determined and the *in vitro* drug release profile ascertained. Furthermore, to impart brittle SAPAEs with flexible, soft tissue-like properties, the polymer was blended with poly(vinyl pyrrolidone) to formulate miscible films that, when hydrated, exhibit hydrogel-like properties. The material's morphology, thermal properties, and *in vitro* drug release profile were elucidated.

In addition to engineering SAPAEs for various applications, hydroxycinnamic acids such as *p*-coumaric, ferulic, and sinapic, which are potent antioxidants with short half-lives and poor chemical stability, were covalently incorporated into a polymer backbone. The chemical composition of precursors and polymers were confirmed and the polymers' physicochemical characteristics and drug release profiles ascertained. Moreover, the ferulic acid-containing polymer chemical structure was tuned to alter the physicochemical properties and drug release rates. The design, synthesis, physicochemical characterization, drug release profiles, bioactivity assessments, device fabrication methods, biocompatibility evaluations, and potential applications of various bioactive-containing poly(anhydride-ester) are discussed herein.

PREFACE

"If a man empties his purse into his head, no man can take it away from him. An

investment in knowledge always pays the best interest."

-Benjamin Franklin

DEDICATION

This work is dedicated to my family and friends, especially my parents and fiancé, who have offered a great deal of love, guidance, and support in my journey through life and especially during my graduate studies.

ACKNOWLEDGEMENTS

I am truly grateful and feel very blessed to have such an amazing support system throughout the years leading up to the writing of this dissertation. I would like to express my sincere appreciation to all of my family, friends, teachers, and mentors who guided and supported me. I have learned a great deal from each of you work described here.

TABLE OF CONTENTS

LIST OF TABLES

LIST OF FIGURES

ABBREVIATIONS

^{1}H NMR	proton nuclear magnetic resonance		g	gram
^{13}C NMR	carbon nuclear magnetic resonance		GPC	gel permeation chromatography
Abs$_t$	absorbance after a period of time		h	hour
			HCl	hydrochloric acid
Abs$_{t0}$	absorbance at time zero		H$_2$O	water
API-ESI	atmospheric pressure ionization-electrospray ion source		HPLC	high performance liquid chromatography
			ICP	inactive control polymer
Ar	Argon		IR	infrared
ArH	aromatic proton		J	coupling constant
ASTM	American Society for Testing and Materials		k'	capacity factor
			KBr	potassium bromide
Au/Pd	gold/palladium		kg	kilogram
CDCl$_3$	deuterated chloroform		kPa	kilopascal
cm^{-1}	wavenumber units		KH$_2$PO$_4$	potassium phosphate monobasic
CO$_2$	carbon dioxide		L	liter
COX	cyclooxygenase		LPS	lipopolysaccharide
C$_p$	heat capacity		log P$_{o,w}$	octanol-water partition coefficient
d	doublet, day			
Da	Dalton		m	multiplet
DCM	dichloromethane		M	molar
DMF	dimethylformamide		mBar	millibar
DI	deionized water		Me	methyl
DMSO	dimethyl sulfoxide		mg	milligram
DMSO-d_6	deuterated dimethyl sulfoxide		MgSO$_4$	magnesium sulfate
			MHz	megahertz
DPPH	2,2-diphenyl-1-1 picrylhydrazyl		min	minute
			mL	milliliter
DSC	differential scanning calorimetry		mm	millimeter
			mM	millimolar
ELISA	enzyme-linked immunosorbant assay		mmHg	millimeters of mercury
			MS	mass spectrometry
eq	equivalence		MTS	(3-(4,5-dimethylthiazol-2-yl)-5-(3-carboxymethoxy phenyl)-2-(4-sulfophenyl)-2H-tetrazolium)
Et$_3$SiH	triethylsilane			
Et$_3$N	triethylamine			
FBS	fetal bovine serum			
FDA	US Food and Drug Administration			
FTIR	Fourier transform infrared spectroscopy		M$_W$	weight averaged molecular weight

MW	molar mass	t-	tert
N	Normal	T_d	thermal decomposition
N_2	nitrogen		temperature
NaCl	sodium chloride	T_g	glass transition
NaH	sodium hydride		temperature
$NaHCO_3$	sodium bicarbonate	TGA	thermal gravimetric
NaOH	sodium hydroxide		analysis
NIH	National Institutes of	THF	tetrahydrofuran
	Health	TLC	thin layer
nm	nanometer		chromatography
NSAID	nonsteroidal anti-	T_m	melting temperature
	inflammatory drug	TMS	trimethylsilane
p-	para	TNF-α	tumor necrosis factor -
PAE	poly(anhydride-ester)		alpha
PBS	phosphate buffered	t_R	sample retention time
	saline	UV	ultraviolet, ultraviolet
PDI	polydispersity index		spectroscopy
$Pd(OAc)_2$	palladium (II) acetate	UV/vis	ultraviolet/visible
PEG	poly(ethylene glycol)		spectroscopy
PHB	p-hydroxybenzoic acid	w_d	dry weight
	(adipic) polymer	w_s	swollen weight
PLGA	poly(lactic-co-glycolic	wt %	weight percent
	acid)	w/v	weight by volume
psi	pounds per square	w/w	weight by weight
	inch	δ	chemical shift
PTFE	polytetrafluoroethylene	°	degrees
PVA	poly(vinyl alcohol)	° C	degrees Celsius
PVP	poly(vinyl pyrrolidone)	λ	wavelength
Q	swelling value	μg	microgram
rad	radians	μL	microliter
RI	refractive index	μm	micron
rp	revolutions per minute	μW	microwatt
RPMI	Roswell-Park-Memorial-	~	approximately
	Institute cell culture	%	percent
	medium		
RT	room temperature		
s	second, singlet		
SA	salicylic acid		
SAA	salicylic acid (adipic)		
	polymer		
SAPAE	salicylic acid-based		
	poly(anhydride-ester)		
SEM	scanning electron		
	microscopy		
t	triplet		
t_0	solvent retention time		

CHAPTER 1:   INTRODUCTION

Modern medicine has been revolutionized by novel therapies to correct bodily imbalances, sometimes reversing the effects of aging, infection, inflammation, and injury.[1]   As the world of medicine evolves and new pharmaceutical drugs are developed, new challenges have emerged including the inability for a drug to be delivered to the intended site before biodegradation occurs, low aqueous solubility, and poor bioavailability.   To overcome such limitations, controlled delivery systems using polymeric materials have received much consideration.

1.1.   Controlled release systems

The drug delivery field has been challenged to develop novel systems that release drugs in a predictable manner.   Such controlled release systems are designed to enhance drug delivery as they enable drug concentration control over time and thus require less dosing, maintain optimal drug levels, enhance drug targeting specificity, and increase patient compliance.[2]   With traditional tablets and injections, the drug concentration in the body increases after each dose and then decreases below the minimal effective level threshold (Figure 1.1).[3, 4]   Furthermore, if drug administration occurs before a previous dose is eliminated from the body, drug concentration may accumulate and rise above the maximum desired drug levels, causing toxicity issues.
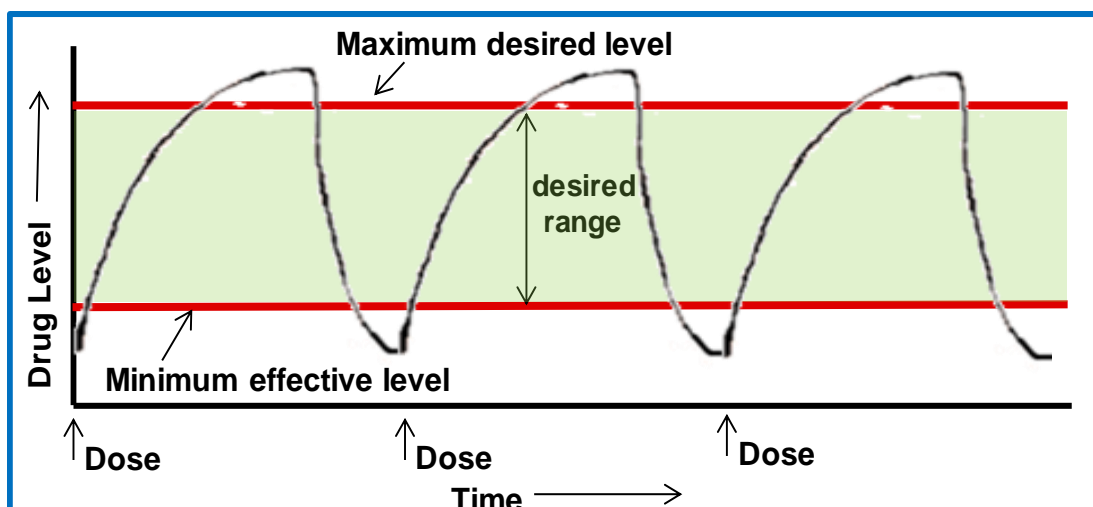
Figure 1.1. Drug levels in the blood using traditional bolus drug dosing, demonstrating issues with maintaining drug within desired, therapeutic range (figure adapted from Brannon-Peppas)[3]

A drug delivery design that would, upon a single administration, allow for a controlled, gradual drug release that remains between the minimum and maximum thresholds is ideal. An optimal drug release profile for such a model is depicted in Figure 1.2. [3, 4] Controlled release systems utilizing polymers have emerged to address the aforementioned issues from bolus dosing as they can achieve optimal clinical effects upon administration, while maintaining drug concentrations within a desired range for a predetermined time period.
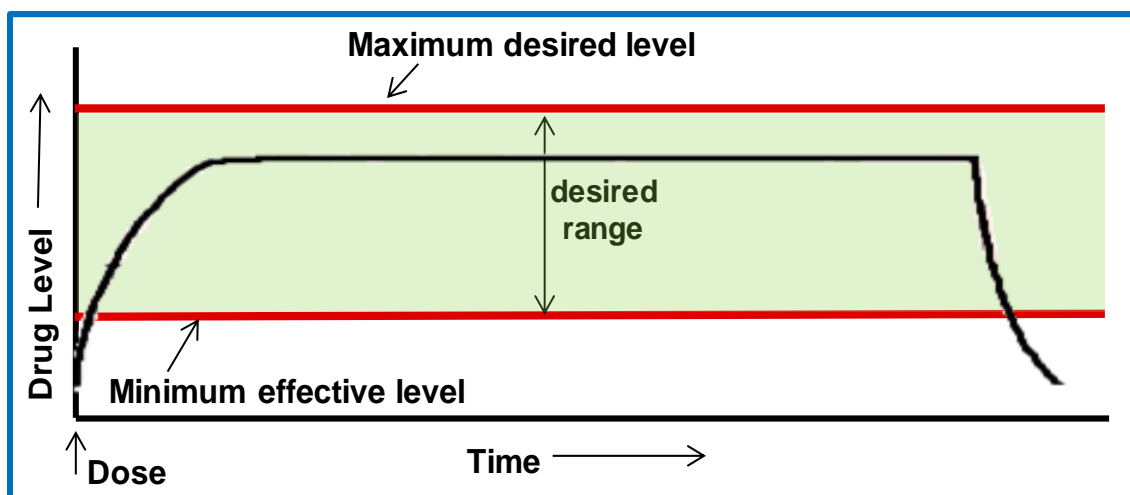
Figure 1.2. Ideal controlled release profile that maintains drug concentration levels within the desired, therapeutic window (figure adapted from Brannon-Peppas)[3]

1.2.   Polymers for controlled release drug delivery

Numerous polymer architectures have been designed and explored to enable control over drug release. Such materials include a diverse range of both degradable and non-degradable systems in which drug molecules are physically incorporated into a polymeric matrix. Non-degradable polymers require retrieval once introduced into the body, which may lead to complications, whereas degradable polymers should be chemically inert (i.e., will not interact with the drug or elicit an immune response) and degrade into non-toxic entities with no adverse effects, overcoming the need for post-application removal.[5] Polymers including poly(α-hydroxy acids) such as poly(lactic-co-glycolic) (PLGA) have gained considerable attention for these applications given their tunable degradation rates and bioresorbable degradation products.

Once incorporated into a polymeric controlled release system, drug molecules can be released via various pathways. Non-degradable polymers typically exhibit diffusion-based drug release, whereas drug release from degradable polymers is influenced by polymer degradation and subsequent erosion. Diffusion occurs when the loaded drug passes between polymer chains or through pores within the polymer matrix. Degradation is defined as the chain scission process where polymer chains are cleaved,[6] whereas erosion is described as the depletion of a material.[2, 6] Such degradation can be further classified into two erosion mechanisms: bulk and surface erosion (Figure 1.3). Both of these erosion mechanisms may occur in a given biodegradable polymer, but the relative erosion extent will vary based on the polymer's chemical structure.

Bulk erosion (Figure 1.3, right) takes place when water penetrates into the bulk of the polymer and degrades uniformly throughout the matrix. Consequently, such erosion results in limited erosion predictability and limited protection of drug molecules.[6] Surface erosion (Figure 1.3, left) occurs when degradation is at the polymer surface, resulting in a release rate relative the drug system's surface area.[3, 5-7] Surface erosion of polyanhydrides enables a near zero-order release of physically entrapped actives upon hydrolytic degradation.[2, 6, 8] Zero order, or constant drug release, is preferred to minimize fluctuations within drug concentration.
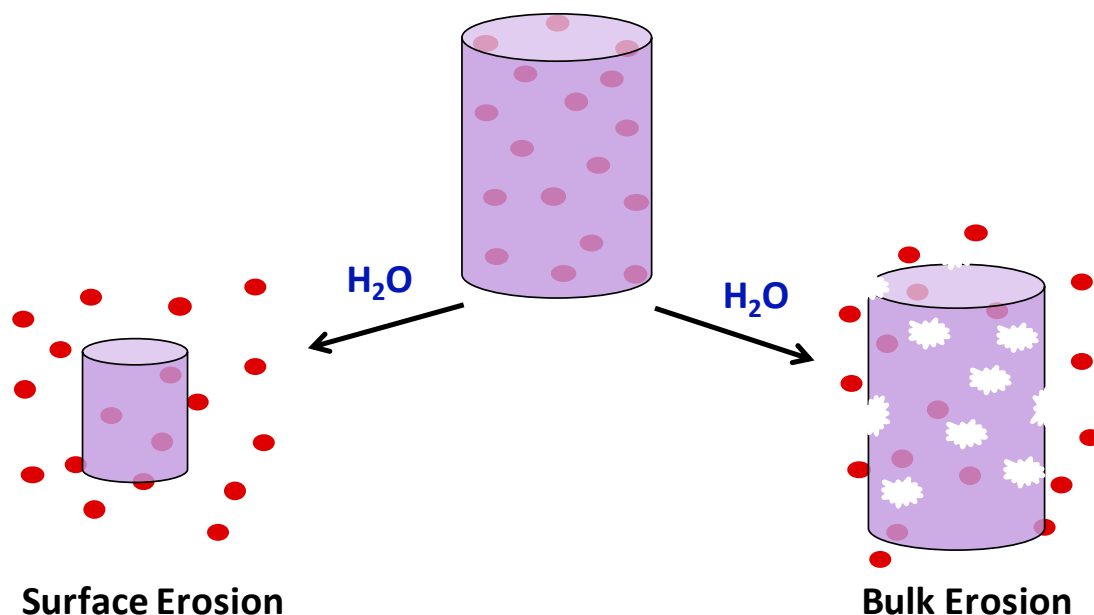
Figure 1.3. Biodegradable polymer (purple) hydrolytic degradation schematic via surface erosion (left) and bulk erosion (right) to deliver physically encapsulated bioactives (red)

1.2.1.   Polyanhydrides

Polyanhydrides (Figure 1.4) are a promising class of biodegradable polymers for controlled release applications due to their surface-eroding behavior, biodegradation into non-cytotoxic products, and tunable degradation rate based on polymer composition.[5, 9, 10] Langer et al. initiated and pioneered the development of polyanhydrides for use as delivery systems due to their hydrolytic instability and surface eroding matrix.[2, 9, 11, 12]
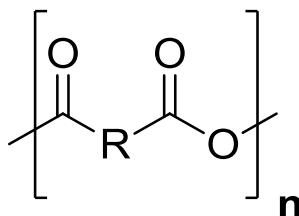
Figure 1.4. General polyanhydride chemical structure

1.2.1.1.　　Polyanhydride synthesis

Several polymerization methods have been used to synthesize polyanhydrides including melt-condensation, solution, inter-facial, and ring-opening approaches.[13] For the polymers described within this dissertation, melt-condensation and solution methods have been successfully employed.[14-17] In melt-polymerization, a diacid is first activated with an excess of acetic anhydride to yield the monomer. The monomer is then melted under high temperature (e.g., 160 – 180 ∘C) and vacuum (e.g., < 2 mm Hg) to initiate polymerization (Figure 1.5). Although this method is highly reproducible and allows for easy scale-up, it may not be suitable for thermally sensitive bioactives, especially if the difference between a monomer's melting temperature and decomposition temperature is narrow.
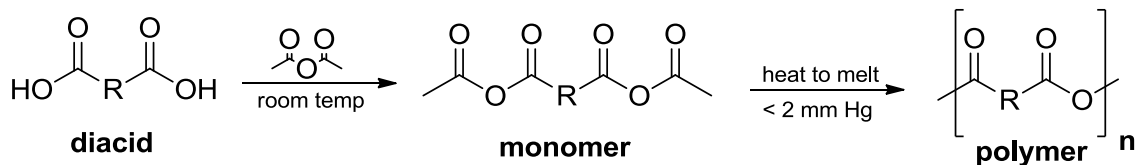
Figure 1.5. Synthetic scheme demonstrating polyanhydride synthesis using melt-condensation polymerization methods by acetylating the diacid with acetic anhydride and polymerizing monomer under vacuum at high temperatures

For these thermally sensitive monomers, solution polymerization at low or ambient temperatures is necessary. A one step polymerization method was developed by Domb et al. using coupling agents such as phosgene (Figure 1.6).[18, 19] Phosgene analogues including diphosgene (liquid at room temperature) and triphosgene (solid at room temperature), both form phosgene *in situ*, and as such were also investigated as coupling agents.[9, 18, 19] In the solution polymerization methods described herein, triphosgene was the chosen coupling agent as it was easiest to handle in its solid state. Limitations to solution polymerization include the strict stoichiometry required[13, 19] and that lower molecular weight polymers are obtained, making scale-up processes difficult.[14]
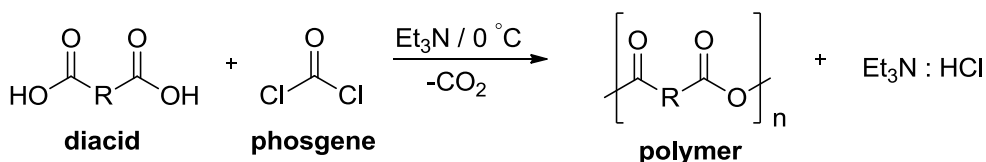
Figure 1.6. Synthetic scheme demonstrating polyanhydride synthesis using phosgene as a coupling agent via solution polymerization methods

1.2.1.2. Polyanhydride degradation

Polyanhydrides are comprised of diacid monomers connected via hydrolytically labile anhydride bonds. As the polymer degradation products include such carboxylic acids, which are more soluble in basic conditions, polyanhydride degradation occurs more rapidly in basic media as compared to acidic media.[5] Despite their based-catalyzed hydrolysis, polyanhydrides' exceptionally hydrophobic nature protects/shields anhydride bonds within the device interior. Degradation consequently occurs at the device surface via the aforementioned surface erosion. Given the well-established, zero-order release profiles of surface eroding polymers, polyanhydrides are thus desirable controlled release systems enabling extrapolation of predicted drug release profiles.

In many polyanhydride delivery systems, the active molecules are physically entrapped within the polymer matrix. One such example receiving FDA approval in 2002 includes the use of carmustine, a chemotherapeutic agent, physically mixed in a biodegradable polyanhydride Gliadel® wafer.[20] This biodegradable polymer-drug mixture is clinically used for the treatment of malignant glioma.[21-23]

1.2.2. Bioactive-based poly(anhydride-esters)

Although most polymeric controlled release systems physically incorporate a bioactive within a polymer matrix, this physical incorporation often results in low bioactive loading and limited control over the bioactive's release rate. Furthermore, the polymer's mechanical properties can be compromised by the

bioactive molecule utilized during physical encapsulation due to plasticizing effects.[24]

As an alternative, polymeric drugs, specifically bioactive-based poly(anhydride-esters), are a unique class of therapeutic polymers that hydrolytically degrade into bioactive components. In this class, bioactives are chemically conjugated as pendant groups or directly incorporated into the polymer backbone (Figure 1.7). This incorporation allows for controlled drug delivery, higher drug loading compared to physical incorporation,[25] and fabrication into various devices depending on the end use.
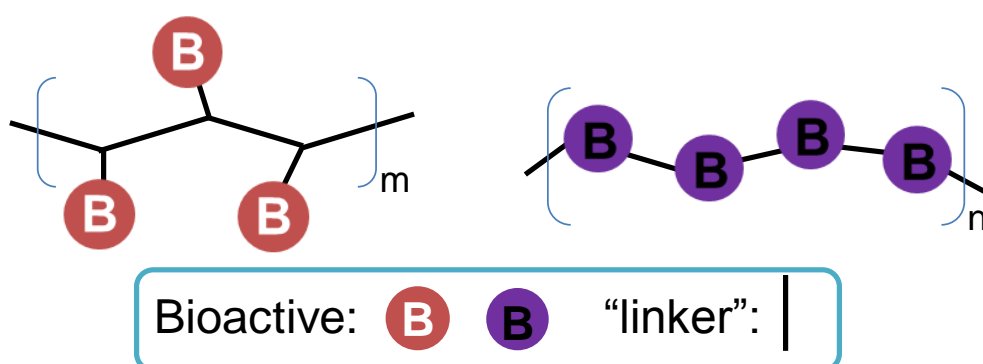
Figure 1.7. Representation of polymeric drugs with a bioactive incorporated as a pendant group (left) or within the polymer backbone (right)

1.2.2.1.   Salicylic acid-based poly(anhydride-esters)

One well-established class of bioactive-based poly(anhydride-esters) is unique in that it chemically incorporates salicylic acid, a non-steroidal anti-inflammatory drug, into the polymer backbone via a "linker" molecule.[16, 17, 26] Salicylic acid is released in a near zero-order fashion as the labile anhydride and

ester bonds within the polymer are hydrolytically cleaved (Figure 1.8). These polymers have been extensively studied for the past decade and are biocompatible,[14, 27-29] stable under storage conditions,[30] and can be exposed to ionizing radiation for sterilization without changing their physicochemical properties.[31] Furthermore, these polymers allow for a higher percentage of drug loading (60-80 %) in microsphere formulations, compared to other biodegradable polymers such as PLGA microspheres encapsulating salicylic acid (20 %).[25]
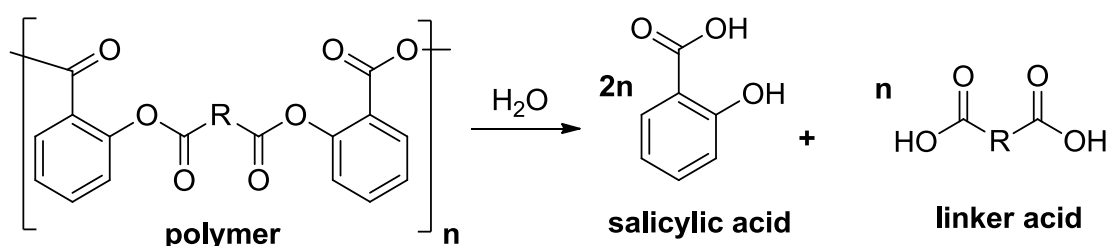
Figure 1.8. Salicylic-acid based polymer hydrolytically degrades into salicylic acid and biocompatible linker acid

1.2.2.2. Salicylic acid-based poly(anhydride-esters): Tunability

Depending upon the predetermined application, salicylic acid-based polymers physicochemical properties can be easily manipulated. Using the previously discussed synthetic methods, these properties could be altered by changing the chemical structure of the linker (Figure 1.9).[14-17] Uhrich et al. demonstrated that salicylic acid-based polymers' glass transition temperatures, hydrophobicities, and release rates were altered as the previously described linker molecules were changed. Several linkers were evaluated including linear

and branched aliphatic, heteroatomic, and aromatic structures.[15, 17]   Glass transition temperatures decreased with increasing alkyl chain length, and polymers containing aromatic linkers exhibited the highest glass transition values.   Polymer hydrolytic degradation to release salicylic acid was influenced by linker structure.   The general trends demonstrated that more hydrophilic linkers (leading to a more hydrophilic polymer overall) exhibited faster *in vitro* degradation than did more hydrophobic structures.[15, 32]
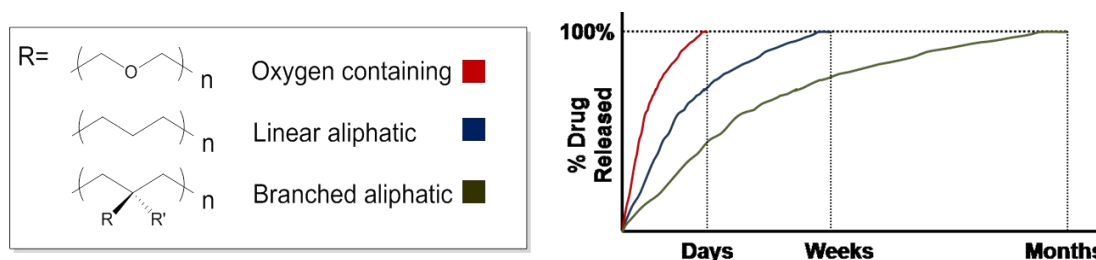
Figure 1.9. Representation of control over drug release profile based upon linker structure

1.2.2.3.   Salicylic acid-based poly(anhydride-esters): Fabrication

In addition to their linker-guided tunability, drug delivery devices based on bioactive-based poly(anhydride esters) can be formulated into various geometries, including microspheres, hydrogels, and electrospun fibers, depending upon their intended application (Figure 1.10). These polymer formulations provide novel biomaterials capable of sustained bioactive release upon polymer hydrolytic degradation.   Furthermore, the specific polymer design allows for more control over current delivery systems and can thus improve

current therapies. The drug release rate tunability, ease of fabrication, and ability to change the bioactive molecule allows for these polymers to be employed in a broad range of applications within the biomaterial field. These topics will be elaborated upon throughout this dissertation.

Random Fibers   **Aligned Fibers**   **Microspheres**   **Discs**

Films   **Stents**   **Conduits**   **Coatings**
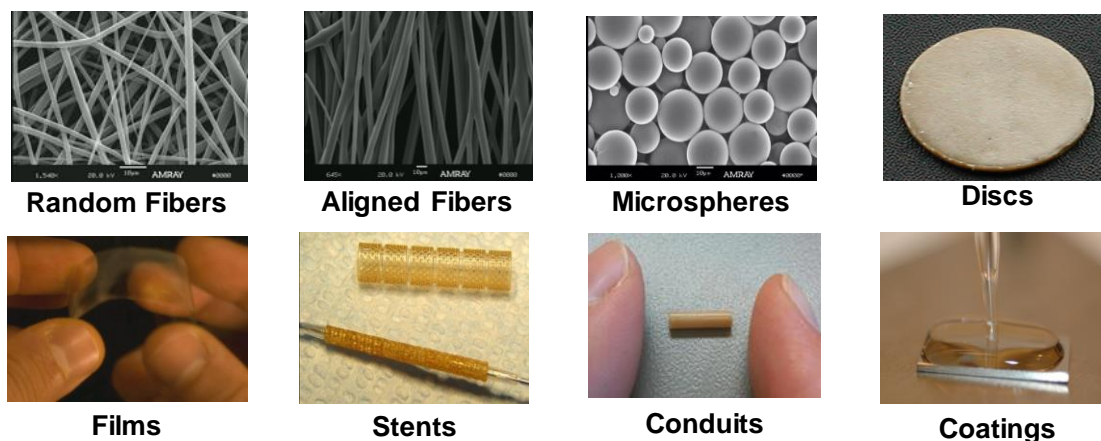
Figure 1.10. Salicylic acid-based polymers have been fabricated for a wide variety of applications

1.3. Research projects

Previous research efforts have been made towards chemically incorporating a variety of salicylates for drug delivery applications.[8, 14-17, 26-44] Within this dissertation, novel and optimized formulations as well as different bioactive-based poly(anhydride-esters) have thus been developed to broaden the application range and diversify the group's polymer library.[45-51] An overview for each project is provided below.

1.3.1. Tunable drug release profiles from salicylic acid-based poly(anhydride-esters)

Salicylic acid-based poly(anhydride-esters) hydrolytically degrade to release salicylic acid over extended time periods (>30 days); however, an initial lag period of no salicylic acid release is observed. This lag period could be unfavorable in applications where immediate salicylic acid release is desired. A poly(anhydride-ester) with a two-day lag period was therefore admixed with various small molecules as a means to shorten or eliminate the lag period.[46] Salicylic acid (Figure 1.11, blue), diacid (Figure 1.11, red), and 1:1 combinations of the two, each at 1%, 5%, and 10% (w/w), were physically admixed with the polymer. All admixtures resulted in immediate salicylic acid release and a decrease in glass transition temperatures compared to polymer alone. By varying the amounts of salicylic acid and salicylic acid prodrugs incorporated into the polymer matrix, immediate and constant salicylic acid release profiles over varied time periods were achieved (Figure 1.11).
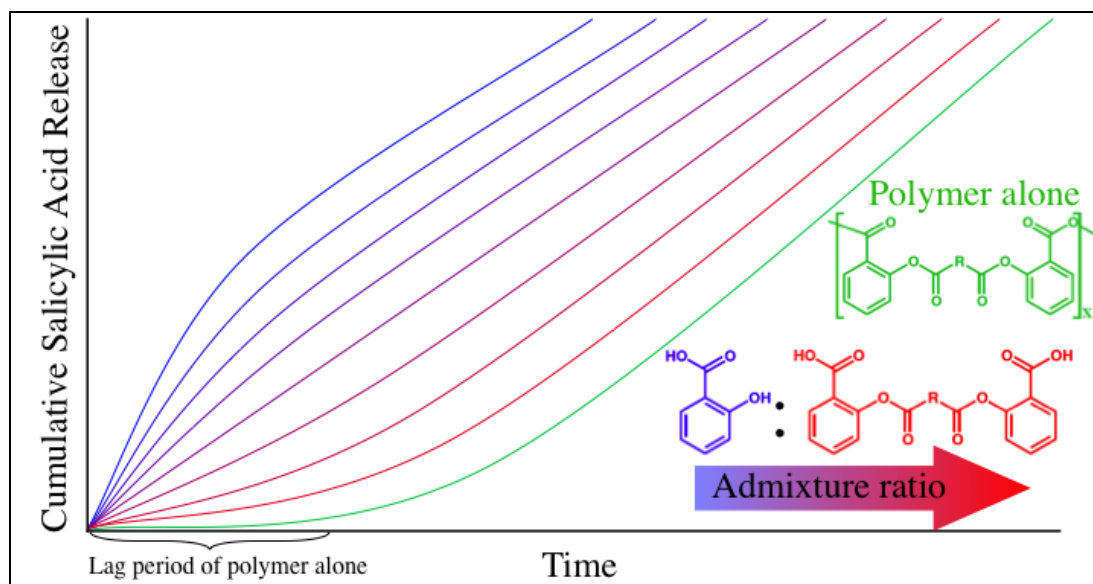
Figure 1.11. Depiction of tunable salicylic acid release profile from salicylic acid-based polymers (green) admixed with salicylic acid (purple) and diacid (red)

1.3.2. Optimized synthesis and formulation of salicylic acid-based poly(anhydride-ester) microspheres

The synthesis of fast-degrading salicylic acid-based poly(anhydride-esters) was optimized to improve polymer yield and minimize impurities by altering temperature and reaction time. This optimized polymer was subsequently used for formulation into microspheres, investigating polymer concentration and homogenization speed to improve overall microsphere morphology (Figure 1.12).[49] The molecular weights (M_w), polydispersity indices (PDI), and glass transition temperatures (T_g) of the formulated polymers were compared to the unformulated polymers. In general, the M_w and PDI exhibited decreased and increased values, respectively, after formulation, whereas the T_g changes increased post-formulation. *In vitro* release studies of the chemically

incorporated salicylic acid displayed release profiles within 3 days. These polymers broadened the range of complete salicylic acid release to now include days, weeks and months.
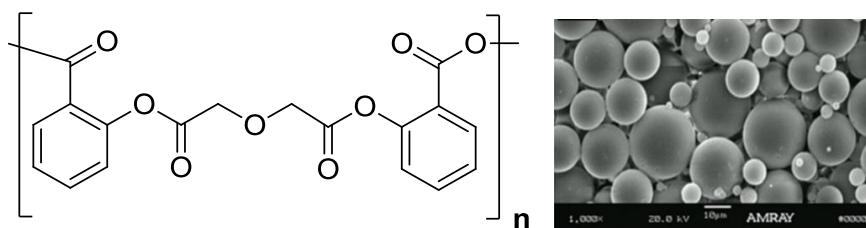
Figure 1.12. Salicylic acid (diglycolic) polymer used to formulate microspheres using an oil-in-water method

1.3.3. Poly(vinyl pyrrolidone) and salicylic acid-based poly(anhydride-ester) blends as hydrogel drug delivery systems

Polymers such as poly(N-vinyl-2-pyrrolidone) (PVP) have been used to prepare hydrogels, or crosslinked polymer networks that imbibe water, for wound dressing applications but are not inherently bioactive. For enhanced healing, the release of physically admixed therapeutics from hydrogels has been studied, but with limited control over drug release profiles. To overcome the limitations of current systems, salicylic acid-based poly(anhydride-esters) have been physically blended with PVP at various ratios to generate a novel material that exhibits hydrogel properties after swelling (Figure 1.13). Scanning electron microscopy images and differential scanning calorimetry confirmed the formation

of miscible blends. The drug release profiles of the blends were studied *in vitro,* demonstrating the chemically incorporated drug was released from the polymer blends over 3-4 days, instead of 3 hours, which is found with diffusion controlled drug release.   Generally, higher PVP content blends exhibited greater swelling values and increased drug release rates.   The polymer blends were found to significantly reduce the inflammatory cytokine TNF-alpha *in vitro* without any cytotoxic or anti-proliferative effects, demonstrating their potential as a wound dressing for enhanced healing and decreased scar tissue formation.

Figure 1.13. Formulation of salicylic acid-based polymers blended with PVP to create materials that exhibit hydrogel-like properties

1.3.4.   Biodegradable   coumaric   acid-based   poly(anhydride-ester) synthesis and subsequent controlled release

p-Coumaric   acid   (pCA),   a   naturally   occurring   bioactive,   has   been chemically   incorporated   into   a   poly(anhydride-ester)   backbone   through   solution polymerization to overcome drug delivery issues associated with its short *in vivo* half-life.   Nuclear   magnetic   resonance   and   Fourier   transform   infrared

spectroscopies indicated that pCA was successfully incorporated without noticeable alterations in structural integrity. The weight-average molecular weight and thermal properties were determined for the polymer. In addition, *in vitro* pCA release via hydrolytic anhydride and ester bond cleavage demonstrated pCA release over 30 days when an adipic acid linker molecule was used, demonstrating its potential as a controlled release system (Figure 1.14).
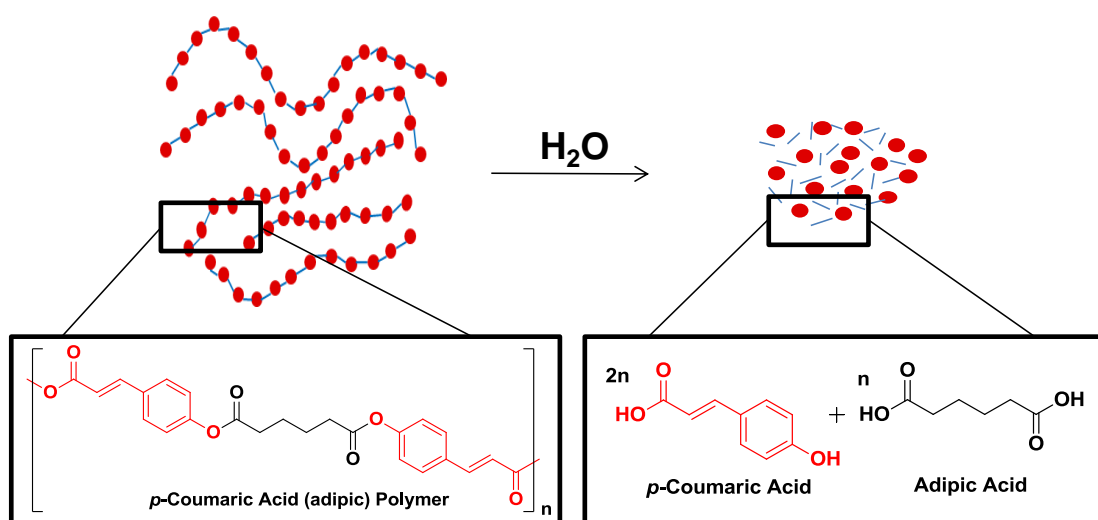
Figure 1.14. Depiction of *p*-coumaric acid-based polymers that release *p*-coumaric acid upon hydrolytic degradation

1.3.5. Biodegradable antioxidant-containing poly(anhydride-esters)

Ferulic acid (FA) and sinapic acid (SinA) are antioxidant and photoprotective hydroxycinnamic acids (HCs) used in biomedical and cosmetic formulations to prevent skin cancer and senescence. Although these bioactives exhibit numerous health benefits, physicochemical instability leading to

decomposition hinders their efficacy. To minimize inherent decomposition, HC-containing biodegradable polymers were prepared via solution polymerization to chemically incorporate FA and SinA into a poly(anhydride-esters).[51] The polymers were characterized using nuclear magnetic resonance and Fourier transform infrared spectroscopies. The molecular weights and thermal properties were also determined. *In vitro* studies demonstrated that the polymers were hydrolytically degradable, thus providing controlled release of the chemically incorporated HC with no detectable decomposition. The polymer degradation products were found to exhibit antioxidant and antibacterial activity comparable to free FA and SinA (Figure 1.15). *In vitro* cell viability studies demonstrated that the polymers were non-cytotoxic towards fibroblasts. This work indicates HC-based polymers as potential candidates for use as controlled release systems for skin care formulations.
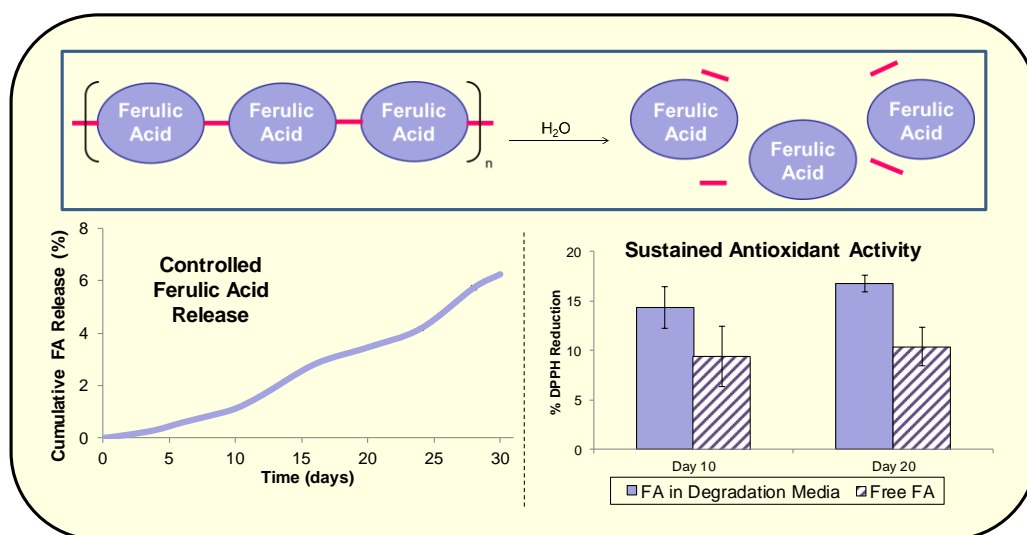
Figure 1.15. Depiction of ferulic acid-based polymer with respective release profile and antioxidant activity

1.3.6. **Ferulic acid-containing poly(anhydride-esters) with glycol functionality for tailoring physicochemical properties and release profiles**

The HC-based polymers synthesized thus far release the chemically incorporated bioactive at a slower rate than that desired for topical applications. Therefore, there is a need for a more rapid release rate for use in skin care formulations. To demonstrate this, a series of ferulic acid-containing polymers with ethylene glycol linkages were synthesized via solution polymerization methods. The polymers were characterized using nuclear magnetic resonance and Fourier transform infrared spectroscopies. The molecular weights and thermal properties were also determined. The glass transition temperatures and contact angles were obtained and the polymers compared. The polymer chemical structures and physical properties were shown to impact the release rates and antioxidant activity as drug delivery systems demonstrating the ability to strategically select polymers for various applications.
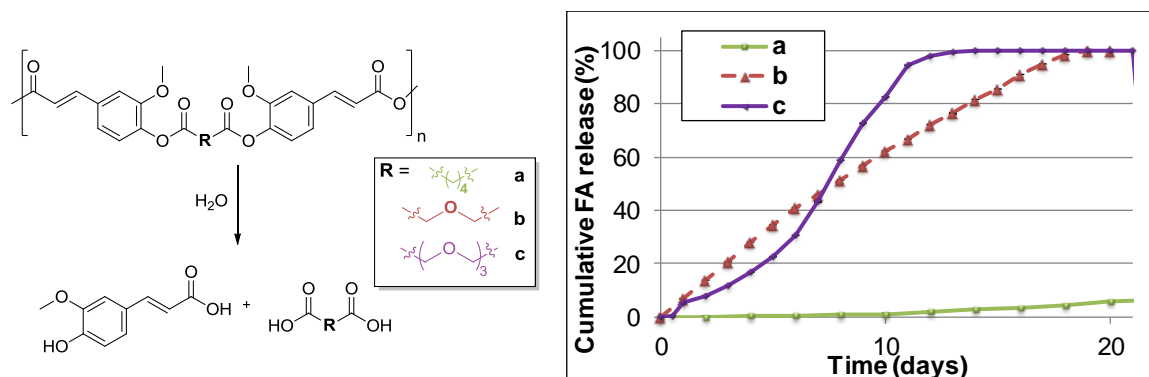
Figure 1.16. Depiction of ferulic acid-based polymers with varying hydrophilicity and tunable release profiles

1.4.   Summary

Biodegradable polymers play an integral role in biomaterials, particularly in the realm of drug delivery. Bioactive-based polyanhydride delivery systems offer advantages over other polymeric delivery systems due to the ability to release a high bioactive loading in a controlled manner. Rather than physically entrapping active molecules, such polymers allow for the chemical incorporation of high levels of bioactive materials, well-controlled and tailored release profiles, and formulation into a variety of devices. Such drug delivery systems are finding significant and diverse applications ranging from biomedical devices to consumer products. This dissertation describes how polymeric systems have been strategically designed and engineered, as the polymers' chemical structures and physical properties directly impact their functionality as controlled release drug delivery systems. Several examples of bioactive-based polyanhydrides will be discussed including those containing hydroxy acids, antimicrobials, and antioxidants that can be strategically chosen for various applications.

1.5.   References

1.   Wilson CG, **2012**, 3-18.

2.   Uhrich KE, Cannizzaro SM, Langer RS, Shakesheff KM, *Chem Rev* **1999**, *99*, 3181-98.

3.   Brannon-Peppas L. Polymers in Controlled Drug Delivery. Medical Plastics and Biomaterials Magazine. 1997.

4.   Neuse EW, *Metal-Based Drugs* **2008**, *2008*, 1-19.

5.   Göpferich A, Tessmar J, *Adv Drug Deliv Rev* **2002**, *54*, 911-31.

6.   Gopferich A, *Biomaterials* **1996**, *17*, 103-14.

7. Katti DS, Lakshmi S, Langer R, Laurencin CT, *Adv Drug Deliv Rev* **2002**, *54*, 933-61.

8. Whitaker-Brothers K, Uhrich K, *J Biomed Mater Res Part A* **2006**, *76A*, 470-9.

9. Kumar N, Langer RS, Domb AJ, *Adv Drug Deliv Rev* **2002**, *54*, 889-910.

10. Amass W, Amass A, Tighe B, *Polym Int* **1998**, *47*, 89-144.

11. Leong KW, Kost J, Mathiowitz E, Langer R, *Biomaterials* **1986**, *7*, 364-71.

12. Rosen HB, Chang J, Wnek GE, Linhardt RJ, Langer R, *Biomaterials* **1983**, *4*, 131-3.

13. Leong KW, Simonte V, Langer R, *Macromolecules* **1987**, *20*, 705-12.

14. Schmeltzer RC, Johnson M, Griffin J, Uhrich K, *J Biomater Sci Polym Ed* **2008**, *19*, 1295-306.

15. Carbone AL, Uhrich KE, *Macromol Rapid Commun* **2009**, *30*, 1021-6.

16. Schmeltzer RC, Anastasiou TJ, Uhrich KE, *Polym Bull* **2003**, *49*, 441-8.

17. Prudencio A, Schmeltzer RC, Uhrich KE, *Macromolecules* **2005**, *38*, 6895-901.

18. Domb AJ, Langer R, *J Polym Sci, Part A: Polym Chem* **1987**, *25*, 3373-86.

19. Domb AJ, Amselem S, Shah J, Maniar M, *Adv Polym Sci* **1993**, *107*, 93-141.

20. Domb AJ, Israel ZH, Elmalak O, Teomim D, Bentolila A, *Pharm Res* **1999**, *16*, 762-5.

21. Westphal M, Ram Z, Riddle V, Hilt D, Bortey E, *Acta Neurochir (Wien)* **2006**, *148*, 269-75; discussion 75.

22. Brem H, Lawson HC, *Cancer* **1999**, *86*, 197-9.

23. Valtonen S, Timonen U, Toivanen P, Kalimo H, Kivipelto L, Heiskanen O, Unsgaard G, Kuurne T, *Neurosurgery* **1997**, *41*, 44-8; discussion 8-9.

24. Siepmann F, Le Brun V, Siepmann J, *J Controlled Release* **2006**, *115*, 298-306.

25. Tang Y, Singh J, *Int J Pharm* **2008**, *357*, 119-25.

26. Erdmann L, Uhrich KE, *Biomaterials* **2000**, *21*, 1941-6.

27. Erdmann L, Macedo B, Uhrich KE, *Biomaterials* **2000**, *21*, 2507-12.

28. Reynolds MA, Prudencio A, Aichelmann-Reidy ME, Woodward K, Uhrich KE, *Curr Drug Deliv* **2007**, *4*, 233-9.

29. Bryers JD, Jarvis RA, Lebo J, Prudencio A, Kyriakides TR, Uhrich K, *Biomaterials* **2006**, *27*, 5039-48.

30. Deronde BM, Carbone AL, Uhrich KE, *Polym Degrad Stab* **2010**, *95*, 1778-82.

31. Rosario-Meléndez R, Lavelle L, Bodnar S, Halperin F, Harper I, Griffin J, Uhrich KE, *Polym Degrad Stab* **2011**, *96*, 1625-30.

32. Prudencio A, Schmeltzer RC, Uhrich KE, *Macromolecules* **2005**, *38*, 6895-901.

33. Whitaker-Brothers K, Uhrich K, *J Biomed Mater Res Part A* **2004**, *70A*, 309-18.

34. Harten RD, Svach DJ, Schmeltzer R, Uhrich KE, *J Biomed Mater Res Part A* **2005**, *72*, 354-62.

35. Schmeltzer RC, Schmalenberg KE, Uhrich KE, *Biomacromolecules* **2005**, *6*, 359-67.

36. Yeagy BA, Prudencio A, Schmeltzer RC, Uhrich KE, Cook TJ, *J Microencapsulation* **2006**, *23*, 643-53.

37. Schmeltzer RC, Uhrich KE, *Polym Bull* **2006**, *57*, 281-91.

38. Rosenberg LE, Carbone AL, Romling U, Uhrich KE, Chikindas ML, *Lett Appl Microbiol* **2008**, *46*, 593-9.

39. Carbone AL, Song M, Uhrich KE, *Biomacromolecules* **2008**, *9*, 1604-12.

40. Johnson ML, Uhrich KE, *J Biomed Mater Res Part A* **2009**, *91*, 671-8.

41. Prudencio A, Carbone AL, Griffin J, Uhrich KE, *Macromol Rapid Commun* **2009**, *30*, 1101-8.

42. Carbone AL. Ph.D. thesis. Rutgers, The State University of New Jersey, New Brunswick, 2009.

43. Griffin J, Carbone A, Delgado-Rivera R, Meiners S, Uhrich KE, *Acta Biomater* **2010**, *6*, 1917-24.

44. Griffin J, Delgado-Rivera R, Meiners S, Uhrich KE, *J Biomed Mater Res Part A* **2011**, *97A*, 230-42.

45. Fogaça R, Ouimet M, Catalani L, Uhrich K, *Proc ACS Div Polym Mater Sci Eng* **2010**.

46. Ouimet MA, Snyder SS, Uhrich KE, *Abstr Pap Am Chem S* **2011**, *242*.

47. Ouimet MA, Snyder SS, Uhrich KE, *J Bioact Compat Pol* **2012**, *27*, 540-9.

48. Ouimet MA, Nguyen V, Smith K, Uhrich KE, *Polymer Prepr* **2012**, *53*, 548-9.

49. Rosario-Meléndez R, Ouimet MA, Uhrich KE, *Polym Bull* **2013**, *70*, 343-51.

50. Fogaca R, Ouimet M, Uhrich K, Catalani LH. In ACS Symposium Series, in press. Scholz C, Kressler J, editors 2013.

51. Ouimet MA, Griffin J, Carbone-Howell AL, Wu WH, Stebbins ND, Di R, Uhrich KE, *Biomacromolecules* **2013**, *14*, 854–61.

CHAPTER 2:   TUNABLE DRUG RELEASE PROFILES FROM SALICYLIC

ACID -BASED POLY(ANHYDRIDE-ESTERS)

2.1.   Introduction

Salicylic acid (SA), the major metabolite of aspirin, has been used for centuries for its analgesic, anti-inflammatory, and antipyretic effects.[2] Recently, SA has been found to be beneficial for many other applications such as wound healing, diabetes, arthritis, and cancer treatment.[3-7] The best results are obtained when SA is maintained at therapeutic levels at the desired area for as long as it is needed.[8] Oral SA delivery is systemic and potentially causes gastrointestinal problems, while not maintaining steady SA concentrations at the desired location.[9] Localized delivery from polymers can help overcome undesired side effects and allow for higher, localized SA levels than systemic delivery.[10, 11]

Previous attempts to control localized SA release have been through the physical mixture of SA into a biodegradable polymer matrix.[12-16] This type of drug incorporation, however, generally results in a burst of SA,[12-15] where large amounts of drug are released before the release rate stabilizes.[17] Burst profiles of drugs tend to be unpredictable[17] and can lead to toxic SA concentrations. Additionally, the maximum amount of drug loading is limited before it begins affecting the device's mechanical and degradation properties.[12]

Many drug-eluting polymer matrices exhibit a burst release without sustaining the drug concentration for the duration of complete polymer degradation.[12-15] Wang et al. have demonstrated sustained release with minimal control over the degradation profile by altering polymer composition. Although the authors were able to obtain zero-order release, the SA amount required to achieve this (40 % in poly(lactide-*co*-glycolide) (PLGA)) significantly increased polymer degradation rates.[16]

To better control SA concentrations, salicylic acid-based poly(anhydride-esters) (SAPAEs) were developed, in which SA is chemically incorporated into the polymer backbone via a biocompatible linker molecule. These polymers have been studied both *in vitro*[18, 19] and *in vivo*[20, 21] and have been found to be biocompatible. The polymers hydrolytically degrade to exhibit near zero-order SA release after an initial lag period, where minimal-to-no drug is measured. SAPAEs are designed to fully degrade over a matter of days to many months.[22, 23] The SA chemical incorporation enables inherent drug loading capacities up to 85 % (w/w), with the ability to physically admix additional drug to obtain even higher loading.[24]

The length of the lag period and the subsequent release rate is a direct function of the linker structure as shown for various polyanhydrides.[23, 25, 26] The linker used herein was linear aliphatic that generally results in a two-day lag period. While the SAPAE release rate can be easily changed for different applications via the linker molecule, the lag period is an important consideration. A lag period may be beneficial for applications, such as bone regeneration,

where an initial inflammatory response is desired and localized, reduced inflammation is beneficial at a later time point.[27, 28] On the other hand, a lag period could be a disadvantage if SA was desired immediately following implantation, as for instances where inflammation is already present (e.g., arthritis and diabetes).

One method used to adjust the length of a lag period is admixing small molecules into the polymer matrix to act as channeling agents.[29] As these channeling agents are solubilized, pores are created in the disc surface, increasing water penetration and subsequent polymer degradation.[30] This effect has been observed using salt leaching techniques,[31] as well as admixing molecules such as drugs[16, 32] or inert polymer precursors into the polymer matrix.[33, 34] For example, PLGA monomers (10 % w/w) acting as channeling agents in drug-loaded PLGA discs resulted in the absence of a lag period in drug release.[34]
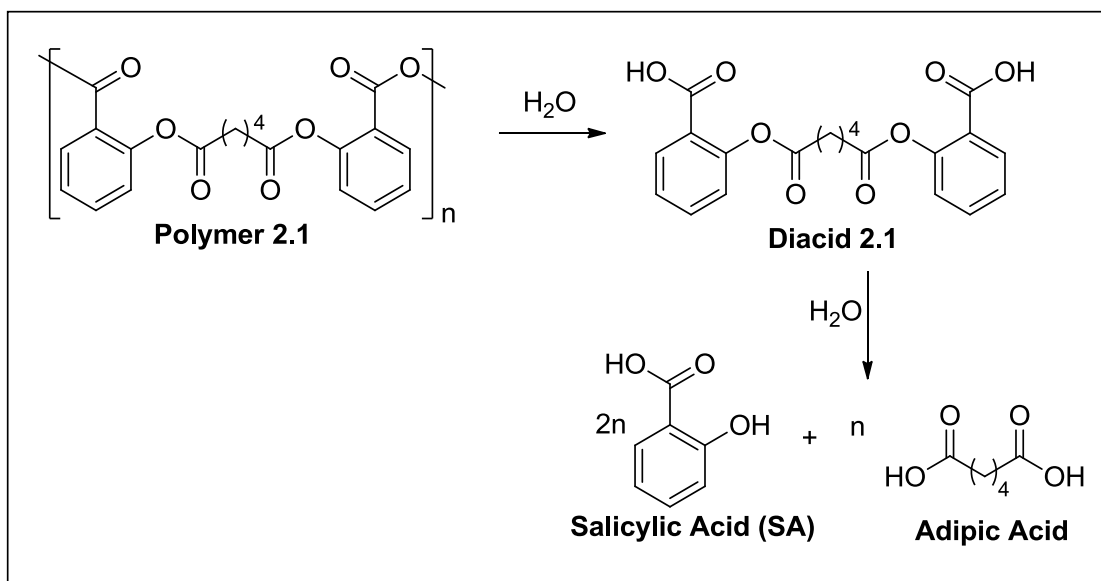
Figure 2.1. Hydrolytic degradation scheme of polymers with an adipic linker that releases SA and corresponding carboxylic acid

In this chapter, free SA and degradable polymer precursors, hereafter referred to as diacids (Figure 2.1), were physically admixed with SAPAEs at different ratios and weight percentages, as described in Table 2.1, to overcome the lag period. Polymers with admixed drug were compressed into discs, and drug release was monitored *in vitro* for 30 days. The admixture effects on drug release and thermal properties of the polymer matrices were determined.

2.2.   Experimental
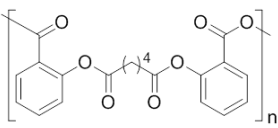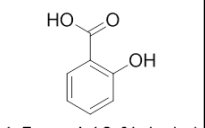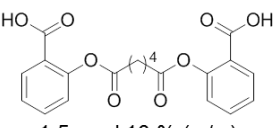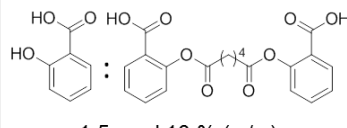
2.2.1.   Materials

Acetic anhydride was purchased from Fisher (Fair Lawn, NJ). All other chemicals and reagents were purchased from Sigma-Aldrich (Milwaukee, WI) and used as received.

2.2.2.   Polymer synthesis and characterization

SAPAEs were synthesized according to previously described methods.[23, 35, 36] In short, SA (2 equivalents (eq)) were dissolved in tetrahydrofuran (THF) and pyridine (4 eq). Adipoyl chloride (1 eq) was dissolved in THF and added drop-wise forming a white suspension. The reaction mixture was stirred overnight, quenched over water, and acidified to pH 2 using concentrated hydrochloric acid. The formed precipitate was filtered, washed with water (3 × 250 mL), and dried *in vacuo* to yield diacid. The diacid was activated in an excess of acetic anhydride at room temperature, concentrated, and polymerized via melt-condensation polymerization at 180 °C for 6 h at 160 rpm *in vacuo* to yield a tan powder. $M_W = 18,500$ Da, PDI = 1.3. $T_g = 42°C$.

Table 2.1. Representation of 1, 5, and 10 % (w/w) admixtures used for various polymer **2.1** sample disc compositions (R = adipic linker).

Polymer Alone	SA	Corresponding Diacid	SA : Diacid (1:1)
	1,5, and 10 % (w/w)	1,5, and 10 % (w/w)	1,5, and 10 % (w/w)

2.2.3. Disc preparation

SA, diacid, and SA:diacid (1:1 by weight) mixtures were separately mixed with polymer at 1 %, 5 %, and 10 % (w/w) (Table 2.1) and ground with mortar and pestle to achieve a homogenous mixture. Polymer discs were prepared by pressing ground polymer mixtures (160 ± 5 mg) into 13 mm diameter × 1 ± 0.5-mm-thick discs in an infrared pellet die (International Crystal Laboratories, Garfield, NJ) with a bench-top hydraulic press (Carver, Inc. Model M; Wabash, IN) at 10,000 psi for 5 min at room temperature. Polymer discs without admixtures were prepared as controls. All samples were prepared in triplicate to give a total of 30 discs.

2.2.4. *In vitro salicylic acid release*

Each disc was placed in 20 mL Wheaton glass scintillation vials containing 10 mL phosphate buffered saline (PBS) at pH 7.40. Samples were incubated at 37 °C with agitation at 60 rpm in a controlled environment incubator shaker (Excella E25; New Brunswick Scientific Co., Edison, NJ). All

media were collected and replaced with fresh PBS (10 mL) at pre-designated time points for 30 days. Spent media were analyzed by ultraviolet (UV) spectrophotometry using a Perkin Elmer Lambda XLS spectrophotometer (Perkin Elmer, Waltham, MA) to specifically monitor SA release. Measurements were obtained at λ = 303 nm, the maximum absorbance of SA that did not overlap with other polymer degradation products. Data were calculated against a calibration curve of absorbance values from standard solutions of known SA concentrations in PBS. All pH measurements were performed using an Accumet$^{®}$ AR15 pH meter (Fisher Scientific, Fair Lawn, NJ).

2.2.5. Influence on glass transition temperature

Differential scanning calorimetry (DSC) was performed to determine glass transition (T_g) values using a Thermal Advantage (TA) DSC Q200 running on an IBM ThinkCentre computer equipped with TA Universal Analysis software for data collection and processing. Samples (5-8 mg) were heated under dry nitrogen at 10 °C/min heating and cooling rate from -10 °C to 200 °C with a two-cycle minimum. TA Instruments Universal Analysis 2000 software, version 4.5A was used to analyze the data. Glass transition temperatures were calculated as half Cp extrapolated.

2.3.   Results and Discussion

Free SA and diacids were physically admixed into SAPAE matrices that exhibit a lag periods to combine the immediate drug release commonly observed in physical mixtures[17] with the zero-order characteristics of SAPAEs.[37] Addition of these molecules at all weight percentages increased SA release during the typical polymer lag period while having little effect on the release rate at later times. The amount of SA released was dependent upon both the type of molecules admixed and the weight percentage within the matrix (Table 2.2).

Table 2.2. Theoretical drug loading for all samples

	None	SA			Diacid			SA:diacid (1:1)		
Polymer **2.1**										
Admixture amount (%)	—	1	5	10	1	5	10	1	5	10
Drug loading (%)	72.2	72.5	73.6	75.0	72.2	72.2	72.2	72.4	72.9	73.6

2.3.1.   *In vitro* salicylic acid release

In vitro drug release was measured by quantifying the SA concentrations in PBS over 30 days using UV spectrophotometry. The inflection point in the polymer release profiles was used to define the lag periods and subsequent period of zero-order drug release. A short lag period of 2 days was observed for polymer **2.1** alone (Figure 2.2). The spent media pH was monitored through the lag periods with the greatest pH differential observed as 0.6, which should have negligible effects on polymer degradation rates. As shown in Figure 2.2, the lag period for polymer alone was overcome by all admixtures within the first 24 h where SA samples

exhibited the highest SA concentration for their respective weight percentages, followed by the 1:1 mixture, and then diacid.
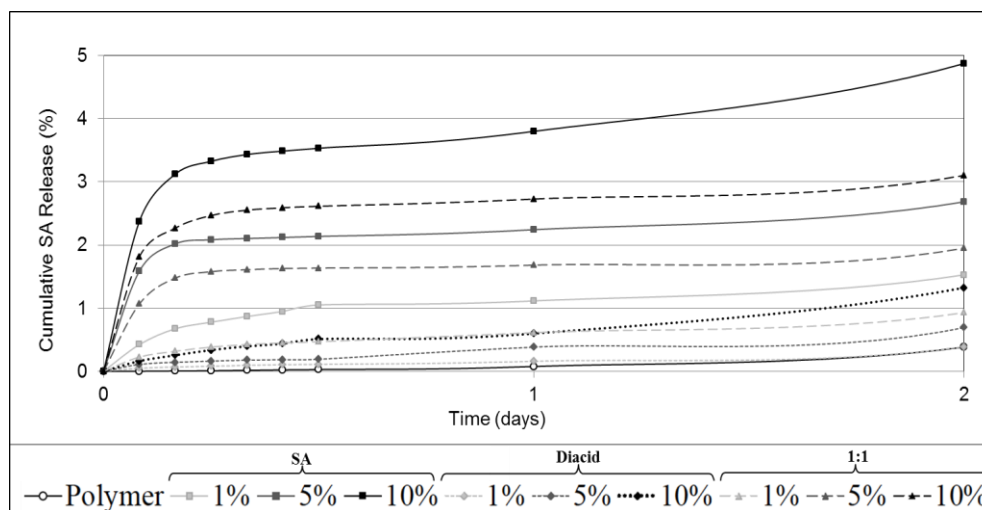
Figure 2.2. SA release profiles during the typical lag period of 0-2 days for polymer **2.1** alone (open circles) against 1, 5, and 10 % (w/w) admixtures.

As expected, larger weight percentages of the SA-based additives resulted in higher SA concentrations over the initial time period. However, differences in weight percentage on early release were dependent on the admixed molecules. The incorporation of SA and 1:1 SA:diacid resulted in distinct differences in SA concentration as a function of weight percentage (Figure 2.3A and B), whereas the differences for the diacid incorporation were not as distinct (Figure 2.3C). After early stage release, all samples maintained near zero-order profiles of SA release (Figure 2.3D), with a post-lag period average of 2.06 % ± 0.38 % and 2.33 % ± 0.1 8 % released per day from polymer **2.1** alone and for polymer **2.1** admixtures, respectively.
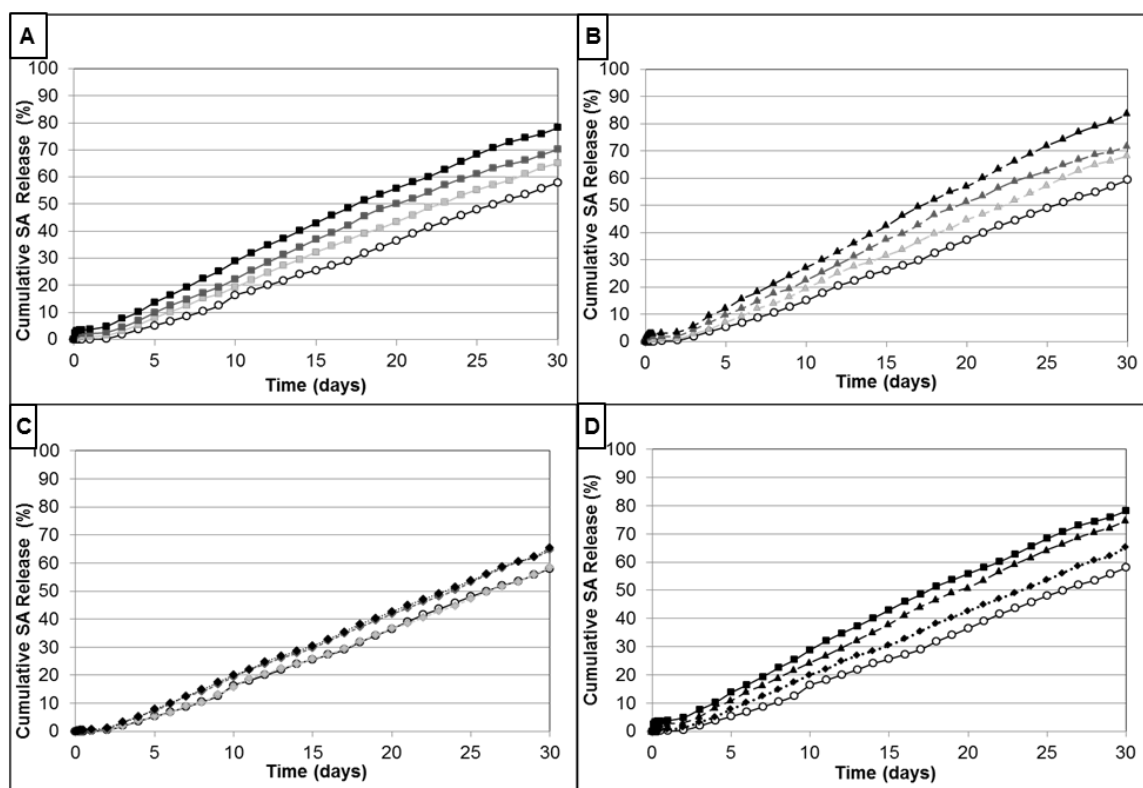
Figure 2.3. Cumulative release profiles of polymer **2.1** (open circles) against 1 % (light gray), 5 % (medium gray), and 10 % (black) (w/w) admixtures of SA (squares) (A), SA:diacid combination (triangles) (B), and diacid (diamonds) (C) over 30 days with a comparison of the three different admixtures at the same weight percentage (10 % w/w) (D).

It is important to note that the samples in this study were compression-molded into discs. If these systems were formulated into fibers or microspheres, for example, the release profiles would likely differ as the geometry and increased surface area influences the erosion characteristics of the polyanhydride matrix.[38, 39] *In vivo* results may also differ as the degradation media do not contain enzymes or other proteins.

2.3.2.   Influence on glass transition temperature

The incorporation of small molecules into a polymer matrix often alters the thermal properties.[40] DSC measurements indicate a 42 °C T_g for polymer alone. A characteristic lowering of the polymers' T_g was noted as the weight percentage of the additive increased (Figure 2.4). This observation is consistent with previously reported results on diffusion-controlled drug release from polymers, where the admixed small molecules act as plasticizers.[40] This aspect constrains the maximum weight percent for some SAPAEs as the device may not retain its shape *in vivo* if a polymeric device's T_g is near or below physiological temperature (37°C). Deformation after implantation could alter the surface area, resulting in unpredictable drug release since these PAEs are primarily surface eroding.[37]
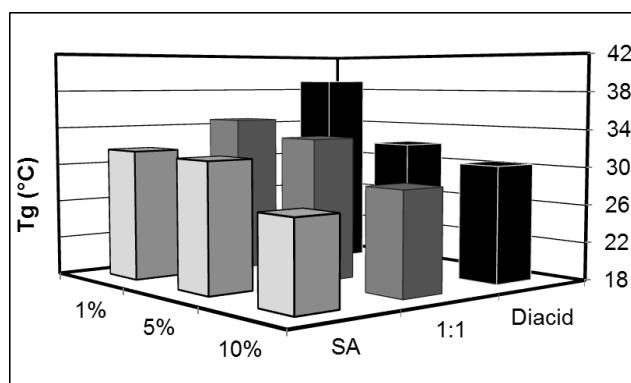
Figure 2.4. Glass transition temperatures measured for polymer 2.1 and various admixtures. The highest point on the y-axis corresponds with the T_g of polymer alone.

2.4.   Conclusion

As an anti-inflammatory drug, SA can be useful for the treatment of a wide range of diseases. Furthermore, localized, sustained release of SA can both minimize side effects and improve patient compliance. To develop a polymeric device that would ensure the desired amount of SA is being released at any given time, SA and diacids were used to alter the polymer release profiles and overcome the lag period. The duration as well as the amount of SA at early and late time points was easily controlled by adjusting multiple factors: polymer composition via the linker molecule, weight ratio of admixed molecules, and ratios of those molecules. With this ability to fine-tune the amount of SA present at various times over sustained periods, devices can be prepared that fit the specific needs of many different applications.

2.5.   References

1.   Ouimet MA, Snyder SS, Uhrich KE, *J Bioact Compat Pol* **2012**, *27*, 540-9.

2.   Wu KK, *Circulation* **2000**, *102*, 2022-3.

3.   Roseborough IE, Grevious MA, Lee RC, *J Natl Med Assoc* **2004**, *96*, 108-16.

4.   Rumore MM, Kim KS, *Ann Pharmacother* **2010**, *44*, 1207-21.

5.   Yamazaki R, Kusunoki N, Matsuzaki T, Hashimoto S, Kawai S, *J Pharm Pharmacol* **2002**, *54*, 1675-9.

6.   Perugini RA, McDade TP, Vittimberga FJ, Jr., Duffy AJ, Callery MP, *J Gastrointest Surg* **2000**, *4*, 24-32.

7.   Spitz GA, Furtado CM, Sola-Penna M, Zancan P, *Biochem Pharmacol* **2009**, *77*, 46-53.

8. Uhrich KE, Cannizzaro SM, Langer RS, Shakesheff KM, *Chem Rev* **1999**, *99*, 3181-98.

9. Amann R, Peskar BA, *Eur J Pharmacol* **2002**, *447*, 1-9.

10. Domb AJ, *Mol Med Today* **1995**, *1*, 134-9.

11. Jain JP, Modi S, Domb AJ, Kumar N, *J Controlled Release* **2005**, *103*, 541-63.

12. Tang Y, Singh J, *Int J Pharm* **2008**, *357*, 119-25.

13. Tada D, Tanabe T, Tachibana A, Yamauchi K, *J Biosci Bioeng* **2005**, *100*, 551-5.

14. Hu Y, Zhou X, Lu Y, Hu C, Hu X, *Int J Pharm* **2009**, *371*, 89-98.

15. Wenk E, Wandrey AJ, Merkle HP, Meinel L, *J Controlled Release* **2008**, *132*, 26-34.

16. Wang Q, Zhang N, Hu X, Yang J, Du Y, *J Biomed Mater Res Part A* **2008**, *85*, 881-7.

17. Huang X, Brazel CS, *J Controlled Release* **2001**, *73*, 121-36.

18. Schmeltzer RC, Johnson M, Griffin J, Uhrich K, *J Biomater Sci Polym Ed* **2008**, *19*, 1295-306.

19. Griffin J, Delgado-Rivera R, Meiners S, Uhrich KE, *J Biomed Mater Res Part A* **2011**, *97A*, 230-42.

20. Erdmann L, Macedo B, Uhrich KE, *Biomaterials* **2000**, *21*, 2507-12.

21. Harten RD, Svach DJ, Schmeltzer R, Uhrich KE, *J Biomed Mater Res Part A* **2005**, *72*, 354-62.

22. Carbone AL, Uhrich KE, *Macromol Rapid Commun* **2009**, *30*, 1021-6.

23. Prudencio A, Schmeltzer RC, Uhrich KE, *Macromolecules* **2005**, *38*, 6895-901.

24. Johnson ML, Uhrich KE, *J Biomed Mater Res Part A* **2009**, *91*, 671-8.

25. Vogel B, *Biomaterials* **2005**, *26*, 721-8.

26. Torres MP, Vogel BM, Narasimhan B, Mallapragada SK, *J Biomed Mater Res Part A* **2006**, *76A*, 102-10.

27. Mountziaris PM, Mikos AG, *Tissue Eng Pt B-Rev* **2008**, *14*, 179-86.

28. Simon AM, O'Connor JP, *J Bone Joint Surg* **2007**, *89*, 500-11.

29. Gonzalez-Rodriguez ML, Perez-Martinez JI, Merino S, Fini A, Rabasco AM, *Drug Dev Ind Pharm* **2001**, *27*, 439-46.

30. Shen E, Kipper MJ, Dziadul B, Lim MK, Narasimhan B, *J Controlled Release* **2002**, *82*, 115-25.

31. Sibambo SR, Pillay V, Choonara YE, Penny C, *J Bioact Compat Pol* **2008**, *23*, 132-53.

32. Kishida A, Goto H, Murakami K, Kakinoki K, Akashi M, Endo T, *J Bioact Compat Pol* **1998**, *13*, 222-33.

33. Kim JM, Seo KS, Jeong YK, Lee HB, Kim YS, Khang G, *J Biomater Sci Polym Ed* **2005**, *16*, 991-1007.

34. Yoo JY, Kim JM, Khang G, Kim MS, Cho SH, Lee HB, Kim YS, *Int J Pharm* **2004**, *276*, 1-9.

35. Erdmann L, Uhrich KE, *Biomaterials* **2000**, *21*, 1941-6.

36. Schmeltzer RC, Schmalenberg KE, Uhrich KE, *Biomacromolecules* **2005**, *6*, 359-67.

37. Whitaker-Brothers K, Uhrich K, *J Biomed Mater Res Part A* **2006**, *76A*, 470-9.

38. Göpferich A, Tessmar J, *Adv Drug Deliv Rev* **2002**, *54*, 911-31.

39. Akbari H, D'Emanuele A, Attwood D, *Int J Pharm* **1998**, *160*, 83-9.

40. Siepmann F, Le Brun V, Siepmann J, *J Controlled Release* **2006**, *115*, 298-306.

CHAPTER 3:   OPTIMIZED SYNTHESIS AND FORMULATION OF

SALICYLIC ACID-BASED POLY(ANHYDRIDE-ESTER)

MICROSPHERES

Reprinted and edited with permission from Rosario-Meléndez R, Ouimet MA, Uhrich KE, *Polym Bull* 2013, *70*, 343-51. *Copyright 2013 Springer.*[1]

3.1.   Introduction

The previous chapter discussed tailoring salicylic acid release profiles using small molecule admixtures.[2, 3] In this chapter, a different method utilizing polymer microspheres to tailor drug release profiles is discussed.   Polymer microspheres have garnered significant attention in recent years as they can be used as delivery systems for encapsulated drugs,[4-7] proteins,[8] and genes/DNA[4-6, 9] for a variety of biomedical applications.   As a result, compounds with pharmaceutical activity are routinely encapsulated within polymer microspheres.[4-7] Microencapsulation also offers advantages for cosmetics and personal care applications as this methodology has the potential to increase the efficacy of topical formulations by controlling the release of bioactive molecules.[10-12]

Salicylic acid, an over-the-counter monograph drug approved by the FDA for acne treatment, is an example of a cosmetic active for which a delivery system would be desired.   In addition to its anti-acne properties, salicylic acid is often incorporated into various skin care products due to its keratolytic properties. Hydroxy acids such as salicylic acid have been utilized for skin benefits including rejuvenation and for the treatment of dry skin, wrinkles, photoaged skin, and skin

pigmentation disorders.[13] As an acid, however, this active sometimes causes skin irritation and dermatitic inflammation due its lowering of a formulation's pH.[13-15] To overcome these drawbacks, an appropriate delivery system can be developed. Recently, Dayan demonstrated that a porous nylon polymer-based controlled release delivery system could deliver 15% of physically entrapped salicylic acid while reducing skin irritation and prolonging the bioactive's efficacy.[11, 12] Rhein designed a salicylic acid delivery system by physical entrapment in porous hydrophobic polyurethane for sustained salicylic acid release.[16] In both examples above, however, the loading and relative salicylic acid release is dependent on the porous polymeric carrier, which limits the ability to tailor the release of the bioactive material.

For biomedical applications, salicylic acid-based poly(anhydride-esters) have been designed to release chemically incorporated salicylic acid over prolonged periods of time (e.g., weeks to months).[17, 18] For personal care and cosmetics, however, the delivery rate needs to be such that it is controlled, yet rapid, releasing the bioactive within 6-12 hours in most cases.[19, 20] A desirable release rate for salicylic acid will be within a 12-24 hour time frame as a consumer will most likely not retain a cosmetic product in their skin for more than 24 hours due to their daily routines (e.g., face washing and showering).[21, 22]

Previous work on salicylic acid-based polymers using discs[18] and microspheres[23] has shown that drug release can be tuned to last over varying time periods by using different linkers within the polymers, but release occurred beyond the desired window (12-48 h). To meet the degradation profile needed

for personal care and cosmetic applications, a salicylic acid-based polymer using a heteroatom, specifically an oxygen-containing linker (Figure 3.2, **3.1**), was used and compared to that of a linear aliphatic linker (Figure 3.2, **3.2**), which can prolong the release to weeks and months.[18] The formulation and characterization of fast-degrading polymer microspheres are reported herein for the first time and an aliphatic linker-containing polymer is used for comparison to previous work.

In this chapter, a previously published microsphere preparation method that would release salicylic acid in a relatively fast timeframe was optimized, while not significantly altering physicochemical properties. The initial polymer-based microsphere formulation was prepared by a well-established oil-in-water single emulsion solvent evaporation method. [23] However, the initial microsphere formulation exhibited significant aggregation and non-spherical morphology, which are undesirable for uniform and predictable drug release. Therefore, to improve the quality of the microspheres, homogenization speed was decreased and polymer concentration was increased during formulation.

Microsphere molecular weight (M_w), polydispersity index (PDI) and glass transition temperature (T_g) were measured and compared to the pre-formulated polymer to determine the formulation effect on the polymer. Scanning electron microscopy (SEM) was used to determine the microsphere size and morphology. *In vitro* studies were performed on the polymer microspheres to investigate bioactive release.

3.2.   Experimental

3.2.1.   Materials

All chemicals and reagents were purchased from Sigma-Aldrich (Milwaukee, WI) and used as received unless otherwise noted.

3.2.2.   Optimized Polymer Synthesis

Salicylic acid (diglycolic) diacid was prepared using previously published methods.[24]   In short, salicylic acid (2 eq) was dissolved in THF and pyridine (4.4 eq) is added. Diglycolyl chloride (1 eq) dissolved in minimal THF was added dropwise via syringe pump at 20 mL/h and reaction stirred for 24 h. Reaction progress was monitored via TLC.   Once complete, the reaction mixture was quenched over 20-fold DI water and acidified with concentrated HCl to pH ~2. Contents were isolated via vacuum filtration and residue washed with additional water to remove residual THF.   The residue was immediately dissolved in acetone and precipitated over hexanes. The contents were isolated via vacuum filtration and dried in a desiccator at room temperature *in vacuo*.

Table 3.1. Various conditions used to prepare poly(anhydride-esters) by solution polymerization

Reaction Temperature	Reaction Time	Ether Temperature	Yield (%)
-78 °C	2 h	RT	27
-78 °C	3 h	RT	29
-78 °C	6 h	RT	37
0 °C	3 h	RT	54
0 °C	6 h	RT	58
0 °C	3 h	chilled	73
0 °C	6 h	chilled	76
0 °C	8 h	chilled	61

Salicylic acid (diglycolic) polymer (5 g, **3.1**) was prepared by stirring diacid (1 eq) in DCM to which Et_3N (4 eq) was added causing dissolution. The reaction was cooled to specified temperature (see Table 3.1) to which triphosgene (0.33 eq) dissolved in minimal DCM is added dropwise. The reaction mixture is stirred for the times outlined in Table 3.1. Once completed, the reaction was precipitated over ether (either at RT or chilled). The precipitate was isolated via vacuum filtration. The residue was washed with acidic water (pH ~2) and dried in the Buchner funnel with high vacuum for 20 minutes. Product was dried *in vacuo* overnight and subsequently characterized via nuclear magnetic resonance (NMR), Fourier transform infrared spectroscopy (FTIR), gel permeation chromatography (GPC), differential scanning calorimetry (DSC), and thermal gravimetric analysis (TGA).

3.2.3. ^{1}H NMR and FTIR spectroscopies

^{1}H and ^{13}C NMR spectra were recorded on a Varian 400 MHz or 500 MHz spectrometer using deuterated dimethyl sulfoxide (DMSO-d_6) as solvent and internal reference. FTIR spectra were obtained using a Thermo Nicolet/Avatar 360 spectrometer, samples (1 wt %) ground and pressed with KBr into a disc. Each spectrum was an average of 32 scans.

3.2.4. Microsphere preparation

Polymers were formulated into microspheres using a modified procedure of a published oil-in-water single emulsion solvent evaporation technique.[23] In general, salicylic acid-based polymers (0.50 g) were dissolved in dichloromethane (3 mL) and added drop-wise to 1% aqueous poly(vinyl alcohol) (PVA) solution (80 mL) at room temperature. The emulsion was homogenized for 2 min using an IKA Ultra-Turrax T8 homogenizer at approximately 10,000 rpm. The homogenized solution was left stirring for 2 h to allow microsphere formation by solvent evaporation. Microspheres were transferred to sterile 50 mL polypropylene conical tubes (30 x 115 mm style, BD Falcon, Franklin Lakes, NJ), washed with acidic water (pH 1) to remove residual PVA, and isolated by centrifugation at 3,000 rpm for 10 min. Microspheres were frozen by placing the conical tubes in a dry ice/acetone bath and lyophilized for 24 h at -40 ˚C and 133x10^{-3} mBar (LABCONO Freeze Dry System/Freezon 4.5).

3.2.5. **Microsphere size and morphology**

Size and morphology of the microspheres were determined using SEM. Images for each set of microspheres were obtained using an AMRAY-1830I microscope (AMRAY Inc.) after coating the samples with Au/Pd using a sputter coater (SCD 004, Blazers Union Limited). SEM images of each polymer microsphere sample were then analyzed using NIH ImageJ software. Distributions of particle diameter were obtained by evaluating > 50 particles per sample.

3.2.6. **Molecular weight and thermal analyses**

Gel permeation chromatography (GPC) was used A Perkin-Elmer LC system consisting of a Series 200 refractive index detector, a Series 200 LC pump, and an ISS 200 advanced sample processor were used to determine molecular weights (M_w) and polydispersity indices (PDI) of polymer and microspheres. A Dell OptiPlex GX110 computer running Perkin-Elmer TurboChrom 4 software was utilized for data collection and control. The connection between the LC system and the computer was made using a Perkin-Elmer Nelson 900 Series Interface and 600 Series Link. Samples were dissolved in dichloromethane (10 mg/mL) and filtered through 0.45 µm polytetrafluoroethylene (PTFE) syringe filters (Whatman, Clifton, NJ) prior to elution through a Jordi divinylbenzene mixed-bed GPC column (7.8 x 300 mm) (Alltech Associates, Deerfield, IL) at a rate of 1 mL/min for a total run time of 30

min. M_w was calculated relative to narrow molecular weight polystyrene standards (Polysciences, Dorval, Canada).

Differential scanning calorimetry (DSC) was performed to determine glass transition (T_g) values using a Thermal Advantage (TA) DSC Q200 running on an IBM ThinkCentre computer equipped with TA Universal Analysis software for data collection and processing. Samples (5-8 mg) were heated under dry nitrogen at 10 °C/min heating and cooling rate from -10 °C to 200 °C with a two-cycle minimum. TA Instruments Universal Analysis 2000 software, version 4.5A was used to analyze the data. Glass transition temperatures were calculated as half Cp extrapolated.

3.2.7.   *In vitro* salicylic acid release

Salicylic acid release from polymer microspheres was studied at 37 °C in phosphate buffered saline (PBS) at pH 7.4 with agitation (60 rpm) to mimic physiological conditions. Triplicate samples of each set of microspheres (20.0 mg) were suspended in 20 mL of PBS. At predetermined time points, samples were centrifuged at 3,000 rpm for 5 min (Hettich Zentrifugen EBA12) such that microspheres would settle to the bottom. Aliquots of the supernatant (15 mL) were collected and replaced with fresh PBS (15 mL). Spent media was analyzed via ultraviolet/visible spectroscopy at $\lambda = 303$ nm (wavelength at which salicylic acid is the only degradation product to absorb) using a Perkin Elmer Lambda XLS spectrophotometer to monitor bioactive release. Data was analyzed against known salicylic acid concentrations and normalized.

3.3.   Results and Discussion

3.3.1.   Optimized polymer synthesis

Previously, our laboratory reported the synthesis of fast-degrading poly(anhydride-esters) comprised of SA.[24]   This polymer synthesis (outlined in Figure 3.1) was optimized to improve polymer yield by altering solution polymerization reaction conditions: temperature during addition, temperature during workup, and reaction time (outlined in Table 3.1).   In preparation of 5 g salicylic acid (diglycolic) polymer, the reaction conditions were varied to increase yield.   With a -78 °C reaction temperature, the reaction time was varied and room temperature ether used.   No specific trend was observed and yields were low (< 37 %).   Polymer yield increased up to 76% with increasing temperature and reaction time.   The key finding for this study was using cold ether to precipitate the completed polymer.   This change allowed pure polymer to precipitate out in high yield with optimal reaction conditions at 0 °C for 6 hours.   Once polymer synthesis was optimized, the methodology was used to synthesize polymers for formulation into microspheres as injectable drug delivery systems and/or dual delivery systems.[1]
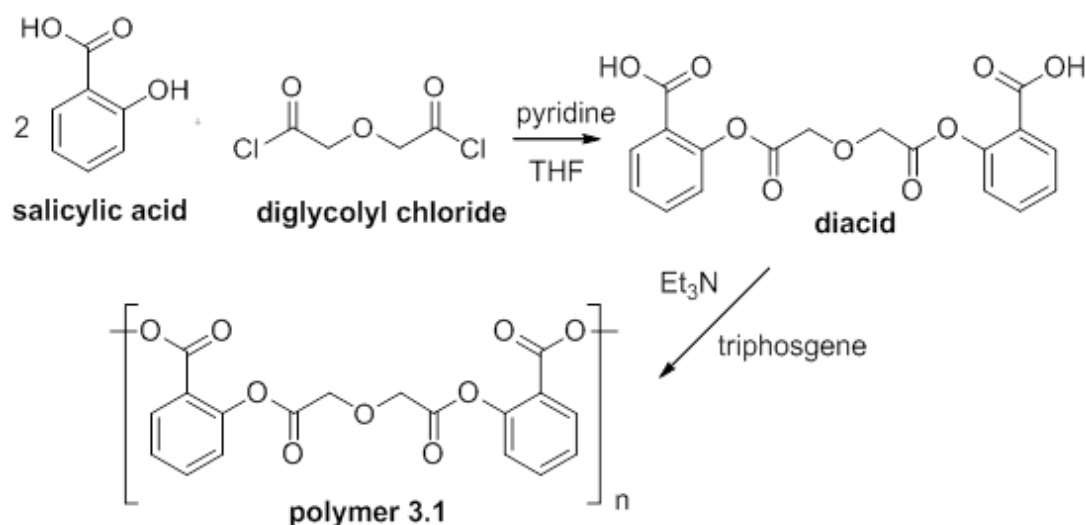
Figure 3.1. Synthetic scheme for diacid and polymer synthesis of polymer **3.1**

3.3.2. Microsphere preparation

Previous work on salicylic acid-based polymers using the free powder or pressed discs demonstrated that the physical properties and the salicylic acid release rate can be significantly altered by changing the chemical composition of the polymer via the linker.[18] Polymers with linear aliphatic linkers were previously formulated into microspheres, but were relatively small in size (i.e., 1-10 μm in diameter), exhibited aggregation, and achieved drug release for 12 days.[23] In this study, the formulation was improved to overcome the aforementioned issues in addition to formulating polymer **3.1** to achieve short-term salicylic acid release.
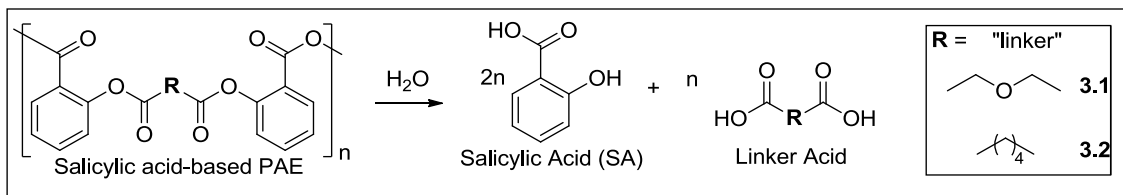
Figure 3.2. Structure of polymers **3.1-3.2** used to formulate salicylic acid-based polymer microspheres hydrolyzing into salicylic acid and linker acid

To enhance microsphere formulation, a modified oil-in-water single emulsion solvent evaporation technique was used.[23] The formulation was first attempted using polymer **3.2** at a concentration of 0.10 g/mL and homogenization speed of ~25,000 rpm. Yeagy *et al.* had used neutral pH water to remove residual PVA. An acidic medium retards polymer hydrolysis; therefore, acidic water (pH 1) was used to decrease potential polymer degradation when removing residual PVA.[17] Two methods were used to isolate the microspheres: 1) vacuum filtration and drying at room temperature overnight *in vacuo* and 2) centrifugation with freeze-drying overnight. Microspheres of 1-10 μm in diameter with minimal aggregation were obtained (data not shown), but an increased yield obtained using centrifugation (80 %) compared to vacuum filtration (60 %). To negate aggregation and increase microsphere size (surface area-to-volume ratio increases with decreasing particle size to increase degradation rates),[6, 25] the formulation method was further optimized by increasing polymer **3.2** concentration to 0.16 g/mL and decreasing homogenization speed to 10,000 rpm. This optimized method was also used to formulate polymer **3.1** microspheres.

3.3.3.   Microsphere size and morphology

When evaluating morphology, narrow size distribution and smooth surfaces are essential properties to ensure uniform microsphere degradation and uniform drug release. Also, aggregated microspheres could be detrimental to the injection process by not passing through the needle.[26]   With this optimized formulation, microspheres 2-34 μm in diameter were obtained in 80% yield without aggregation.   Microspheres comprised of polymer **3.1** and **3.2** demonstrated size distributions of 2-30 μm and 4-34 μm, respectively, as depicted in the representative SEM images (Figure 3.3 A-B).   The size distribution of microsphere diameters are demonstrated in Figure 3.4 exhibiting mean values of 11±7 μm and 19±7 μm for polymer **3.1** and **3.2**, respectively. Overall, these microspheres are larger in size as compared to previously published data (1-10 μm in diameter).[23] No signs of aggregation were noted and all microspheres displayed smooth surfaces, and are therefore viable candidates as drug delivery systems.
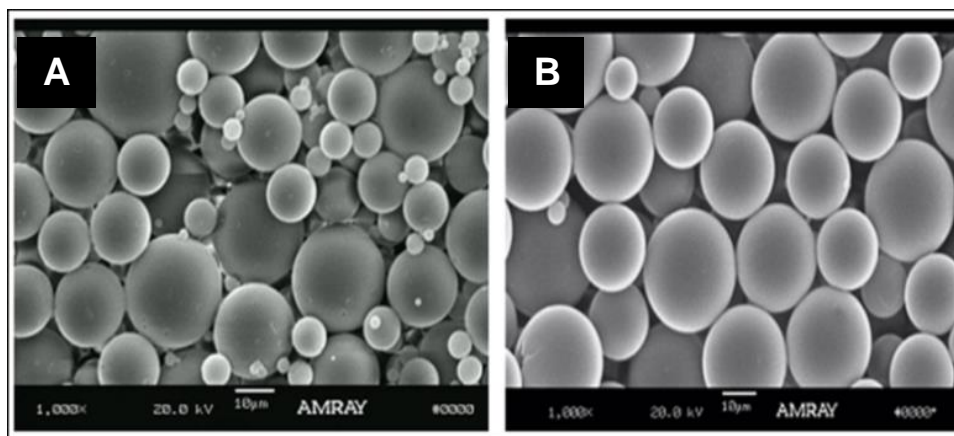
Figure 3.3. Representative scanning electron microscopy images of microspheres prepared from polymer **3.1** (A) and **3.2** (B).
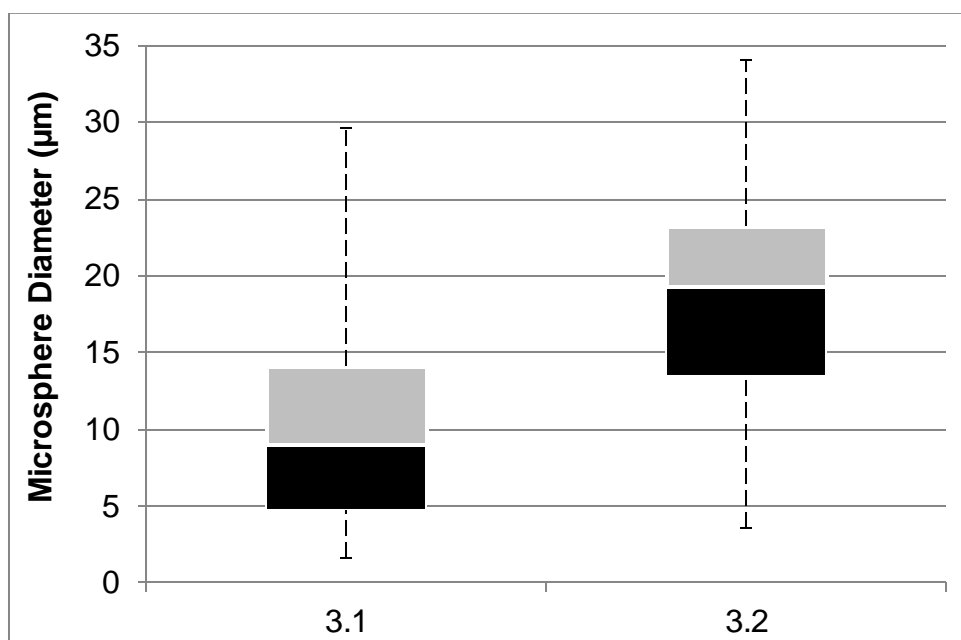
Figure 3.4. Box plots demonstrating the percentage of microsphere size for polymers **3.1-3.2** from representative SEM images using NIH ImageJ Software where top and bottom bars represent maximum and minimum values, respectively, black and grey potions represent the 25-50 % and 50-75 % portion of the sample set, respectively, and the white line represents the median value.

3.3.4. Molecular weight and thermal analyses

The M_w and T_g of the microspheres were determined and compared to the values obtained for the unprocessed polymers (Table 3.2). A consistent decrease in M_w and increase in PDI compared to the unprocessed polymer was observed for both microsphere samples. These changes were expected for these hydrolytically degradable polymers due to water exposure during formulation. Polymer **3.2** microspheres preserved a relatively high M_w (only decreasing 7 %) with a larger decrease observed for polymer **3.1** microspheres (40 %), which can be attributed to the more hydrophilic nature of the linker. The changes in T_g values increased slightly post formulation but not significantly. Both samples had T_g values above 37 ^{o}C, which ensure their integrity will remain *in vivo*.

Table 3.2. Physical and thermal properties of polymers **3.1** and **3.2** and respective microspheres including M_W, PDI, and T_g values.

	M_w (Da) Polymer	M_w (Da) Microspheres	PDI Polymer	PDI Microspheres	T_g (°C) Polymer	T_g (°C) Microspheres
3.1	12,000	7,200	1.2	1.9	68	70
3.2	18,000	16,800	1.3	1.9	50	51

3.3.5. *In vitro* salicylic acid release

To investigate the different time frames of complete salicylic acid release, polymer **3.1** was used to create faster-degrading microspheres that achieve release within days, polymer **3.2** was used as a reference point to compare microsphere properties against previously published data with an extended drug release profile (weeks).[23]   *In vitro* drug release from the microspheres was studied to determine the release profiles shown in Figure 3.5.   Microspheres prepared from polymers **3.1** and **3.2** released 100 % salicylic acid without the presence of a lag period (i.e., an initial time period where bioactive is not released).   Release rates for both polymer microspheres (26.5 and 5.1 percent SA released/day for **3.1** and **3.2**, respectively) correlate to the linkers used: the microspheres containing the relatively more hydrophilic polymer **3.1** (contact angle 50°) [24] released 100 % of the drug in a shorter period of time (3 days), followed by polymer **3.2** (21 days).
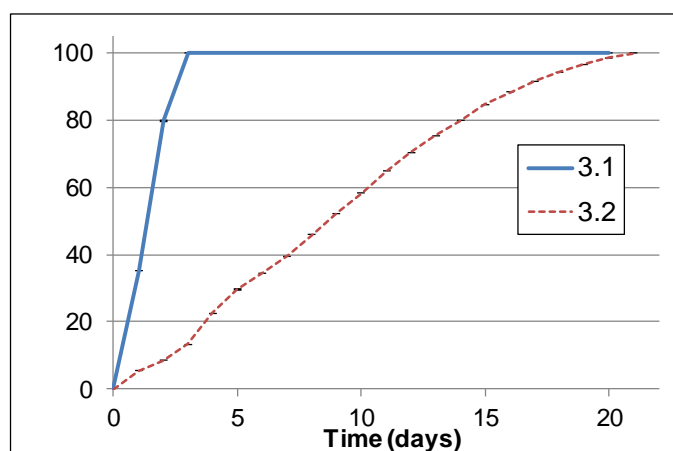
Figure 3.5. Normalized *in vitro* salicylic acid release from polymer microspheres (bioactive ± standard deviation) for polymer **3.1** and **3.2**

3.4.   Conclusion

Microspheres were prepared using two different salicylic acid-based polymers. The modified oil-in-water single emulsion solvent evaporation method was successfully used to obtain microspheres with size distributions ranging from 2-34 μm and smooth surfaces without aggregation. The T_g and M_w of the microspheres were studied and compared to the polymer prior to formulation where only minor changes in the T_g and decreases in M_w were observed. The release profiles showed salicylic acid release can be completed within days, a feature not yet attained from previous salicylic acid-based polymer microspheres, by changing the polymer chemical composition via the linker molecule. An additional benefit is that the microspheres may be carriers for additional bioactive molecules; skin care formulations often contain multiple bioactive molecules, and the ability to use a multi-drug delivery system may be desirable.

3.5.   References

1.   Rosario-Meléndez R, Ouimet MA, Uhrich KE, *Polym Bull* **2013**, *70*, 343-51.

2.   Ouimet MA, Snyder SS, Uhrich KE, *Abstr Pap Am Chem S* **2011**, *242*.

3.   Ouimet MA, Snyder SS, Uhrich KE, *J Bioact Compat Pol* **2012**, *27*, 540-9.

4.   Vasir JK, Tambwekar K, Garg S, *Int J Pharm* **2003**, *255*, 13-32.

5.   Freitas S, Merkle HP, Gander B, *J Controlled Release* **2005**, *102*, 313-32.

6.   Freiberg S, Zhu XX, *Int J Pharm* **2004**, *282*, 1-18.

7.   Edlund U, Albertsson A. Degradable Polymer Microspheres for Controlled Drug Delivery Degradable Aliphatic Polyesters. Springer Berlin / Heidelberg; 2002. pp. 67-112.

8.   Lee KY, Yuk SH, *Prog Polym Sci* **2007**, *32*, 669-97.

9.   Díez S, Tros de Ilarduya C, *Eur J Pharm Biopharm* **2006**, *63*, 188-97.

10. Baudonnet L, Grossiord JL, Rodriguez F, *Drug Dev Ind Pharm* **2004**, *30*, 975-84.

11. Dayan N, Basak K. A Delivery System for Salicylic Acid to Overcome the Drawbacks of its Use in Topically Applied Formulations. C&T Manufacture World Wide Magazine. 2003:114-8.

12. Dayan N, Basak K, editors. Epidermal Targeting: Controlled Topical Delivery of Salicylic Acid. HBA Product Development Presentations, , Session PD2; 2002; New York, NY.

13. Gupta S. Hydroxy Acids Delivery Systems. Skin delivery systems: transdermals, dermatologicals, and cosmetic actives. 1st ed. Ames, Iowa: Blackwell Pub.; 2006.

14. Gupta S, *HAPPI* **2003**, *January*, 49-59.

15. Kligman A, *J Geri Derm* **1997**, *5*, 128-31.

16. Rhein L, Chaudhuri B, Jivani N, Fares H, Davis A, *Int J Cosmet Sci* **2004**, *26*, 218-9.

17. Erdmann L, Uhrich KE, *Biomaterials* **2000**, *21*, 1941-6.

18. Prudencio A, Schmeltzer RC, Uhrich KE, *Macromolecules* **2005**, *38*, 6895-901.

19. Huang X, Brazel CS, *J Controlled Release* **2001**, *73*, 121-36.

20. Peppas NA, BrannonPeppas L, *J Controlled Release* **1996**, *40*, 245-50.

21. Abrahamse W, Steg L, Vlek C, Rothengatter T, *J Environ Psychol* **2007**, *27*, 265-76.

22. Wilkes CR, Mason AD, Hern SC, *Risk Anal* **2005**, *25*, 317-37.

23. Yeagy BA, Prudencio A, Schmeltzer RC, Uhrich KE, Cook TJ, *J Microencapsulation* **2006**, *23*, 643-53.

24. Carbone AL, Uhrich KE, *Macromol Rapid Commun* **2009**, *30*, 1021-6.

25. Ferrari M, Lee AP, Lee LJ, **2006**, *l*.

26.   Kawaguchi H, *Prog Polym Sci* **2000**, *25*, 1171-210.

CHAPTER 4:   POLY(VINYL PYRROLIDONE) AND SALICYLIC ACID-BASED POLY(ANHYDRIDE-ESTER) BLENDS AS HYDROGEL DRUG DELIVERY SYSTEMS

4.1.   Introduction

As outlined in the previous chapters, salicylic acid-based polymers fabricated into discs and microspheres have been the main focus.   A new formulation not yet investigated using such polymers includes hydrogels, which is addressed in this chapter.   Hydrogels are crosslinked networks comprised of polymers, such as poly(N-vinyl-2-pyrrolidone) (PVP) (Figure 4.1A), that imbibe large amounts of water without dissolving due to the presence of physical (e.g., intermolecular interactions and entanglements) or chemical crosslinks (e.g., covalent bonding).[1-5]   These systems are becoming increasingly important for a variety of biomedical applications[1, 6, 7] because they are biocompatible and have properties similar to natural living tissue given their high water content and pliable consistency.[2, 8]   Hydrogels are particularly suitable as wound-dressings due to their intrinsic softness, flexibility, adhesion to healthy skin without affecting the wound bed, low transition temperatures resulting from the continuous water evaporation, and their ability to prevent nerve ending exposure, thereby decreasing pain.[7, 9]

PVP is commonly used to prepare hydrogels due to its mechanical and water-absorption properties when chemically crosslinked.[5, 10]   One major drawback, however, is that PVP alone does not exhibit inherent bioactivity and

cannot reduce inflammation associated with wounds. The ability for wound therapies to address inflammation and its role in scarring pathogenesis would be advantageous; prolonged inflammation and proliferative phases of the wound healing process greatly increase the occurrence of hypertrophic and keloid scars.[11]

To combat inflammation-related issues associated with, researchers have investigated combined hydrogel therapies that utilize bioactives. One such example includes a topical therapy in which salicylic acid (SA), a non-steroidal anti-inflammatory drug, was combined with a hydrogel dressing and shown to be efficient in reducing hypertrophic scars.[12] Additionally, researchers have developed PVP/poly(vinyl alcohol) (PVA) membranes with added SA to mitigate systemic side effects.[13] Utilizing these PVP blends as controlled drug delivery systems is limited by the relatively rapid SA release where >50% SA was released within the first 4 hours, presumably due to high water content and large pore size.[1, 13] Ideally, the drug release profile could deliver a nearly instantaneous drug dose followed by sustained drug release to maintain drug concentrations at therapeutic levels.[14]

SA-based poly(anhydride-esters) (SAPAEs) are innovative degradable materials that have been evaluated over the past decade for SA delivery.[15-17] Compared to other biodegradable delivery systems, they are unique in that the bioactive molecules are chemically incorporated into the polymeric backbone via linker molecules (Figure 4.1B), rather than physically admixed,[18-20] leading to high drug loading (up to 85%).[16] Upon hydrolytic degradation, SA and

biocompatible linker molecules are released in a controlled, sustained manner[16] contributing to their utility as drug delivery systems. Despite SAPAEs' inherent bioactivity upon degradation and controlled SA release profiles, they can be brittle and lack the swelling properties necessary to form hydrogels. A combinatorial approach utilizing the bioactivity from SAPAE degradation products with hydrogel characteristics was therefore investigated.
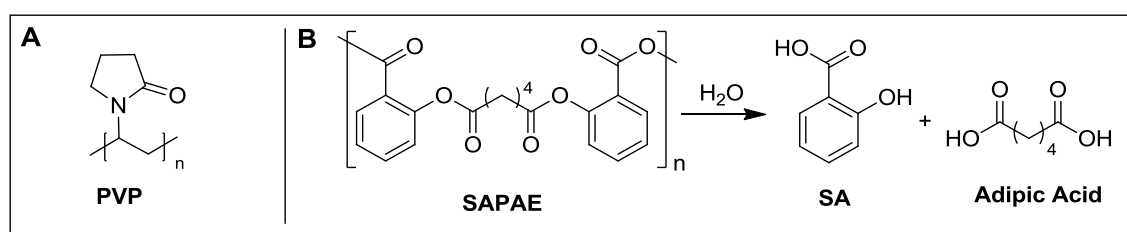
Figure 4.1. Structure of poly (vinyl pyrrolidone) (PVP) (A); structure of SAPAE blended with PVP and subsequent polymer degradation into SA and adipic acid (B).

In this chapter, PVP and SAPAE ratios were blended in various ratios to generate hydrogels with sustained SA delivery. SAPAE degradation controls drug release and enables high drug loading while PVP improves SAPAE mechanical properties by increasing plasticity and hydrophilicity. Once formed, characterization and degradation studies on the blends were carried out. Among many potential applications of these polymer blends, a smart wound-dressing for wound treatment and scar prevention is an appropriate application.

4.2. **Experimental**

4.2.1. **Materials**

Acetic anhydride and hydrochloric acid were purchased from Fisher (Fair Lawn, NJ). All other chemicals and reagents were purchased from Sigma-Aldrich (Milwaukee, WI) and used as received.

Table 4.1. Amounts of each polymer used for specified ratios and theoretical SA amount chemically incorporated within designated amount of SAPAE.

Ratio PVP:SAPAE	PVP Amount (g)	SAPAE Amount (g)	Theoretical SA Amount (g)
7:3	0.525	0.225	0.163
6:4	0.450	0.300	0.217
5:5	0.375	0.375	0.271

4.2.2. **Formulation of blended polymer films**

PVP solutions were stirred for 48 hours in anhydrous dimethylformamide/anhydrous chloroform (1:1 v/v) at room temperature. SAPAE of varying amounts (Table 4.1) were each added separately to the PVP solutions and stirred for 24 hours. These blends were prepared at 3 different ratios: 7:3, 6:4, and 5:5 PVP:SAPAE. The resulting solutions (15 % w/v total polymer, 1 mL) were cast onto Teflon plates (28 mm diameter) via syringe and dried in a vacuum oven to form films (n=3). Miscibility analyses were performed via scanning

electron microscopy (SEM) and differential scanning calorimetry (DSC). SEM images were obtained using an AMRAY-1830I microscope (AMRAY Inc.) after films were dried in a vacuum, stored under N_2, and coated with Au/Pd using a sputter coater (SCD 004, Blazers Union Limited). DSC measurements were carried out on TA Instrument Q200 to determine glass transition (T_g) temperatures of the blended films. Measurements on samples (4-6 mg) heated under nitrogen atmosphere from -10 °C to 200 °C at a heating rate of 10 °C/min and cooled to -10 °C at a rate of 10 °C/min with a two-cycle minimum were performed. TA Instruments Universal Analysis 2000 software, version 4.5A was used to analyze the data. Glass transition temperatures were calculated as half Cp extrapolated. The Fox equation (Equation 1) was used for this binary system to calculate the predicted T_g values for the blends where $T_{g,blend}$ pertains to the miscible blend, $T_{g,i}$ to the pure components, and w_i to the weight fraction of component i.

$$\frac{1}{T_{g,blend}} = \frac{w_{PVP}}{T_{g,PVP}} + \frac{w_{SAPAE}}{T_{g,SAPAE}} \qquad \text{Equation 1}$$

4.2.3. PVP:SAPAE film swelling values

The films (in triplicate for each ration) were immersed in deionized water for 2, 6, and 24 hours (separately) at room temperature. Swelling values (Q) were calculated according to Equation 2, where w_s and w_d represent the weight of swollen and dried films, respectively.

$$Q = \frac{W_s - W_d}{W_d} \qquad \text{Equation } 2$$

4.2.4.   Rheological testing and mechanical properties

The rheological testing studies were performed by Sameer Sathaye, Ph.D. candidate in Department of Materials Science and Engineering (University of Delaware, Newark, DE) supervised by Dr. Darrin Pochan

Differences in mechanical properties of the films were monitored using oscillatory rheology. Oscillatory time sweep experiments were carried out on the PVP:SAPAE films (7:3, 6:4, and 5:5 PVP:SAPAE). Each time sweep step was carried out for 9 hours. For each ratio, a film was soaked in deionized water for 2 hours prior to the measurements to swell the films. Then, the film was removed from the water and placed between the upper plate and the lower Peltier plate of a TA Instruments ARG2 stress controlled rheometer. A stainless steel serrated parallel plate geometry (20 mm) was chosen as the upper plate. Samples (20 mm diameter) were used. Water evaporation from the swollen hydrogel films was prevented by covering the sides of the plate with low viscosity mineral oil. After completion of the oscillatory time sweep step, oscillatory frequency sweep and oscillatory strain sweep steps were also carried out. The gap height used for the experiments was 400 μm. The time sweep measurements were carried out at a constant angular frequency of 6 rad/s and strain of 1 %. The frequency sweep measurements were carried out at a constant oscillatory strain of 1 % and

the strain sweep measurements were carried out a constant oscillatory frequency of 6 rad/s.

4.2.5.   *In vitro* salicylic acid release

To determine whether the chemically incorporated SA is advantageous over physically incorporated SA, an inactive control polymer (ICP), a SA-based poly(anhydride-ether), was used to prepare PVP:ICP blended films at 7:3, 6:4, and 5:5 ratios. These control polymers were similarly prepared to PVP:SAPAE films in that ICP replaces SAPAE in the formulation. Additionally, the theoretical SA amount for each ratio (see Table 4.1) was added with the appropriate amount of ICP to the solution 24 hours before casting. For the PVP:ICP ratios, 0.163, 0.217, 0.271 g of SA were added to the 7:3, 6:4, and 5:5 ratios, respectively.
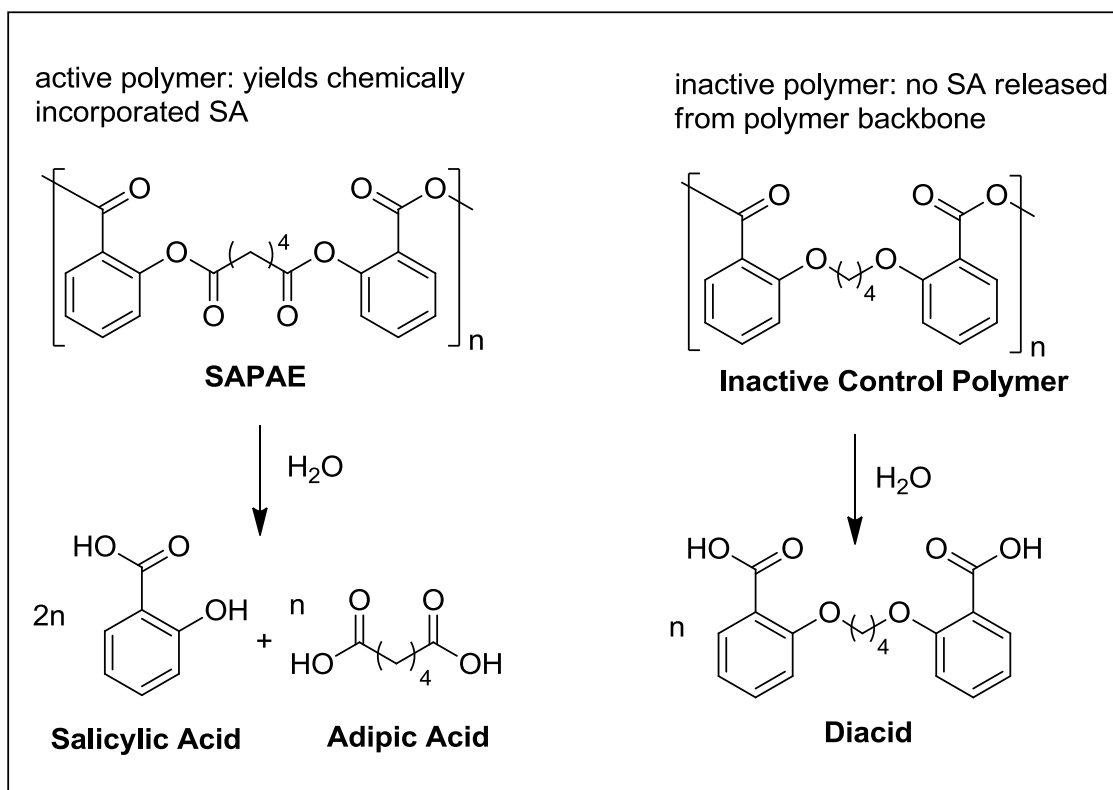
Figure 4.2. Degradation of active poly(anhydride-esters), referred to as SAPAEs, releases SA and adipic acid compared with degradation of inactive poly(anhydride-ether), referred to as inactive control polymer (ICP).

Films (80 ± 5 mg) were immersed in 20 mL glass scintillation vials containing 10 mL phosphate buffered saline (PBS) at pH 7.40. The vials were stored at 37 °C with agitation at 60 rpm in a controlled environment incubator shaker (New Brunswick Scientific Excella E25) to mimic physiological conditions. A 5 mL aliquot of the spent media was removed and replaced with 5 mL of fresh PBS every 24 hours. The spent media was analyzed by UV spectrophotometry using a Perkin Elmer Lambda XLS spectrophotometer to monitor SA release. Measurements were obtained at λ = 303 nm, the maximum SA absorbance that

did not overlap with PVP or other polymer degradation products. Data were calculated against a calibration curve from standard SA solutions in PBS. All sets of experiments were performed in triplicate, carried out until drug release was no longer detected, and normalized to 100 %.

4.2.6. TNF-α secretion assay

The TNF-alpha secretion assay was performed by Dr. Sabrina Snyder, Ph.D. graduate in Biomedical Engineering (Rutgers University, Piscataway, NJ) supervised by Dr. Kathryn Uhrich

Human blood-derived monocytes (Blood Center of New Jersey) were used to determine the efficacy to decrease inflammatory cytokine secretion. The cell isolation and purification protocol used was previously described by Kim et al. (2009).[21] Briefly, peripheral blood mononuclear cells were collected from blood of healthy donors by density gradient separation using ficol at a density of 1.077 (GE Healthcare, Piscataway, NJ). Red blood cells were lysed by incubation in Ammonium-Chloride-Potassium (ACK) lysing buffer for 5 min, washed with PBS and counted. Monocytes were cultured on 175 cm^2 flasks (BD, Franklin Lakes, NJ) at a concentration of $8x10^6$ cells/mL in RPMI-1640 media (GIBCO BRL, Rockville, MD). RPMI media was supplemented with 10 % fetal bovine serum (FBS) (GIBCO BRL), 100 units/mL penicillin (GIBCO BRL), 100 ug/mL streptomycin (GIBCO BRL) and 400 mM L-glutamine (GIBCO BRL). Monocytes were allowed to adhere for 2 hours and then washed 3 times with PBS to remove non-adherent cells. Monocytes were cultured for 7 days at 37 °C and 5 % CO_2 in

RPMI supplemented with 5 ng/mL granulocyte-macrophage colony-stimulating factor (GM-CSF) (R&D Systems, Minneapolis, MN) to generate macrophages. After 7 days of culture, macrophages were washed once with PBS and then detached with trypsin-EDTA (GIBCO) for 30 minutes at room temperature. Cells were re-suspended in culture medium (RPMI), counted, re-plated at 8 x 10^3 cells/well in a 96 well plate, and allowed to attach overnight. The following day, the media was replaced with the various sample groups: polymer-containing media (0.1 mg/mL polymer, 10 ng/mL lipopolysaccharide (LPS), 1% DMSO), a positive control (10 ng/mL LPS, 1% DMSO), and a negative control (no LPS, 1% DMSO). All cell studies were performed in triplicate. TNF-α secretion was achieved by activation of the macrophages with LPS (10 ng/mL). After 48 hours, media was collected and TNF- α secretion was determined with an ELISA kit against human TNF- α (BioLegend, San Diego, CA). A CellTiter 96®AQueous One Solution Cell Proliferation Assay (Promega, Madison, WI) was used to ensure that differences in cell viability did not account for differences in TNF-α secretion. A one-way ANOVA followed by Bonferroni's all-pairs comparison was used to determine significance ($p < 0.05$).

4.2.7. *In* vitro cytotoxicity and proliferation assay

The cytotoxicity studies were performed by Dr. Sabrina Snyder, Ph.D. graduate in Biomedical Engineering (Rutgers University, Piscataway, NJ) supervised by Dr. Kathryn Uhrich

Hydrogel cytocompatibility was performed by culturing NCTC clone 929 (strain L) mouse areolar fibroblast cells (ATCC, Manassas, Virginia) in media containing the dissolved polymer blends. These L929 fibroblast cells are a standard cell type for cytocompatibility testing as recommended by ASTM.[22] The polymer blends were dissolved in dimethyl sulfoxide (10 mg/mL; DMSO, Sigma, St. Louis, MO) as a stock solution and serially diluted with cell culture media to a 0.1 mg/mL concentration). Cell culture media consisted of Dulbecco's Modified Eagle's Medium (DMEM, Sigma-Aldrich, St. Louis, MO), 10 % v/v fetal bovine serum (Atlanta Biologicals, Lawrenceville, GA), 1 % L-glutamate (Sigma) and 1 % penicillin/streptomycin. The polymer-containing media was distributed into a 96-well plate and seeded at an initial concentration of 2,000 cells per well. The media with dissolved polymer was compared to DMSO-containing media (1 % v/v) and media alone. For the L929 fibroblasts, cell viability was determined by using a CellTiter 96®AQueous One Solution Cell Proliferation Assay (Promega, Madison, WI) at 24, 48, and 72 hours. After 2 hours incubation, the absorbance was recorded with a microplate reader at λ = 490 nm. Cell numbers were calculated based upon a standard curve created 24 hours after original seeding.

4.2.8. Hydrogel morphology

SEM was used to monitor hydrogel morphology. Films were swelled in deionized water for 24 h and then lyophilized prior to SEM analysis. Images were obtained using an AMRAY-1830I microscope (AMRAY Inc.) after coating the samples with Au/Pd using a sputter coater (SCD 004, Blazers Union Limited).

4.3.   Results and Discussion

These polymer blends exhibit hydrogel properties within a particular time window: the materials first swell, the SAPAEs begin to degrade, and the materials then dissociate and eventually fall apart and/or solubilize. This time window is advantageous (e.g., hours to days) for potential wound care applications.   Similar behavior is observed in other physical hydrogels (i.e., networks that swell until dissolution). While most recently published hydrogel work involves molecular design of specific covalent or physical crosslinks, the PVP-SAPAE hydrogels are simply prepared by blending in organic solvents.

4.3.1.   Formulation of PVP:SAPAE blended films

SAPAEs were blended with PVP and cast into films at ratios of 7:3, 6:4, and 5:5 PVP:SAPAE. Additional crosslinking methods (i.e., ultraviolet or gamma irradiation) were not necessary to generate hydrogels because the films became soft, stable, three-dimensional structures upon swelling, demonstrating that physical hydrogels were formed.   This structural stability decreased over time after water immersion; hydrolytic degradation of the SAPAEs yields completely dissociated films over 3 weeks at 25 °C and 6 days at elevated temperatures (37 °C). When attempting to blend PVP with the SA (diglycolic) polymer described in Chapter 3 (Polymer **3.1**), these hydrogels dissolved within hours under the same conditions.   The lack of solid residues and complete PVP solubilization for all blends also demonstrate its physical crosslinking character.
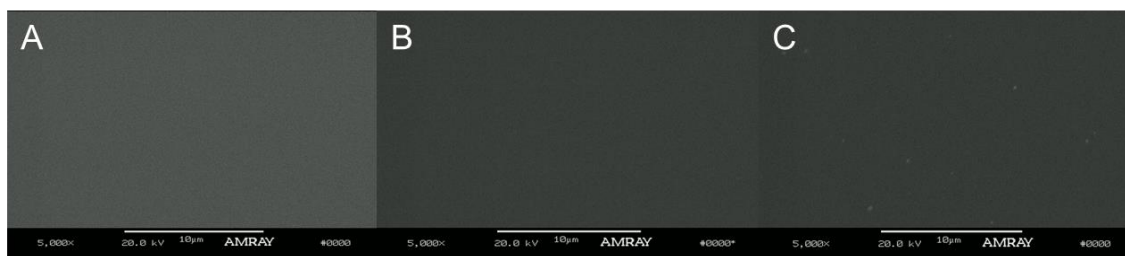
Figure 4.3. SEM image of blended PVP:SAPAE films prior to hydration at 5000x magnification with a homogenous morphology (no phase separation)

To elucidate the structure formed, the polymer miscibility was determined for the polymer blends. The surface morphology was homogenous; as shown in the SEM images (Figures 3A-C) of the non-hydrated films, all three blends exhibit uniform morphologies without phase separation or aggregation indicating blend miscibility. Correspondingly, the DSC results for pure polymers and blends are summarized in Figure 4.4 as "experimental". DSC analyses showed single, intermediary T_g values for the blends relative the pure polymer values. Figure 4.4 demonstrates the behavior of the measured T_g against PVP weight fraction and compares values predicted by Fox analytical equation for a binary system.[23] In short, the T_g increases with increasing PVP content; Fox's equation proves a relationship between the individual homopolymers and respective blends' T_g values. Accordingly, the measured T_g values are very close to the values predicted for a miscible polymer blend.
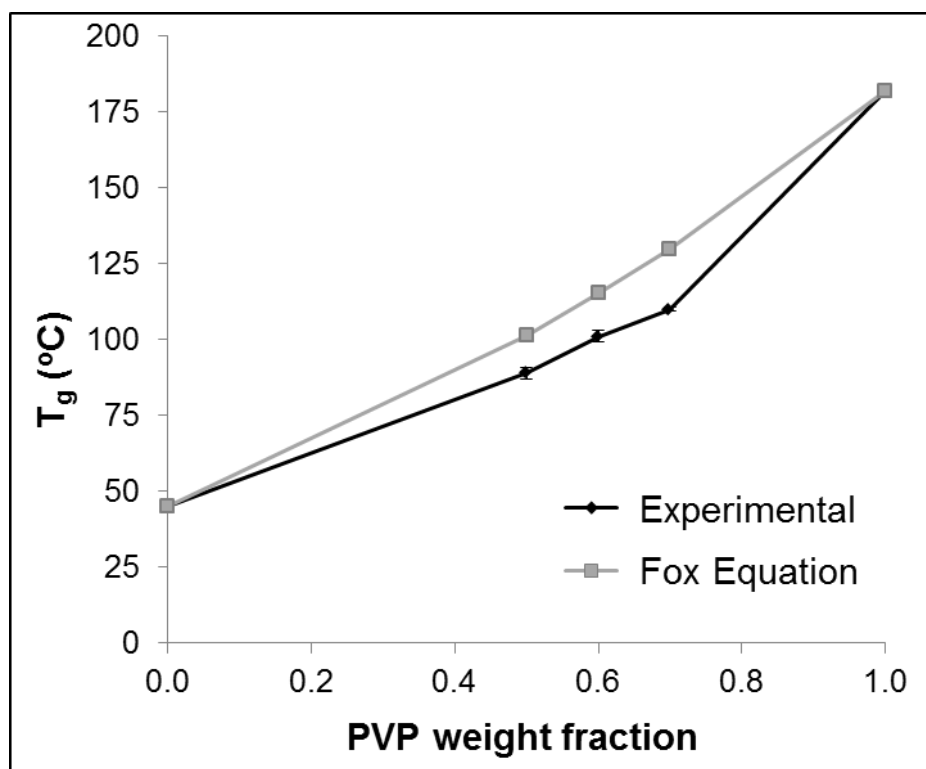
Figure 4.4. Experimental glass transition temperatures for pure PVP and SAPAE polymers and respective blends as a function of PVP weight fraction compared to values predicted by the Fox equation.

4.3.2.   Swelling values of PVP:SAPAE blended films

When comparing swelling values, the PVP concentration affected swelling: higher PVP content led to higher swelling values. This effect is likely due to the PVP hydrophilicity and its ability to attract water. The film thickness, before and after swelling, showed increased swelling with increased PVP content. PVP alone dissolves in an aqueous medium; in contrast, when blended with SAPAE, dissolution occurs at a much slower rate as SAPAE interacts with the PVP via physical interactions yielding a hydrogel.

To formulate a physically crosslinked network, entanglements and intermolecular interactions between PVP and SAPAE must take place. Fourier transform infrared spectroscopy analyses of the blends (not shown) indicated that dipole-dipole interactions were not responsible for the miscibility, as no clear signs of absorption band shifting were observed. Therefore, the hydrophobic interactions are likely responsible for the polymer miscibility. As such, the swelling values observed (compared to immediate dissolution) may result from the intermolecular interactions taking place between the hydrophobic portion of PVP and the hydrocarbon chains of the SAPAE linker.

Table 4.2. Swelling values (Q) for the PVP:SAPAE blends at various ratios according to Equation 1 (n=3).

PVP:SAPAE Ratio	PVP:SAPAE (Q after 2 hours)	PVP:SAPAE (Q after 6 hours)	PVP:SAPAE (Q after 24 hours)
7:3	7.7 ± 1.0	8.5 ± 0.5	11.1 ± 0.9
6:4	4.7 ± 0.3	5.3 ± 0.3	7.2 ± 0.8
5:5	3.6 ± 0.4	4.0 ± 0.6	4.9 ± 0.1

4.3.3. Hydrogel Morphology

SEM images (Figure 4.5) of the swollen lyophilized hydrogels show a macroporous structure with pore sizes ranging 1.3 – 12.9, 4.3 – 48.6, and 15.4 – 100 µm for 5:5, 6:4, and 7:3 ratios, respectively. Porous hydrogels are beneficial

for wound dressing and drug delivery applications as it allows for both gas exchange and drug diffusion. In the formation of hydrogels via free-radical polymerization, macroporosity is explained as a result of phase separation leading to heterogeneities, where voids of low polymer density become pores.[24] A similar argument can be used to explain the porosity seen in Figure 4.5, as hydrophobic interactions between PVP and SAPAE functions as hydrogel crosslinking. It is known that porosity is a function of crosslinking density[24] where the crosslinking density for the hydrogels described herein is a function of SAPAE concentration as this polymer is relatively more hydrophobic. The proposed nature for the observed physical cross-links is hydrophobic interactions between the two polymers; therefore, the higher the SAPAE concentration, the more hydrocarbon chains are available for interactions to occur. It is expected that porosity will decrease with increasing SAPAE, which is supported by the images presented in Figure 4.5.
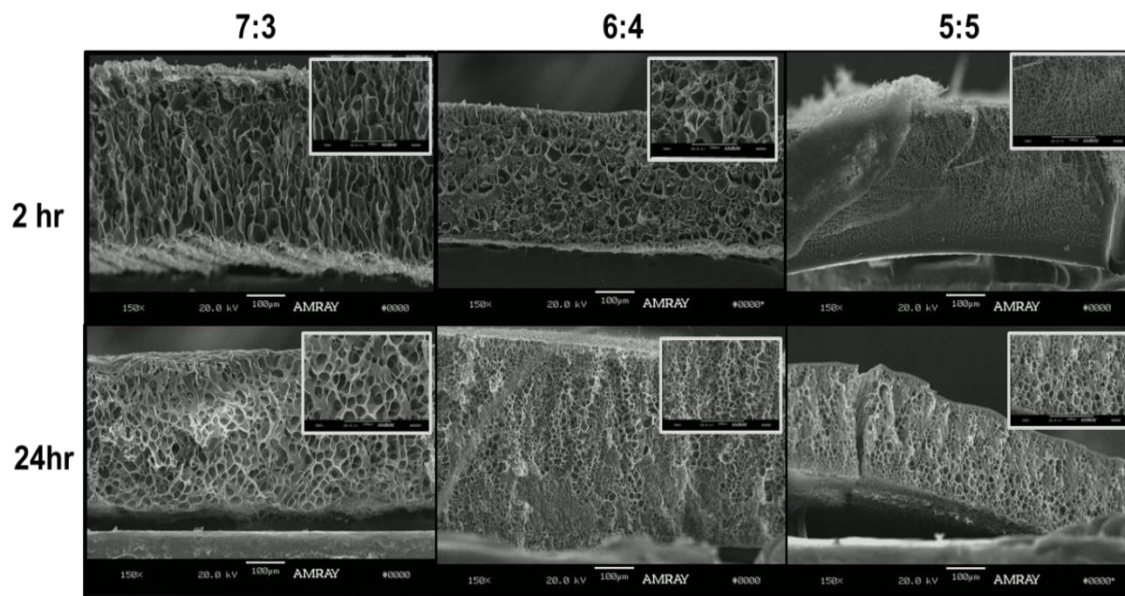
Figure 4.5. SEM image of PVP:SAPAE hydrogels at swelling time points 2 h and 24 h. Films are shown at 150x magnification with 500x inset.

4.3.4.   Rheological testing and mechanical properties

Results from the oscillatory rheological experiments show distinct differences in the mechanical properties of polymer films at the three different blends (PVP:SAPAE, 7:3, 6:4, and 5:5).   Stiffer hydrogel films displayed enhanced structural integrity, which is useful for applications such as drug delivery implants or patches as they are less susceptible to displacement or removal *in vivo*.
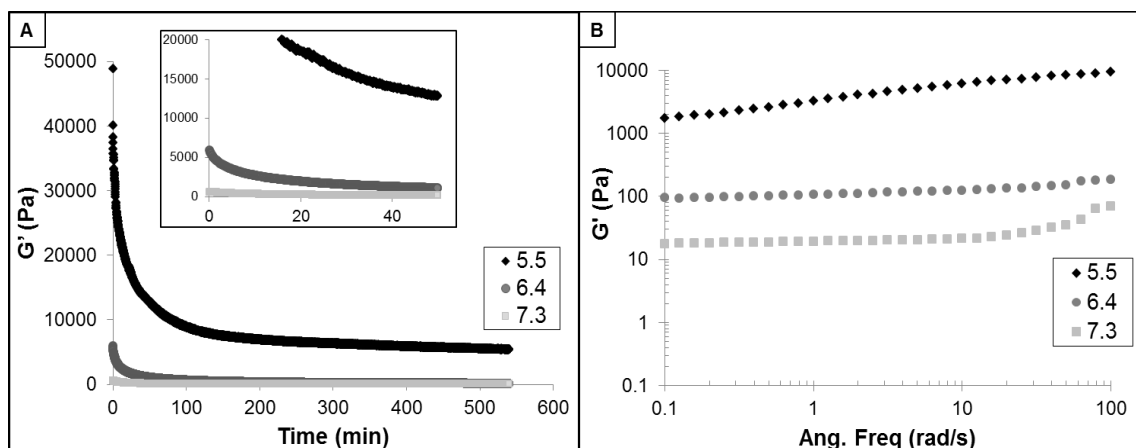
Figure 4.6. Time sweep measurements with 1 % strain and 6 rad/s angular frequency (A) and angular frequency strain sweep measurements at 1 % strain (B). Note the logarithmic scale for Figure 4.6B.

The time sweep measurements show a steady, uniform decline in the storage modulus, or G' (Pa), values. The G' (Pa) is an indicator of the elastic or solid nature of the hydrogel films. The water imbibed by the films during soaking for two hours influences elasticity. The initial values of G' (Pa) for 7:3, 6:4, and 5:5 PVP:SAPAE films are around 600 Pa, 6000 Pa, and 50,000 Pa, respectively. Thus, an order-of-magnitude stiffness increase is observed for decreasing PVP concentrations. This correlation is expected as PVP is hydrophilic, and a higher PVP concentration would yield more flexible films. SAPAE is susceptible to degradation by the entrapped water in the film and, thus, the steady uniform decline in the stiff or elastic nature of the films likely occurs via polymer degradation. At the end of the time sweep measurements, the frequency sweep measurements carried out on all three films indicate some dependence of G' on applied angular frequency. This data indicates that the gel-like nature of the films

reduces over time as the gels begin to lose their integrity at room temperature. The strain sweep measurements indicate the existence of a linear viscoelastic regime up to a certain value of oscillatory strain, after which the films fail. Thus, the initial and final values of G' are directly related to the PVP content in the films. This observation of mechanical properties correlates with the swelling ratio values i.e., higher PVP content provides a higher swelling ratio and less stiff, more flexible hydrogel films.

4.3.5. *In vitro* salicylic acid release

The polymer blends presented herein have the mechanical properties suitable for a wound dressing, but would also be beneficial as a drug delivery system if SA were released in a controlled manner. Therefore, the PVP:SAPAE blends' *in vitro* SA release rates were analyzed. The hydrogels exhibited 100 % SA release over 3-4 days (Figure 4.7). The correlation between the PVP content and SA released per day was observed; as PVP content increased, SA release rate increased. The release kinetics can be compared by the slope of release curve, where 7:3 > 6:4 > 5:5 (1.17, 0.94, 0.93 % SA release per hour, respectively). The 7:3 hydrogels reached 100 % SA release by day 3, whereas ratios 6:4 and 5:5 released 100 % SA by day 4. After these respective time frames, no residual hydrogels were visible in the vials and no SA was detected in the degradation media. This observation further verifies that physical gels were formed as no hydrogel pieces remained. The SA release curves correlate with the swelling values in Table 4.1; higher swelling values correspond to faster SA

release rates. Swelling values are a measure of water uptake by each film; therefore, higher swelling values correlate with higher wettability and higher water diffusion through the film. Moreover, SA release rates are expected to be dependent on water contact with hydrolytically labile anhydride and ester bonds in the SAPAEs.
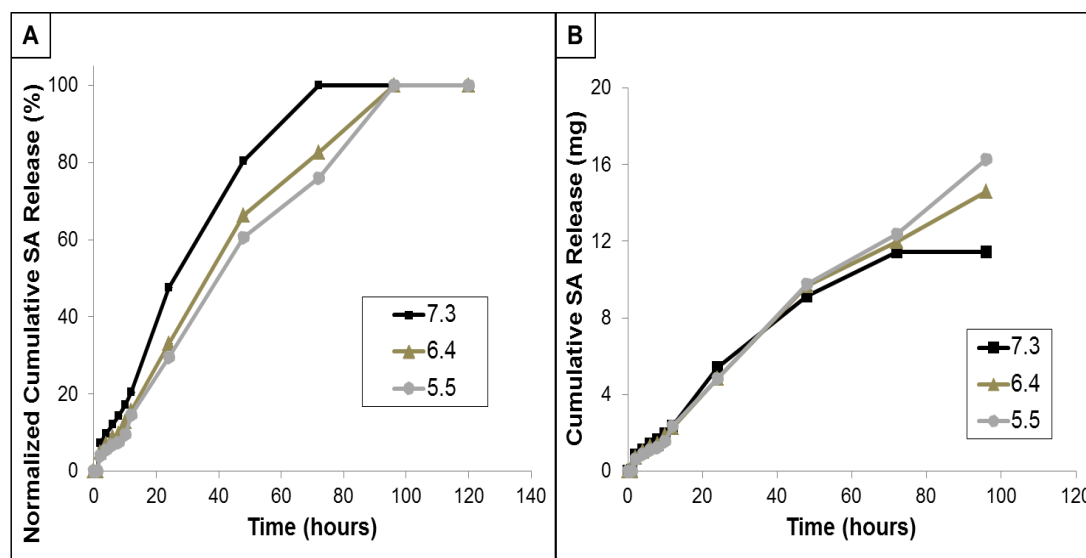
Figure 4.7. *In vitro* SA release from PVP:SAPAE hydrogels represented as normalized cumulative SA release as a percentage (A) and cumulative SA amount in mg (B). For each data point, three samples were measured and the averages graphed. The standard deviations were smaller than or equivalent to the data point symbols.

The PVP:ICP blends with free SA were used as a control to ascertain whether the chemical incorporation of SA into SAPAEs is advantageous over physical incorporation for sustained drug delivery. The ICP was necessary to

mimic the conditions for the active hydrogel formulation, but the UV spectra of other polymer degradation products do not overlap with free SA. As expected, the physically mixed SA was released within 3 hours (Figure 4.8), compared to 3-4 days for PVP:SAPAE samples. Bioactive release within 3 hours would not be advantageous for wound dressing applications as the dressings expected to be stable for longer time periods. The PVP:SAPAE release profiles can be further tuned by substituting SAPAE with ICP if needed.
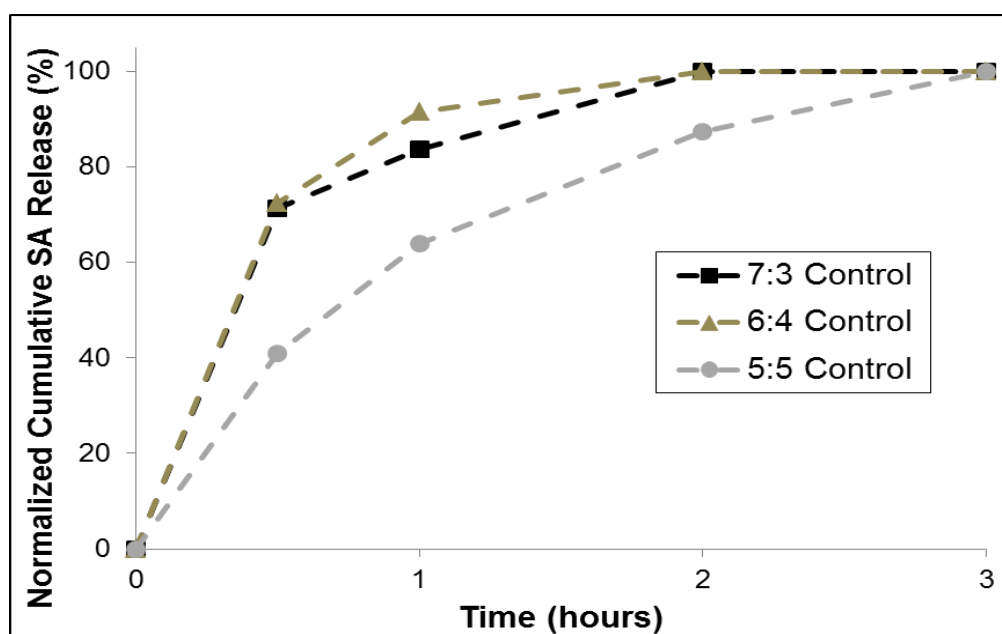
Figure 4.8. SA physically incorporated into PVP and inactive poly(anhydride-ether) blends (ICP) with physically admixed SA. For each data point, three samples were measured and the averages graphed. The standard deviations were smaller than or equivalent to the data point symbols.

4.3.6.   TNF-α secretion assay

Human blood-derived macrophages were activated by LPS to elicit the secretion of TNF-α. Dissolved hydrogels (0.1 mg/mL) were monitored for their effect on the amount of TNF-α secreted (Figure 4.9). The PVP sample increased the amount of TNF-α secreted when compared to the LPS control. This increase in inflammatory cytokines in the presence of high molecular weight PVP is consistent with previous literature.[25] The SAPAE hydrogels showed a reduction in TNF-α, compared to the PVP alone with the 5:5 and 6:4 ratios exhibiting a significant decrease in TNF-α secretion when compared to the LPS control. When correlated with drug loading, the SAPAE hydrogels inhibited TNF-α secretion in a dose-dependent manner, with greater amounts of SA resulting in lowered TNF-α. Cell viability was determined by MTS assay to ensure that differences in TNF-α secretion were not due to differences in cell number; no statistical differences were found in cell viability between the groups (data not shown).
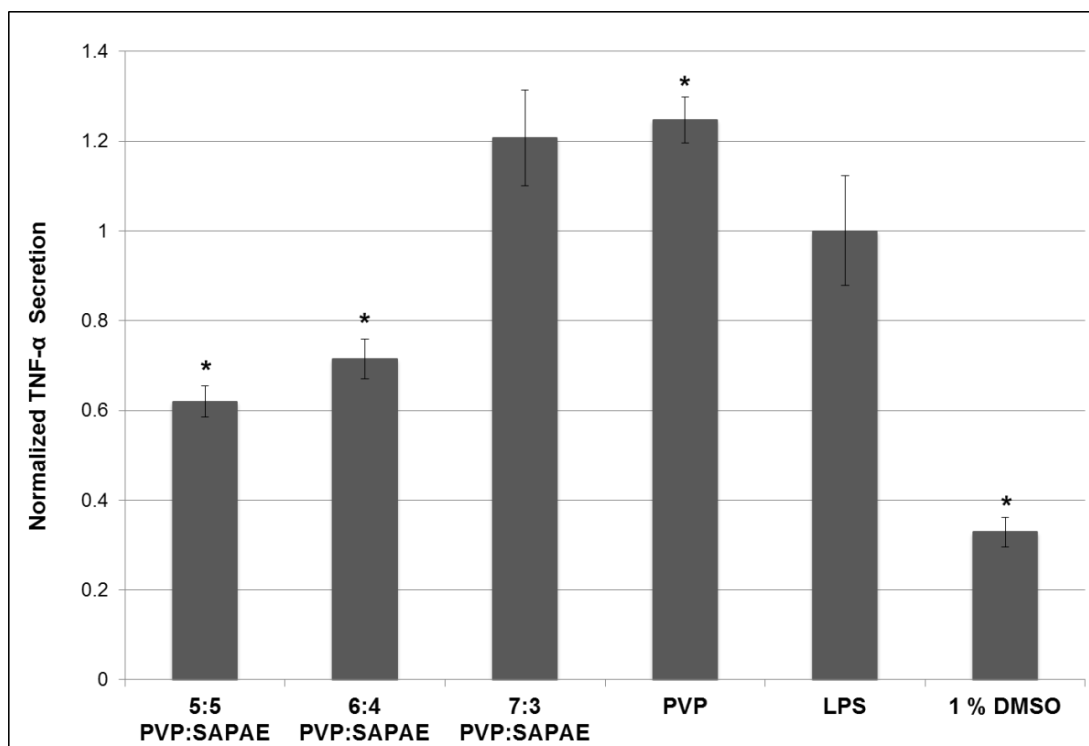
Figure 4.9. TNF-α secretion (normalized to the positive LPS control) from macrophages. The PVP group elicited significantly higher TNF-α than the LPS control, while the 5:5 and 6:4 PVP:SAPAE samples significantly decreased TNF-α secretion compared to the positive LPS. Significant difference denoted by asterisks.

4.3.7. *In vitro* cytotoxicity and proliferation assay

While the TNF-α studies indicated that the dissolved films were not toxic to macrophages at 48 hours, the effect on other relevant cell types needed to be studied. L929 fibroblasts were used to determine the PVP:SAPAE blends' effect on cytotoxicity and cell proliferation. The cells were cultured in the presence of dissolved polymers for three days. At 0.1 mg/mL, a concentration at which anti-inflammatory effects were observed, the hydrogels were not statistically different

from the DMSO controls (1%) in terms of both cell viability and proliferation (Figure 4.10). This study indicates that these polymer hydrogels would be effective as wound dressings without adversely affecting healing.
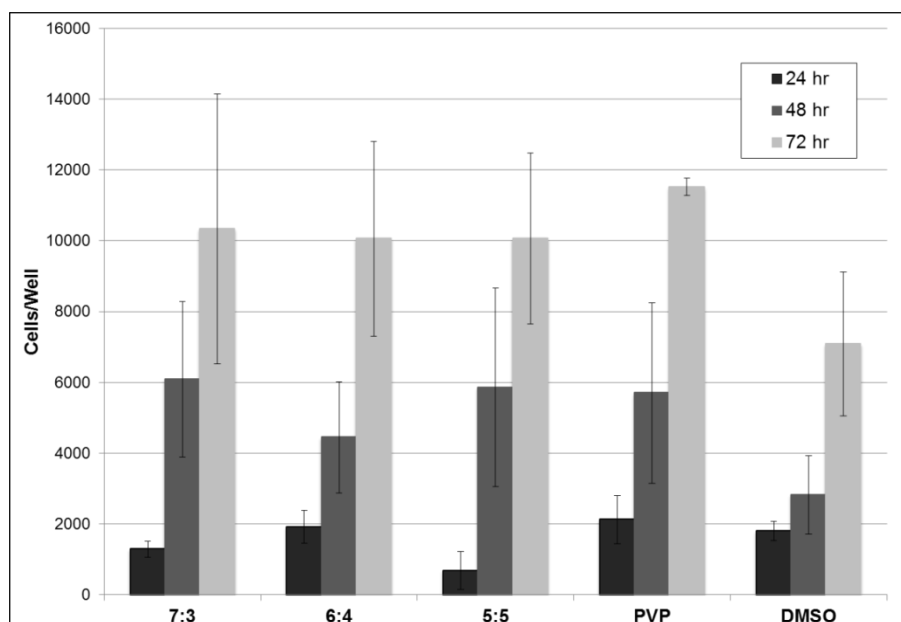
Figure 4.10. L929 cell viability at 24, 48, and 72 hours in the presence of dissolved hydrogels. The hydrogels did not exhibit cytotoxicity compared to the DMSO control.

4.4. Conclusion

A molecularly blended polymer material that exhibits hydrogel properties after swelling and that can be simply prepared by mixing can be advantageous. Formulation of SAPAEs with PVP resulted in miscible film blends that, upon hydration, became physically crosslinked hydrogels at room temperature. These experiments demonstrate that the hydrogels release SA, an anti-inflammatory

and analgesic agent, in a controlled manner over a sustained time period. This blending and subsequent hydration of PVP and SAPAE provides a biocompatible drug delivery system with good handling and swelling capabilities, porosity, and sustained drug release without a burst release, providing a foundation for these blends as promising wound dressings.

4.5. References

1. Hoare TR, Kohane DS, *Polymer* **2008**, *49*, 1993-2007.

2. Devine D, Higginbotham C, *Euro Polym J* **2005**, *41*, 1272-9.

3. Hamidi M, Azadi A, Rafiei P, *Adv Drug Deliv Rev* **2008**, *60*, 1638-49.

4. Peppas NA, Huang Y, Torres-Lugo M, Ward JH, Zhang J, *Annu Rev Biomed Eng* **2000**, *2*, 9-29.

5. Lopérgolo LC, Lugão AB, Catalani LH, *Polymer* **2003**, *44*, 6217-22.

6. Lin C, Metters A, *Adv Drug Deliv Rev* **2006**, *58*, 1379-408.

7. Boateng JS, Matthews KH, Stevens HNE, Eccleston GM, *J Pharm Sci* **2008**, *97*, 2892-923.

8. Shivakumar HG, Satish CS, Satish KP, *Indian Journal of Pharmaceutical Sciences* **2006**, *68*, 133.

9. Rosiak Janusz M. Hydrogel Dressings. Radiation Effects on Polymers: American Chemical Society; 1991. pp. 271-99.

10. Barros JAG, Fechine GJM, Alcantara MR, Catalani LH, *Polymer* **2006**, *47*, 8414-9.

11. Roseborough IE, Grevious MA, Lee RC, *J Natl Med Assoc* **2004**, *96*, 108-16.

12. Danielson JR, Walter RJ, *J Burns Wounds* **2005**, *4*, e6.

13. Şanlı O, Orhan E, Asman G, *J Appl Polym Sci* **2006**, *102*, 1244-53.

14. Costache MC, Qu H, Ducheyne P, Devore DI, *Biomaterials* **2010**, *31*, 6336-43.

15. Schmeltzer RC, Johnson M, Griffin J, Uhrich K, *J Biomater Sci Polym Ed* **2008**, *19*, 1295-306.

16. Prudencio A, Schmeltzer RC, Uhrich KE, *Macromolecules* **2005**, *38*, 6895-901.

17. Carbone AL, Uhrich KE, *Macromol Rapid Commun* **2009**, *30*, 1021-6.

18. de la Torre P, Enobakhare Y, Torrado G, Torrado S, *Biomaterials* **2003**, *24*, 1499-506.

19. Catauro M, Raucci MG, de Marco D, Ambrosio L, *J Biomed Mater Res* **2006**, *77A*, 340-50.

20. Fontana G, Pitarresi G, Tomarchio V, Carlisi B, San Biagio PL, *Biomaterials* **1998**, *19*, 1009-17.

21. Kim J, Hematti P, *Exp Hematol* **2009**, *37*, 1445-53.

22. Duncan E, Lemons J, Mayesh J, Saha P, Saha S, Scranton M. In New products and standards in biomaterials science. New York: Elsevier Academic Press; 2004.

23. Brostow W, Chiu R, Kalogeras IM, Vassilikou-Dova A, *Mater Lett* **2008**, *62*, 3152-5.

24. Okay O, *Prog Polym Sci* **2000**, *25*, 711-79.

25. Zimecki M, Webb DR, Rogers TJ, *Arch Immunol Ther Exp (Warsz)* **1980**, *28*, 179-97.

CHAPTER 5:   BIODEGRADABLE COUMARIC ACID-BASED

POLY(ANHYDRIDE-ESTER) SYNTHESIS AND

SUBSEQUENT CONTROLLED RELEASE

Reprinted with edits as this manuscript was recently accepted: Ouimet MA, Stebbins, N, and Uhrich KE to Macromolecular Rapid Communications (2013).

5.1.   Introduction

The bioactive chemically incorporated into a polymer backbone described thus far includes salicylic acid, a non-steroidal anti-inflammatory drug. Another class of bioactives that may be beneficial for controlled release applications include hydroxycinnamic acids, which are phenolic compounds with anti-inflammatory and antioxidant properties.   Once such example includes *p*-coumaric acid (pCA, Figure 5.1), which a naturally occurring hydroxycinnamic acid derivative found in grains, teas, and fruits that exhibits many beneficial properties.[1, 2]

It is well-known that pCA displays antioxidant, anti-thrombotic, and antimicrobial properties highlight its potential for many applications.[3-5] Notably, pCA has demonstrated both anti-inflammatory and antioxidant activities in the gastrointestinal system.[6, 7]   Research has demonstrated that pCA can reduce oxidative DNA damage and cyclooxygenase-2 (COX 2) overexpression in colonic mucosa of rats and thus has potential for use in treatment of colitis and other related inflammatory conditions.[6]   However, pCA use is currently limited due to its short half-life *in vivo,* necessitating frequent dosing to maintain therapeutically relevant concentrations.[8]

p-coumaric acid (pCA), **5.1**
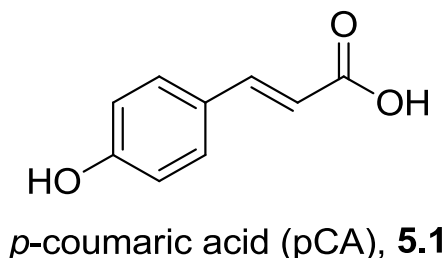
Figure 5.1. Structural representation of pCA (**5.1**)

To control pCA release, researchers have incorporated the bioactive into various matrices. For example, pCA has been physically incorporated into a zinc basic salt hybrid material to achieve pCA release via diffusion, but this system exhibited a burst release and yielded low pCA concentrations.[9] Additionally, pCA homopolymers[10, 11] and copolymers[12-16] have been prepared, but either their delivery wasn't studied or their properties were not ideal (i.e., required enzymatic degradation and exhibited low T_g values, limiting *in vivo* use as the deformation would alter the drug release profile). Therefore, a polymer with a T_g value greater than physiological temperature that releases pCA in a controlled manner over time is desired.

One such method to improve bioactive delivery is through incorporation into a biodegradable polyanhydride backbone, as polyanhydrides undergo surface erosion,[17] unlike the bulk erosion exhibited by polyesters,[18] thus enabling controlled pCA release. This methodology has been demonstrated for salicylic acid by coupling an acyl chloride to the bioactive using pyridine as base and catalyst.[19] This synthetic method was used and multiple purification methods attempted. Additional protection methods were utilized, including a Knoevenagel

condensation, to allow for sole reaction of the phenolic group instead of the carboxylate group.

In this chapter, a biodegradable poly(anhydride-ester) containing pCA in the backbone was synthesized via solution polymerization and characterized using proton and carbon nuclear magnetic resonance (^{1}H and ^{13}C NMR) and Fourier transform infrared (FTIR) spectroscopies. Differential scanning calorimetry (DSC) and thermogravimetric analysis (TGA) were used to determine thermal properties. Gel permeation chromatography (GPC) and mass spectrometry (MS) were used to determine weight-averaged molecular weight (M_w) of polymer and molecular weight of all polymer precursors, respectively. In addition, *in vitro* release studies were performed to study the release of pCA via the hydrolytic degradation of the polymer.

5.2. Experimental

5.2.1. Materials

Silica gel and fetal bovine serum were purchased from VWR (Radnor, PA) and Atlanta Biologicals (Lawrenceville, GA), respectively. Hydrochloric acid (HCl, 1 N), concentrated HCl, poly(vinylidine fluoride) and poly(tetrafluoroethylene) syringe filters, Wheaton glass scintillation vials, and 96-well plates were purchased from Fisher Scientific (Fair Lawn, NJ). All other reagents, solvents, and fine chemicals were purchased from Aldrich (Milwaukee, WI) and used as received.

5.2.2. ^{1}H and ^{13}C NMR and FTIR spectroscopies

^{1}H and ^{13}C NMR spectra were recorded on a Varian 400 MHz or 500 MHz spectrometer using deuterated dimethyl sulfoxide (DMSO-d_6) as solvent and internal reference.   FTIR spectra were obtained using a Thermo Nicolet/Avatar 360 spectrometer, samples (1 wt %) ground and pressed with KBr into a disc. Each spectrum was an average of 32 scans.

5.2.3.   Molecular weight

Polymer precursors were analyzed via MS to determine molecular weights.   A Finnigan LCQ-DUO equipped with Xcalibur software and an adjustable atmospheric pressure ionization electrospray ion source (API-ESI Ion Source) was used with a pressure of 0.8 x 10-5 and 150 °C API temperature. Samples dissolved in methanol (< 10 µg/mL) were injected with a glass syringe. GPC was used to determine polymer weight-averaged molecular weight and polydispersity using a Perkin-Elmer liquid chromatography system consisting of a Series 200 refractive index detector, a Series 200 LC pump, and an ISS 200 autosampler.   Sample automation and data processing were performed using a Dell OptiPlex GX110 computer running Perkin-Elmer TurboChrom 4 software with a Perkin-Elmer Nelson 900 Series Interface and 600 Series Link.   Polymer samples were prepared for autoinjection by dissolving in dichloromethane (DCM, 10 mg/mL) and filtering through 0.45 µm poly(tetrafluoroethylene) syringe filters. Samples were resolved on a Jordi divinylbenzene mixed-bed GPC column (7.8 x 300 mm, Alltech Associates, Deerfield, IL) at 25 °C, with DCM as the mobile

phase at a 1.0 mL/min flow rate. Molecular weights were calibrated relative to broad polystyrene standards (Polymer Source Inc., Dorval, Canada).

5.2.4. Thermal analyses

DSC measurements were carried out on a TA Instrument Q200 to determine melting (T_m) and glass transition (T_g) temperatures. Measurements on samples (4-6 mg) heated under nitrogen atmosphere from –10 °C to 200 °C at a heating rate of 10 °C/min and cooled to –10 °C at a rate of 10 °C/min with a two-cycle minimum were performed. TA Instruments Universal Analysis 2000 software, version 4.5A, was used to analyze the data. Glass transition temperatures were calculated as half Cp extrapolated. TGA was utilized for determining decomposition temperatures (T_d) using a Perkin-Elmer Pyris 1 system with TAC 7/DX instrument controller and Perkin-Elmer Pyris software for data collection. Samples (5-10 mg) were heated under nitrogen atmosphere from 25 °C to 400 °C at a heating rate of 10 °C/min. Decomposition temperatures were measured at the onset of thermal decomposition.

5.2.5. Previous methodology used for pCA diacid synthesis

Previous synthetic methods to prepare diacid by coupling two bioactive equivalents to one linker using pyridine was attempted as outlined in Figure 5.2.[19, 20] Pyridine (4.4 eq) was added to pCA (2 eq) dissolved in THF to which the acyl chloride linker dissolved in minimal THF was added dropwise via syringe pump at 20 mL/h. The reaction was monitored over 24 h and reaction progress

monitored via TLC. At times the reaction would go to completion; during other attempts, the reaction would not progress showing significant starting material present. At these attempts, an additional acyl chloride equivalent was added. Once complete, the reaction mixture was quenched over 20-fold DI water and acidified with concentrated HCl to pH ~2. Contents were isolated via vacuum filtration and residue washed with additional water to remove residual THF. The residue was immediately dissolved (partially) in acetone and precipitated over hexanes. The contents were isolated via vacuum filtration and dried in a desiccator at room temperature *in vacuo*. As an alternative, this reaction was repeated neat in pyridine following the same steps outlined above. Other attempts included utilizing different bases (e.g., triethylamine), covering the reaction mixture with aluminum foil to shield it from light, and attempting the reaction (using each method described here) at various temperatures (-76 °C, 0 °C, and room temperature).
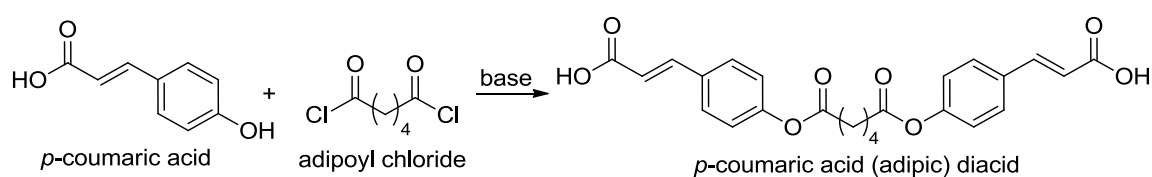
Figure 5.2. Initial synthetic method utilized to prepare pCA polymer precursor

5.2.6.   pCA protection group methods: Methyl esters
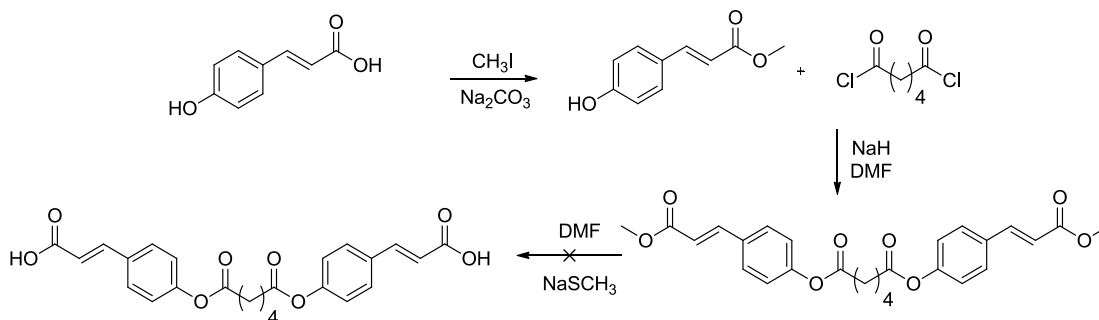
Figure 5.3. Synthesis of pCA-based polymer precursors utilizing a methyl ester protection.

Methyl esters (Figure 5.3) were prepared by dissolving pCA (1 eq) in anhydrous DMF to which Na_2CO_3 (1.2 eq) was added. CH_3I (1.5 eq) was added and the reaction stirred for 2 hours. After monitoring the reaction via TLC indicating completion, solvent was removed *in vacuo* via rotary evaporation. The crude product was diluted in ethyl acetate, washed with DI water, and then washed with an aqueous solution of $NaHCO_3$ (100 mL x 2). The organic layer was dried over $MgSO_4$, filtered, and dried *in vacuo*.

This product (2 eq) was then dissolved in anhydrous DMF. NaH (2.2 eq) was slowly added and the reaction mixture cooled in an ice bath. Adipoyl chloride (1 eq), dissolved in anhydrous DMF was added dropwise via syringe pump. After stirring for 24 hours, the reaction was monitored by TLC, and worked up after completion. Solvent was removed *in vacuo* via rotary evaporation to yield crude product. This product was purified on silica gel via flash chromatography using 4:1 hexane:ethyl acetate as eluent.

The dimethyl ester deprotection was attempted using 90% sodium methane thiolate (NaSCH$_3$). Briefly, the dimethylester pCA intermediate (1 eq) was stirred in anhydrous DMF and NaSCH$_3$ (2.2 eq) was then added. Reaction progress was monitored via TLC. Once starting material was no longer present, the reaction was dried *in vacuo* and subsequently diluted in ethyl acetate and washed with 1 N HCl. The organic layer was collected and dried over MgSO$_4$ for 2 h. The mixture is vacuum filtered and dried via rotary evaporation and analyzed via ^{1}H NMR spectroscopy.

5.2.7. pCA protection group methods: Benzyl esters
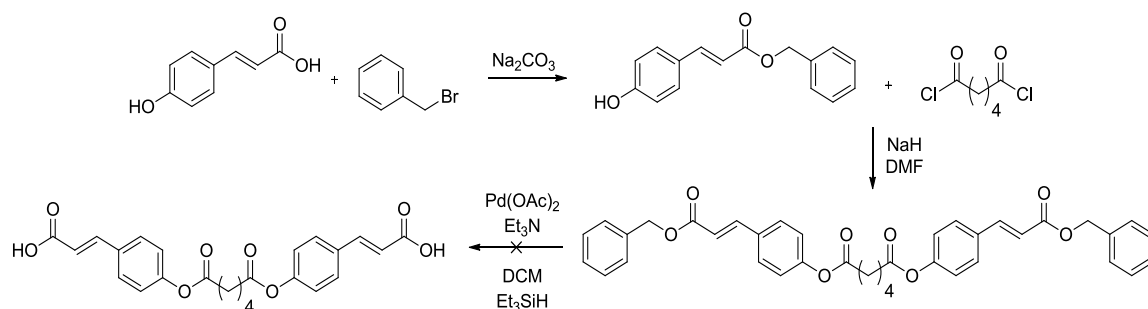
Figure 5.4. Synthesis of pCA-based polymer precursors utilizing a benzyl ester protection

Benzyl esters (Figure 5.4) were prepared by dissolving pCA (1 eq) in anhydrous DMF to which Na$_2$CO$_3$ (2.4 eq) was added. Benzyl bromide (3.5 eq) was added and the reaction stirred for 24 hours at 40 °C. After monitoring the reaction via TLC indicating completion, solvent was removed *in vacuo* via rotary evaporation. The crude product was diluted in ethyl acetate, washed with DI

water, and then with an aqueous solution of $NaHCO_3$ (100 mL x 2). The organic layer was dried over $MgSO_4$, filtered, and dried *in vacuo*. Hexane was added to remove unreacted benzyl bromide and product (residue portion) was isolated via vacuum filtration. Adipoyl chloride (1 eq), dissolved in anhydrous DMF was added dropwise via syringe pump. After stirring for 24 hours, the reaction was monitored by TLC, and worked up after completion. Solvent was removed *in vacuo* via rotary evaporation to yield crude product. This product was purified on silica gel via flash chromatography using 4:1 hexane:ethyl acetate as eluent.

Benzyl ester deprotection was attempted using a mild hydrogenation reaction adapted from Lamiday et al.[21] Briefly, palladium (II) acetate ($Pd(OAc)_2$) (2.5 eq) was added to a pre-dried three-neck round bottom and maintained under argon. To this mixture, triethylamine (2.5 eq) in anhydrous DCM were added. Dibenzyl pCA intermediate (1 eq) in anhydrous DCM was added dropwise. Triethylsilane (Et_3SiH) was then added dropwise. Reaction progress was monitored via TLC. Once all starting material was consumed, methanol was added and reaction filtered over celite in a glass fritted funnel twice. The filtrate was collected, dried *in vacuo*, diluted in ethyl acetate, and washed with 1 N HCl. The organic layer was collected and dried over $MgSO_4$ for 2 h. The mixture is vacuum filtered and filtrate dried via rotary evaporation. Samples were analyzed via ^1H NMR spectroscopy.
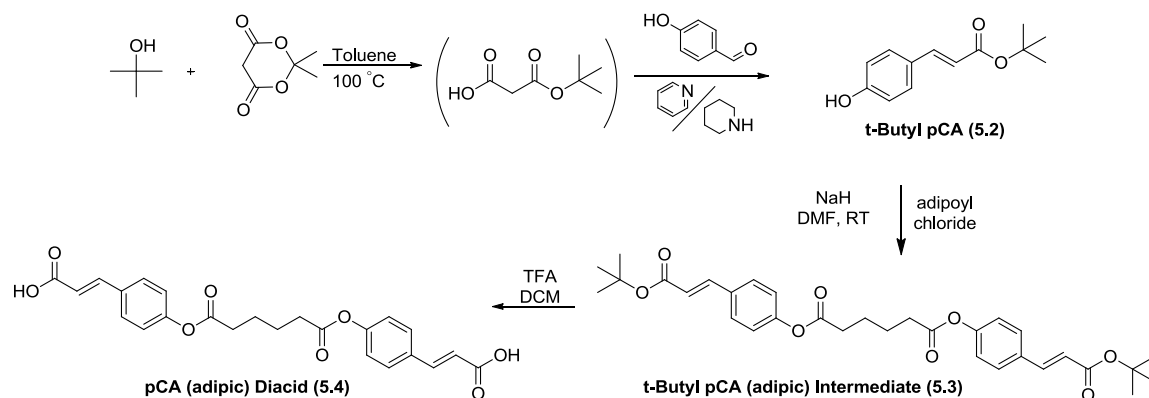
Figure 5.5. Synthesis of coumaric acid-based polymer precursors including *t*-butyl coumaric acid (**5.2**), *t*-butyl coumaric acid (adipic) intermediate (**5.3**), and coumaric acid (adipic) diacid (**5.4**).

5.2.8.   pCA protection group methods: t-Butyl esters

5.2.8.1.   *t*-Butyl pCA

To prepare **5.2** (Figure 5.5), a procedure adapted from Hu. et al.[22] was used where Meldrum's acid (2.5 eq) was dissolved in toluene (50 mL), tertiary butanol (2.5 eq) was added, and the reaction was heated to 100 °C with stirring for 5 h. Without separation, the reaction was cooled to room temperature where vanillin was added followed by pyridine (2.5 mL) and piperidine (0.25 mL), and then heated to 75 °C with stirring for 24 h. The reaction mixture was dried *in vacuo*, and the residue obtained was diluted in diethyl ether, washed with saturated aqueous sodium bicarbonate (2 x 200 mL), 1N HCl (2 x 200 mL), and distilled water (1 x 200 mL). The organic layer was then dried overnight over MgSO$_4$, filtered, and the solvent removed *in vacuo* to yield crude product. This

was purified on silica gel via flash chromatography using 4:1 hexane:ethyl acetate as eluent. Yield: 86 % (white crystals). ^{1}H-NMR (400 MHz, CDCl$_3$): δ 7.54 (d, 1H, *J*=16.0 Hz, R-CH=CH-R), 7.37 (d, 2H, Ar-H), 6.61 (s, 1H, OH), 6.87 (d, 2H, Ar-H), 6.21 (d, 1H, *J*=16.0 Hz, R-CH=CH-R), 1.55 (s, 9H, 3CH$_3$). ^{13}C-NMR (CDCl$_3$): δ 167.8, 158.3, 144.1, 130.1, 127.3, 117.4, 116.1, 81.1, 28.5. IR (KBr, cm^{-1}): 3270 (OH, Ph), 1674 (C=O, ester), 1630 and 1600 (C=C). T$_m$: 98-101 ⁰C.

5.2.8.2.   *t*-Butyl pCA (adipic) intermediate

t-Butyl coumaric acid (**5.2**) (2 eq) was dissolved in anhydrous dimethylformamide (DMF), to which sodium hydride (NaH, 2.2 eq) was slowly added. After 30 min, adipoyl chloride (1 eq) dissolved in DMF (10 mL) was added dropwise at 20 mL/h. Reaction progress was monitored by thin layer chromatography (4:1 hexane:ethyl acetate as eluent). Once completed, the reaction mixture was diluted with ethyl acetate (250 mL) and washed with deionized water (2 x 100 mL). The organic layer was collected, dried over MgSO$_4$, and the solvents removed *in vacuo*. The product was purified on silica gel via flash chromatography using 4:1 hexane:ethyl acetate as eluent. Yield: 70 % (white powder). ^{1}H-NMR (400 MHz, CDCl$_3$): δ 7.58 (d, 2H, *J*=16.0 Hz, R-CH=CH-R), 7.51 (d, 4H, Ar-H), 7.11 (d, 4H, Ar-H), 6.32 (d, 2H, *J*=16.0 Hz, R-CH=CH-R), 2.66 (m, 4H, CH$_2$), 1.89 (m, 4H, CH$_2$), 1.53 (s, 18H, 3CH$_3$). ^{13}C-NMR (CDCl$_3$): δ 171.6, 166.4, 152.0, 142.6, 132.7, 129.3, 122.2, 120.6, 80.8, 34.2,

28.4, 24.4. IR (KBr, cm^{-1}): 1750 (C=O, ester), 1700 (C=O, ester), 1640 and 1600 (C=C). T_m: 150-153 °C.

5.2.8.3.   pCA (adipic) diacid

Compound **5.3** (1 eq) was dissolved in anhydrous DCM to which trifluoroacetic acid (TFA) (40 eq) was added and stirred overnight. Solvent was removed *in vacuo,* and the residue was triturated with DI water (300 mL), isolated via vacuum filtration, and dried *in vacuo* for 24 h. Yield: 99 % (white powder). ^{1}H-NMR (500 MHz, DMSO-d_6): δ 12.49 (s, 2H, COOH), 7.82 (d, 4H, Ar-H), 7.67 (d, 2H, *J*=16.0 Hz, R-CH=CH-R), 7.25 (d, 4H, Ar-H), 6.59 (d, 2H, *J*=16.0 Hz, R-CH=CH-R), 2.74 (m, 4H, CH$_2$), 1.82 (m, 4H, CH$_2$). ^{13}C-NMR (DMSO-d_6): δ 172.2, 168.2, 152.5, 143.6, 132.6, 130.1, 123.0, 120.0, 33.8, 24.3. IR (KBr, cm^{-1}): 2553 (OH, COOH), 1759 (C=O, ester), 1677 (C=O, COOH), 1624 and 1600 (C=C). T_m: 273-274 °C. ESI-MS *m/z*: 437 *z-1*.
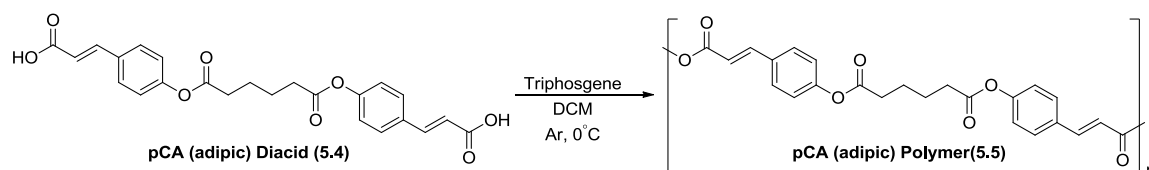
Figure 5.6. Synthesis of pCA (adipic) polymer (**5.5**) via solution polymerization

5.2.8.4.   pCA (adipic) poly(anhydride-ester)

Polymer (**5.5**) was prepared using a modified version of a previously described procedure[23] (Figure 5.6). Diacid **5.4** (1 eq) was dissolved in 20 mL

anhydrous DCM under argon. After adding triethylamine (NEt_3, 4.4 eq), the reaction mixture was cooled to 0 °C. Triphosgene (0.33 eq) dissolved in 10 mL anhydrous DCM was added dropwise (20 mL/h). The reaction was allowed to stir at 0 °C until CO_2 evolution ceased (ca. 6 h). The reaction mixture was precipitated over chilled diethyl ether (400 mL), and the precipitate isolated via vacuum filtration. The residue was dissolved in anhydrous DCM, washed with acidic water (1 x 250 mL), dried over $MgSO_4$, concentrated, and precipitated with an excess of chilled diethyl ether (500 mL). The ether was filtered off via vacuum filtration, and the polymer was dried *in vacuo* at room temperature. Yield: 73 % (white solid). ^{1}H-NMR (500 MHz, DMSO-d_6): δ 7.92 (6H, *J*=16 Hz, R-CH=CH-R, Ar-H), 7.21 (4H, Ar-H), 6.81 (2H, *J*=16 Hz, R-CH=CH-R), 2.65 (4H, CH_2), 1.71 (4H, CH_2). ^{13}C-NMR (DMSO-d_6): δ 172.1, 163.4, 153.4, 148.3, 132.0, 131.1, 123.2, 117.6, 33.8, 24.3. IR (KBr, cm^{-1}): 1800-1720 (C=O, anhydride and ester region), 1630 and 1600 (C=C). M_w = 26,700 Da, PDI = 1.9. T_g = 57 °C. T_d = 302 °C.
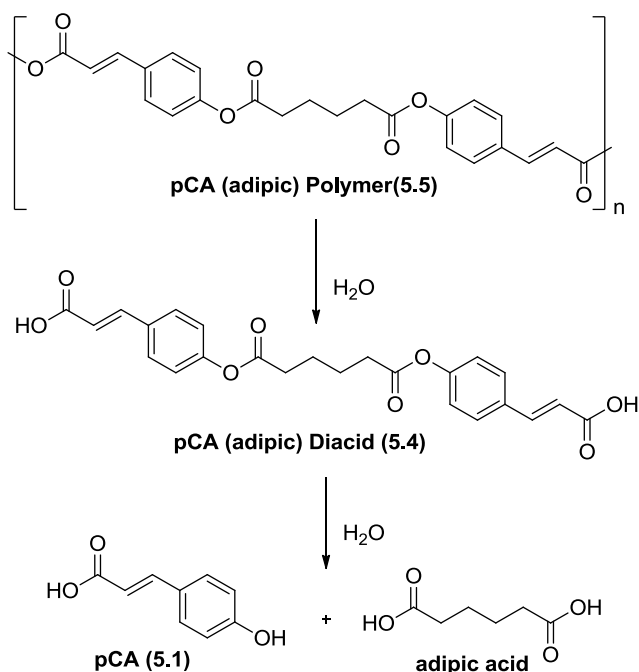
Figure 5.7. Proposed *in vitro* pCA (**5.1**) release via hydrolysis of anhydride and ester bonds within the polymer (**5.5**)

5.2.9. *In vitro* pCA release from polymer

Polymer degradation (Figure 5.7) was monitored via appearance of pCA in phosphate buffered saline (PBS) by high-performance liquid chromatography (HPLC). Polymer discs (n = 3) were prepared by pressing ground polymer (45 ± 5 mg) into 8 mm diameter x 1 mm thick discs in an IR pellet die (International Crystal Laboratories, Garfield, NJ) with a bench-top hydraulic press (Carver model M, Wabash, IN). Pressure of 10,000 psi was applied for 5 min at room temperature. All pH measurements were performed using an Accumet® AR15 pH meter (Fisher Scientific, Fair Lawn, NJ).

Polymer (**5.5**) discs were placed in 20 mL Wheaton glass scintillation vials with 10 mL of PBS and incubated at 37 ºC with agitation at 60 rpm using a controlled environment incubator-shaker (New Brunswick Scientific Co., Edison, NJ). The degradation media was collected every 2 days until day 12 and then collected every 4 days until day 30. At each time point, the buffer solution was replaced by fresh solution (10 mL) and the spent media was analyzed over 30 days by HPLC. An XTerra® RP18 5 µm 4.6x150 mm column (Waters, Milford, MA) on a Waters 2695 Separations Module equipped with a Waters 2487 Dual λ Absorbance Detector was used to analyze and quantify pCA release via HPLC. The mobile phase was comprised of 0.05 M KH_2PO_4 with 1 % formic acid in DI water at pH 2.5 (70 %) and acetonitrile (30 %) run at 1 mL/min flow rate at room temperature. Samples were filtered using 0.22 µm poly(vinylidine fluoride) syringe filters and subsequently injected (20 µL) using an autosampler. Absorbance was monitored at λ = 305 nm. At this wavelength, pCA absorbs and minimal-to-no absorption by the diacid is observed. Amounts were calculated from a calibration curve of known pCA standard solutions.

5.3. Results and Discussion

5.3.1. Synthesis of polymer and precursors

This synthetic approach was used as a continuation of previously performed research.[20] When attempting to utilize the first method outlined in Figure 5.2 (pyridine in THF at room temperature), it was evident that a mixed

product was formed as shown in Figure 5.8. According to the NMR and mass spectra, starting material, monoacid (one bioactive per linker), and diacid (two bioactives per linker) were present. Also present was product from reaction of the carboxylate (compared to phenolic esterification) demonstrating that the linker was reacting at both the phenolic and carboxylate group.
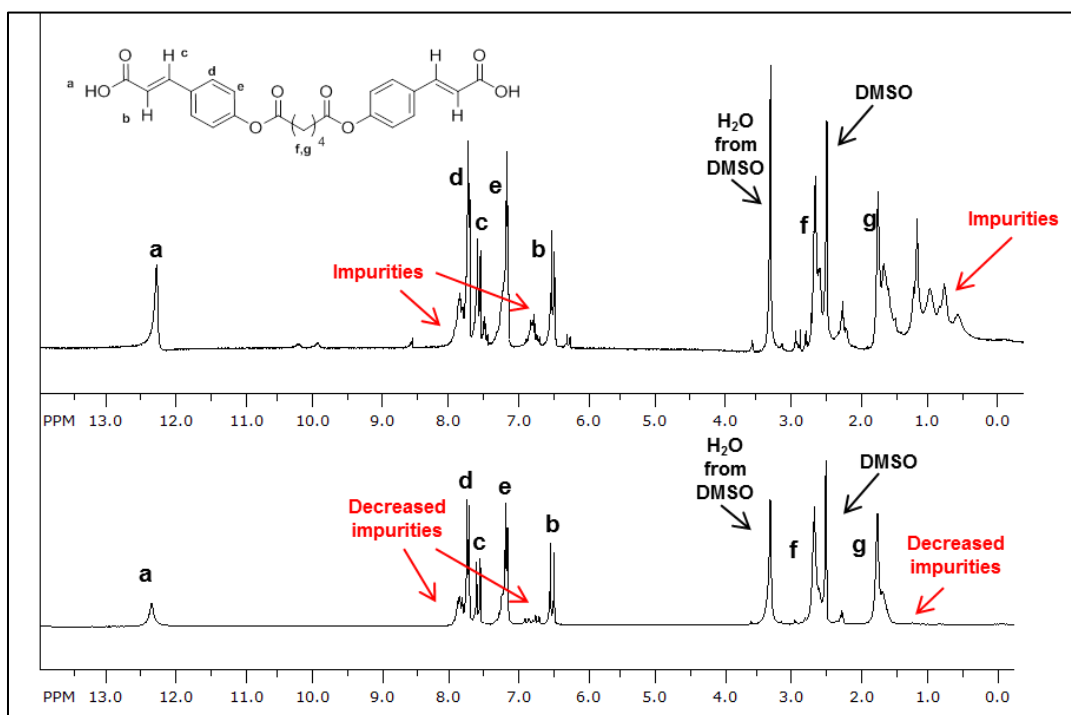
Figure 5.8. ^{1}H NMR spectra after performing triturations (top) and recrystallizations (bottom) in an attempt to remove impurities

To isolate pure product, flash chromatography was attempted using various loading and eluent solvents; however, this method resulted in the product precipitating out of solution. Therefore, dry loading was attempted by dissolving the crude material in DMF, adding silica gel, and removing solvent *in vacuo*. This

process also resulted in impure product (Figure 5.8, top). The crude material was also triturated in different solvents at varying temperatures to differentially solubilize the diacid and other side products. These solutions were separated via vacuum filtration and both residue and filtrate (after solvent removal) were examined. All attempts resulted in reducing impurities, but pure product was never isolated. Although not completely pure, the optimal method to reduce impurities was after a recrystallization from ethanol (Figure 5.8, bottom).
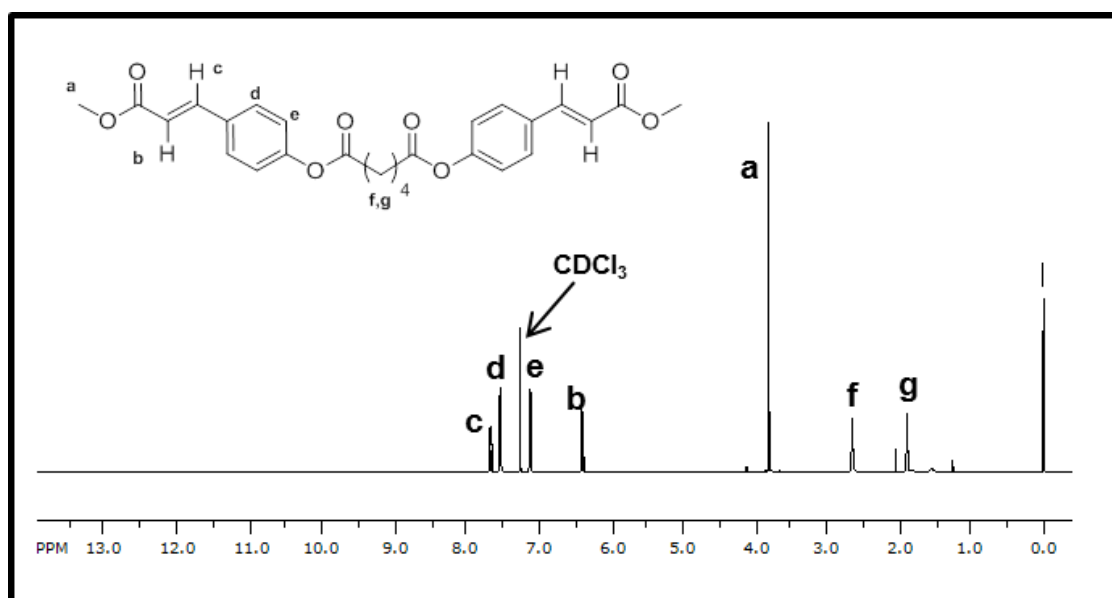
Figure 5.9. ^{1}H NMR spectrum for dimethyl pCA (adipic) intermediate

After all attempts to purify the desired product proved futile, protection methods were investigated. pCA methyl esters were successfully synthesized and reacted with adipoyl chloride to form the protected methyl pCA (adipic) intermediate. After full characterization of the intermediate (Figure 5.9), deprotection methods using NaSCH$_3$ were attempted but not successful. After

^{1}H NMR analysis, only pCA was present following deprotection methods; the thiolate cleaved all four ester bonds within the product, not solely the methyl esters as desired.
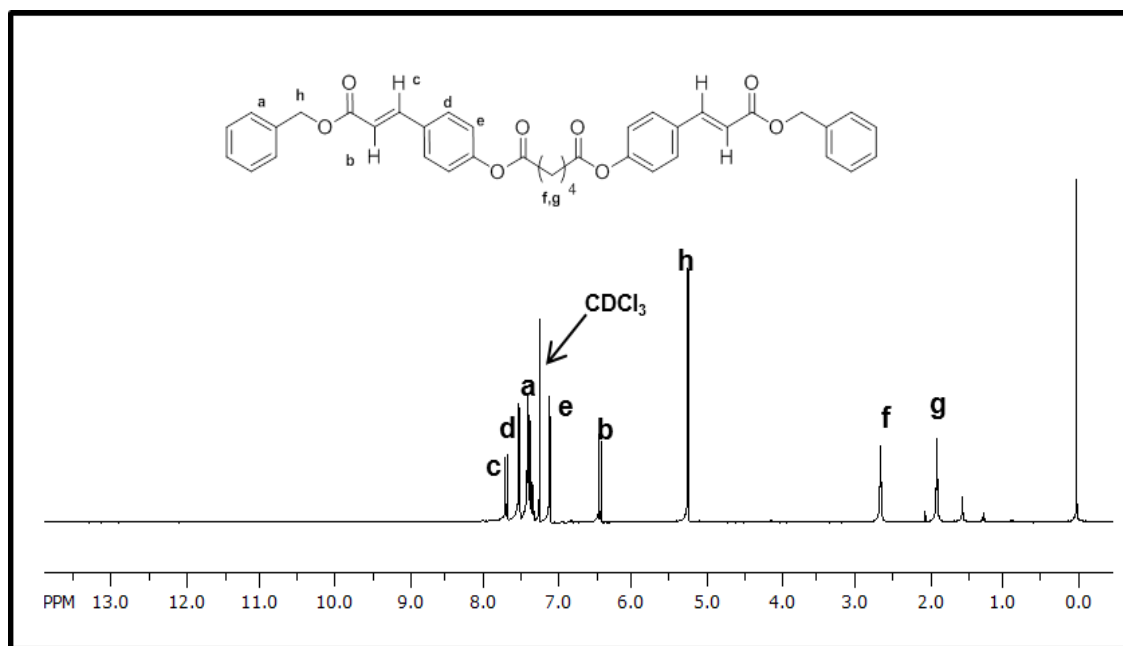
Figure 5.10. ^{1}H NMR spectrum for dibenzyl pCA (adipic) intermediate

A benzyl ester was used to protect pCA's carboxylate group and subsequently reacted with adipoyl chloride to yield clean dibenzyl pCA (adipic) intermediate (Figure 5.10). Once isolated, a mild deprotection method was used to cleave the benzyl esters (hydrogenolysis), while protecting the double bond from hydrogenation. ^{1}H NMR analysis showed the double bonds were no longer present; instead, two new aliphatic peaks between 2 and 4 ppm were noted. This observation demonstrated that the outlined methodology cleaved the dibenzyl esters and double bonds.

5.3.2. Polymer synthesis and characterization

To achieve controlled pCA release, the bioactive (**5.1**) was successfully chemically incorporated into a polymer backbone as outlined in Figure 5.5. A one-pot Knoevenagel condensation reaction was utilized by reacting *t*-butanol with Meldrum's acid to form a malonic acid monoester, which was immediately reacted with 4-hydroxybenzaldehyde in the presence of pyridine and piperidine as catalysts to yield *t*-butyl pCA (**5.2**) (Figure 5.11A). This product was subsequently coupled with adipoyl chloride (1:2 ratio of adipoyl chloride:pCA) to yield the intermediate, **5.3** (Figure 5.11B). Diacid (**5.4**) was formed after removing the *t*-butyl ester from **5.3** with TFA and structure confirmed using ^{1}H NMR (Figure 5.11C), ^{13}C NMR, and FTIR spectra. DSC and MS were utilized for melting point and molecular weight determination, respectively.
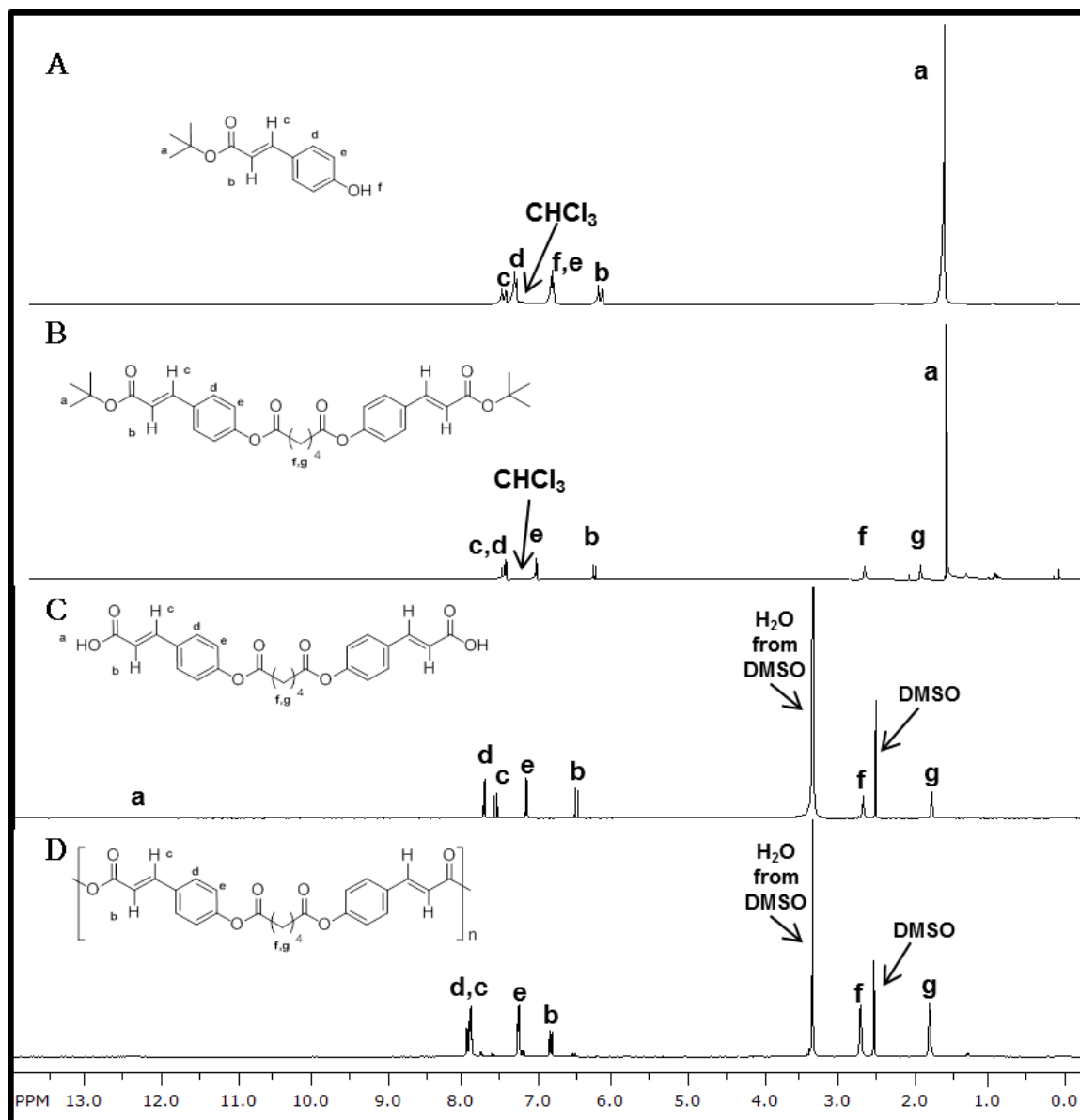
Figure 5.11. ^{1}H NMR spectra of t-butyl pCA, **5.2** (A), t-butyl pCA-based diacid intermediate, **5.3** (B), pCA-based diacid, **5.4** (C), and pCA-based polymer, **5.5** (D) are illustrated above
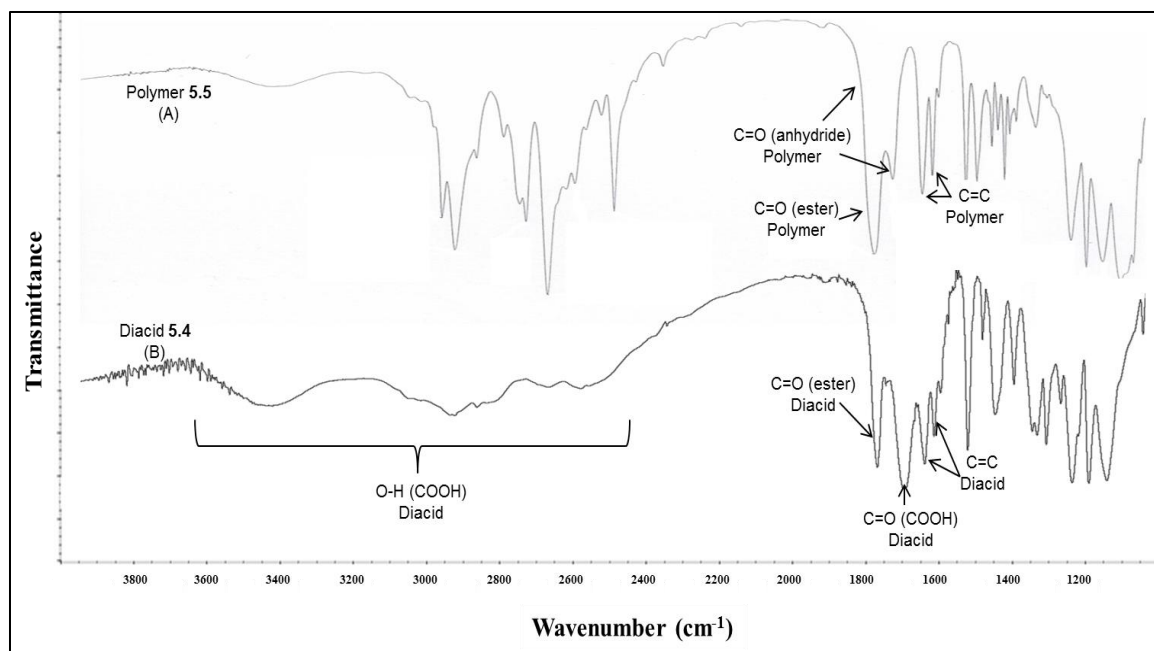
Figure 5.12. FTIR spectra of pCA-based polymer, **5.5** (A), and pCA-based

diacid, **5.4** (B) are illustrated above

Polymer **5.5** was synthesized via solution polymerization using **5.4** in the

presence of triethylamine and triphosgene. As indicated by ^{1}H NMR (Figure

5.11D) and FTIR spectroscopies (Figure 5.12), pCA was successfully

incorporated without noticeable alterations in structural integrity. The bioactive

was preserved after polymerization as observed in the obtained spectra. By

chemically incorporating pCA (**5.1**) into the backbone of a poly(anhydride-ester)

(**5.5**), a high drug loading was obtained (78 % by weight). The polymer exhibited

a M_w and polydispersity index of 26,700 Da and 1.9, respectively with a

decomposition temperature of 302 °C and T_g at 57 °C.

5.3.3. *In vitro* pCA release from polymer

The *in vitro* degradation of the polymer to yield **5.1** and adipic acid (not detected by HPLC) was used to determine the pCA release rate. Polymer **5.5** was pressed into discs and incubated in PBS pH 7.4 at 37 °C to mimic physiological conditions. Polymer degradation is measured by the appearance of pCA in degradation media via HPLC. pCA release is dictated by the hydrolysis of anhydride and ester bonds; previous studies (using salicylic acid as bioactive) indicated more rapid anhydride bond hydrolysis than that of ester bonds.[24] Within this study, however, diacid has limited solubility (<<0.002 mg/mL) relative to pCA under the conditions used and minimal diacid absorbance was observed at the specified wavelength. Although diacid could be present (retention time 7.26 min) following anhydride bond hydrolysis, it was not observed in the degradation media. Over the 30 day timeframe, pCA was detected at a 3.82 min retention time, indicating hydrolysis of both anhydride and ester bonds.

Initially, the polymer displayed an 8 day lag time (i.e., period where minimal pCA release occurs), commonly observed in polyanhydrides due to surface-eroding behavior.[17, 25]   After 30 days, 4.5 % pCA is released from the polymer (Figure 5.13) indicating complete degradation is > 30 days. This system is expected to exhibit a linear release profile, as other poly(anhydride-esters) have demonstrated.[26]   By extrapolating the curve, degradation should be complete in ~14 months (i.e., 100% pCA release with 0.24 % pCA release/day after day 10).
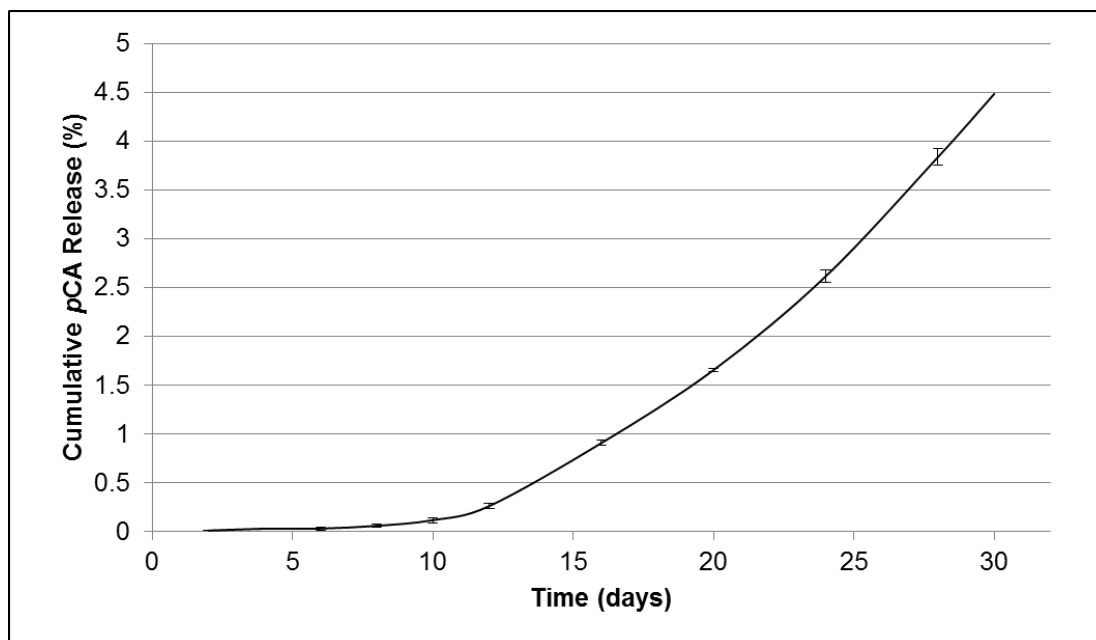
Figure 5.13. *In vitro* cumulative pCA (**5.1**) release from pCA-based poly(anhydride-ester) (**5.5**) (pCA ± standard deviation)

5.4. Conclusion

A pCA-based poly(anhydride-ester) was synthesized using a Knoevenagel condensation, TFA deprotection, and subsequent solution polymerization method. These methods rendered a biodegradable polymer with high drug loading (78 %) that releases pCA over time via hydrolysis of anhydride and ester bonds. Favorable thermal properties including a T_g well above physiological temperature indicate the potential for *in vivo* use. The controlled, sustained release of the bioactive may be beneficial for maintaining pCA concentrations at biologically relevant levels necessary to combat gastrointestinal diseases. Additionally, the successful synthetic method presented herein allows for altering the pCA release rate by changing the structure of the linker molecule.

5.5. References

1. Herrmann K, Nagel CW, *CRC Cr Rev Food Sci* **1989**, *28*, 315-47.

2. El-Seedi HR, El-Said AMA, Khalifa SAM, Göransson U, Bohlin L, Borg-Karlson A-K, Verpoorte R, *J Agr Food Chem* **2012**, *60*, 10877-95.

3. Shahidi F, Chandrasekara A, *Phytochem Rev* **2009**, *9*, 147-70.

4. Ferguson LR, Zhu ST, Harris PJ, *Mol Nutr Food Res* **2005**, *49*, 585-93.

5. Luceri C, Giannini L, Lodovici M, Antonucci E, Abbate R, Masini E, Dolara P, *Br J Nutr* **2007**, *97*, 458-63.

6. Luceri C, Guglielmi F, Lodovici M, Giannini L, Messerini L, Dolara P, *Scand J Gastroentero* **2004**, *39*, 1128-33.

7. Guglielmi F, Luceri C, Giovannelli L, Dolara P, Lodovici M, *Brit J Nutr* **2007**, *89*, 581.

8. Konishi Y, Hitomi Y, Yoshioka E, *J Agric Food Chem* **2004**, *52*, 2527-32.

9. Biswick T, Park D-H, Shul Y-G, Choy J-H, *J Phys Chem Solids* **2010**, *71*, 647-9.

10. Thi TH, Matsusaki M, Shi D, Kaneko T, Akashi M, *J Biomater Sci Polym Ed* **2008**, *19*, 75-85.

11. Kimura K, Inoue H, Kohama SI, Yamashita Y, Sakaguchi Y, *Macromolecules* **2003**, *36*, 7721-9.

12. Matsusaki M, Kishida A, Stainton N, Ansell CWG, Akashi M, *J Appl Polym Sci* **2001**, *82*, 2357-64.

13. Nagata M, Hizakae S, *Macromol Biosci* **2003**, *3*, 412-9.

14. Jin XM, Carfagna C, Nicolais L, Lanzetta R, *Macromolecules* **1995**, *28*, 4785-94.

15. Spiliopoulos IK, Mikroyannidis JA, *J Polym Sci, Part A: Polym Chem* **1996**, *34*, 2799-807.

16. Kaneko T, Kaneko D, Wang S, *Plant Biotechnol* **2010**, *27*, 243-50.

17. Göpferich A, Tessmar J, *Adv Drug Deliv Rev* **2002**, *54*, 911-31.

18.   Nair LS, Laurencin CT, *Prog Polym Sci* **2007**, *32*, 762-98.

19.   Schmeltzer RC, Anastasiou TJ, Uhrich KE, *Polym Bull* **2003**, *49*, 441-8.

20.   Carbone AL. Ph.D. thesis. Rutgers, The State University of New Jersey, New Brunswick, 2009.

21.   Lamidey A-M, Fernon L, Pouységu L, Delattre C, Quideau S, Pardon P, *Helv Chim Acta* **2002**, *85*, 2328-34.

22.   Hu WX, Xia CN, Wang GH, Zhou W, *J Chem Res-S* **2006**, 586-8.

23.   Schmeltzer R, Johnson M, Griffin J, Uhrich K, *J Biomat Sci Polym Ed* **2008**, *19*, 1295-306.

24.   Erdmann L, Uhrich KE, *Biomaterials* **2000**, *21*, 1941-6.

25.   Whitaker-Brothers K, Uhrich K, *J Biomed Mater Res Part A* **2004**, *70A*, 309-18.

26.   Whitaker-Brothers K, Uhrich K, *J Biomed Mater Res Part A* **2006**, *76A*, 470-9.

CHAPTER 6:   BIODEGRADABLE ANTIOXIDANT-CONTAINING POLY(ANHYDRIDE-ESTERS)

6.1.   Introduction

The methodology used in Chapter 5 set the foundation for exploring other types of phenolic compounds that may be beneficial as controlled release systems for biomedical applications. Examples such as hydroxycinnamic acids (HCs) have gained considerable attention in recent years for their use in preventing oxidative stress.[2]   Ferulic acid (FA) and sinapic acid (SinA), in particular, are phenolic compounds that exhibit anti-inflammatory, antimicrobial, and anticancer properties (Figure 6.1).[3-6] Exposure of skin to ultraviolet radiation (UV) causes oxidative stress, which can result in photosensitivity, senescence, and skin cancer.[7]   The prevention of oxidative stress can be achieved using antioxidants as photoprotective agents that absorb UV radiation and scavenge free radicals responsible for causing damage.[2] As photoprotective agents and antioxidants in biomedical and cosmetic formulations, these HCs also prevent harmful radiation effects both as a UV absorber and a free radical scavenger.[2, 8] Although FA and SinA exhibit beneficial properties, each undergo thermal-, air-, and light-induced decomposition through a proposed decarboxylation mechanism,[9] which reduces its efficacy and causes discoloration (Figure 6.2).[10, 11]
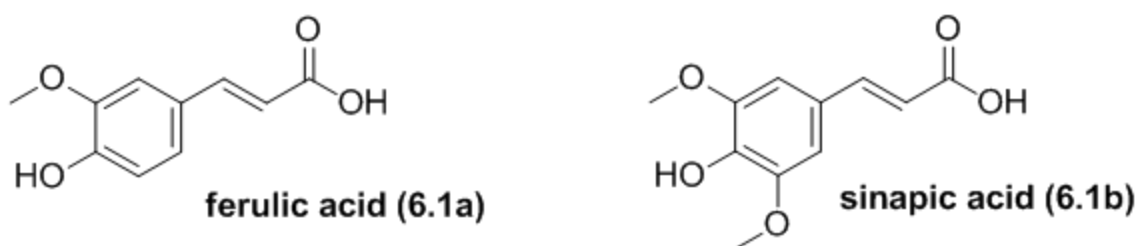
Figure 6.1. Structures of hydroxycinnamic acids (HCs) including ferulic acid (FA, **6.1a**) and sinapic acid (SinA, **6.1b**)

To improve the physiochemical stability of FA and SinA in formulations, researchers have attempted to protect the antioxidants from decomposition via physical incorporation into matrices.[12] For example, FA has been physically incorporated into an organic-inorganic nanohybrid material for controlled release via diffusion, but the low FA concentration samples exhibited minimal antioxidant activity.[13, 14] To overcome this issue with physical incorporation, polymers containing cinnamoyl moieties chemically conjugated as pendant groups have been used to improve photostability, but exhibited low drug loading (ca. 50 %).[15, 16] Polymers containing cinnamoyl groups in the main chain and polymerized with poly(ethylene glycol) derivatives also exhibit lower drug loading and require enzymatic degradation.[17]

Figure 6.2. Discoloration observed from ferulic acid (left) and sinapic acid (right) solutions stored for 10 days at 37 ºC

Other researchers have successfully incorporated antioxidants into a biodegradable polymer backbone to increase drug loading (in some cases, the polymer is comprised entirely of the antioxidant),[18-21] and few examples using FA and SinA are known.[22, 23]   Our work is distinguished by the success at both protecting the unstable HC from decomposition and improving drug loading by chemically incorporating the antioxidants each into a hydrolytically degradable polyanhydride backbone. This polymer is a controlled release system that can offer advantages compared to conventional formulations by reducing the frequency of applications and improving patient compliance.[24]

Here we report the synthesis of biodegradable poly(anhydride-esters) containing antioxidants, FA and SinA, in the backbone via solution polymerization methods and its characterization using proton and carbon nuclear magnetic

resonance (^{1}H and ^{13}C NMR) and Fourier transform infrared (FTIR) spectroscopies. Thermal properties were evaluated using differential scanning calorimetry (DSC) and thermogravimetric analysis (TGA). Gel permeation chromatography (GPC) and mass spectrometry (MS) were used to determine weight-averaged molecular weight (M_w) of the polymer and molecular weights of all polymer precursors, respectively. In addition, *in vitro* HC release studies were performed to measure the polymer hydrolytic degradation. The antioxidant and antibacterial activities of the degradation products were evaluated and compared to free HC. Finally, the polymer cytotoxicity towards fibroblasts was assessed *in vitro*.

6.2. Experimental

6.2.1. Materials

Silica gel and fetal bovine serum were purchased from VWR (Radnor, PA) and Atlanta Biologicals (Lawrenceville, GA), respectively. Hydrochloric acid (HCl, 1 N), concentrated HCl, poly(vinylidine fluoride) and polytetrafluoroethylene syringe filters, Wheaton glass scintillation vials, and 96-well plates were purchased from Fisher Scientific (Fair Lawn, NJ). Mouse areolar fibroblasts were purchased from ATCC (Manassas, VA). All other reagents, solvents, and fine chemicals were purchased from Aldrich (Milwaukee, WI) and used as received.

6.2.2. ^{1}H and ^{13}C NMR and FTIR spectroscopies

^{1}H and ^{13}C NMR spectra were recorded on a Varian 400 MHz or 500 MHz spectrometer using deuterated dimethyl sulfoxide (DMSO-d_6) as solvent and internal reference. FTIR spectra were obtained using a Thermo Nicolet/Avatar 360 spectrometer, samples (1 wt %) ground and pressed with KBr into a disc. Each spectrum was an average of 32 scans.

6.2.3. Molecular weight

Polymer precursors were analyzed via MS to determine molecular weights. A Finnigan LCQ-DUO equipped with Xcalibur software and an adjustable atmospheric pressure ionization electrospray ion source (API-ESI Ion Source) was used with a pressure of 0.8 x 10-5 and 150 °C API temperature. Samples dissolved in methanol (< 10 µg/mL) were injected with a glass syringe. GPC was used to determine polymer weight-averaged molecular weight and polydispersity using a Perkin-Elmer liquid chromatography system consisting of a Series 200 refractive index detector, a Series 200 LC pump, and an ISS 200 autosampler. Sample automation and data processing were performed using a Dell OptiPlex GX110 computer running Perkin-Elmer TurboChrom 4 software with a Perkin-Elmer Nelson 900 Series Interface and 600 Series Link. Polymer samples were prepared for autoinjection by dissolving in dichloromethane (DCM, 10 mg/mL) and filtering through 0.45 µm polytetrafluoroethylene syringe filters. Samples were resolved on a Jordi divinylbenzene mixed-bed GPC column (7.8 x 300 mm, Alltech Associates, Deerfield, IL) at 25 °C, with DCM as the mobile

phase at a 1.0 mL/min flow rate. Molecular weights were calibrated relative to broad polystyrene standards (Polymer Source Inc., Dorval, Canada).

6.2.4. Thermal analysis

DSC measurements were carried out on a TA Instrument Q200 to determine melting (T_m) and glass transition (T_g) temperatures. Measurements on samples (4-6 mg) heated under nitrogen atmosphere from –10 °C to 200 °C at a heating rate of 10 °C/min and cooled to –10 °C at a rate of 10 °C/min with a two-cycle minimum were performed. TA Instruments Universal Analysis 2000 software, version 4.5A, was used to analyze the data. Glass transition temperatures were calculated as half Cp extrapolated. TGA was utilized for determining decomposition temperatures (T_d) using a Perkin-Elmer Pyris 1 system with TAC 7/DX instrument controller and Perkin-Elmer Pyris software for data collection. Samples (5-10 mg) were heated under nitrogen atmosphere from 25 °C to 400 °C at a heating rate of 10 °C/min. Decomposition temperatures were measured at the onset of thermal decomposition.

6.2.5. Polymer precursor and polymer syntheses

6.2.5.1. *t*-Butyl HC

To prepare *t*-butyl HC (Figure 6.3, **6.2**), a procedure adapted from Hu et al.[25] was used where Meldrum's acid (2.5 eq) was dissolved in toluene (50 mL), tertiary butanol (2.5 eq) added, and the reaction was heated to 100 °C with stirring for 5 h. Without separation, the reaction was cooled to room temperature

where vanillin was added followed by pyridine (2.5 mL) and piperidine (0.25 mL),
and then heated to 75 °C with stirring for 24 h. The reaction mixture was dried *in
vacuo*, and the residue obtained was diluted in diethyl ether, washed with
saturated aqueous sodium bicarbonate (2 x 200 mL), 1 N HCl (2 x 200 mL), and
distilled water (1 x 200 mL). The organic layer was then dried overnight over
$MgSO_4$, filtered, and the solvent removed *in vacuo* to yield crude product. This
product was purified on silica gel via flash chromatography using 4:1
hexane:ethyl acetate as eluent.

Figure 6.3. Synthesis of HC-based polymer (**6.5**) and precursors including *t*-butyl
HC (**6.2**), *t*-butyl HC (adipic) intermediate (**6.3**), HC (adipic) diacid (**6.4)**, and HC
(adipic) polymer (**6.5**)

t-Butyl FA (**6.2a**).   Yield: 76 % (white crystals). ^{1}H-NMR (400 MHz, CDCl$_3$): δ 7.53 (d, 1H, *J*=16.0 Hz, R-CH=CH-R), 7.06 (s, 1 H, Ar-H), 7.02 (d, 1H, Ar-H), 6.91 (d, 1H, Ar-H), 6.23 (d, 1H, *J*=16.0 Hz, R-CH=CH-R), 6.06 (s, 1H, OH), 3.91 (s, 3H, OCH$_3$), 1.54 (s, 9H, 3CH$_3$). ^{13}C-NMR (CDCl$_3$): δ 168.9, 147.9, 143.9, 127.5, 123.2, 117.9, 114.9, 109.4, 80.5, 51.2, 28.5.   IR (KBr, cm^{-1}): 3390 (OH, Ph), 1685 (C=O, ester), 1634 and 1605 (C=C).   T$_m$: 90-93 ºC.

t-Butyl SinA (**6.2b**).   Yield: 68 % (white crystals). ^{1}H-NMR (**400** MHz, CDCl$_3$): δ 7.48 (d, 1H, *J*=15.9 Hz, R-CH=CH-R), 6.75 (s, 2 H, Ar-H), 6.23 (d, 1H, *J*=15.9 Hz, R-CH=CH-R), 5.73 (s, 1H, OH), 3.91 (s, 6H, OCH$_3$), 1.54 (s, 9H, 3CH$_3$). ^{13}C-NMR (CDCl$_3$): δ 166.7, 147.4, 144.0, 137.1, 126.4, 118.2, 105.1, 80.6, 56.5, 28.5.   IR (KBr, cm^{-1}): 3358 (OH, Ph), 1692 (C=O, ester), 1633 and 1606 (C=C).   T$_m$: 155-156 ºC.

6.2.5.2.   *t*-Butyl HC (adipic) intermediate

t-Butyl HC (**6.2**) (2 eq) was dissolved in anhydrous dimethylformamide (DMF), to which sodium hydride (NaH, 2.2 eq) was slowly added. After 30 min, adipoyl chloride (1 eq) dissolved in DMF (10 mL) was added dropwise at 20 mL/h.   Reaction progress was monitored by thin layer chromatography (4:1 hexane:ethyl acetate as eluent).   Once completed, the reaction mixture was diluted with ethyl acetate (250 mL) and washed with deionized water (2 x 100 mL).   The organic layer was collected, dried over MgSO$_4$, and the solvents removed *in vacuo*. The product was purified on silica gel via flash chromatography using 4:1 hexane:ethyl acetate as eluent.

t-Butyl FA (adipic) intermediate (6.3a). Yield: 69 % (off-white powder).

^{1}H-NMR (400 MHz, CDCl$_3$): δ 7.54 (d, 2H, J=16.0 Hz, R-CH=CH-R), 7.11 (s, 2 H, Ar-H), 7.08 (d, 2H, Ar-H), 7.04 (d, 2H, Ar-H), 6.31 (d, 2H, J=16.0 Hz, R-CH=CH-R), 3.85 (s, 6H, OCH$_3$), 2.67 (m, 4H, CH$_2$), 1.92 (m, 4H, CH$_2$), 1.54 (s, 18H, 3CH$_3$). ^{13}C-NMR (CDCl$_3$): δ 171.4, 166.3, 151.5, 143.1, 141.4, 133.9, 123.4, 121.4, 120.6, 111.3, 80.9, 56.1, 33.8, 28.4, 24.5. IR (KBr, cm^{-1}): 1765 (C=O, ester), 1695 (C=O, ester), 1634 and 1597 (C=C). T$_m$: 112-115 ºC.

t-Butyl SinA (adipic) intermediate (6.3b). Yield: 84 % (white powder).

^{1}H-NMR (400 MHz, CDCl$_3$): δ 7.50 (d, 2H, J=15.9 Hz, R-CH=CH-R), 6.75 (s, 4 H, Ar-H), 6.30 (d, 2H, J=15.9 Hz, R-CH=CH-R), 3.83 (s, 12H, OCH$_3$), 2.69 (m, 4H, CH$_2$), 1.94 (m, 4H, CH$_2$), 1.54 (s, 18H, 3CH$_3$). ^{13}C-NMR (CDCl$_3$): δ 171.1, 166.3, 152.6, 143.5, 133.2, 130.4, 120.7, 104.7, 80.9, 56.3, 33.7, 28.4, 24.6. IR (KBr, cm^{-1}): 1766 (C=O, ester), 1699 (C=O, ester), 1634 and 1595 (C=C). T$_m$: 180-184 ºC.

6.2.5.3.   HC (adipic) diacid

Compound **6.3** (1 eq) was dissolved in anhydrous DCM to which trifluoroacetic acid (TFA) (40 eq) was added and left to stir overnight. Solvent was removed *in vacuo,* and the residue was triturated with DI water (300 mL), isolated via vacuum filtration, and dried *in vacuo* for 24 h.

FA (adipic) diacid (6.4a). Yield: 97 % (light pink powder). ^{1}H-NMR (500 MHz, DMSO-d_6): δ 12.43 (s, 2H, COOH), 7.56 (d, 2H, J=16.0 Hz, R-CH=CH-R), 7.47 (s, 2 H, Ar-H), 7.25 (d, 2H, Ar-H), 7.10 (d, 2H, Ar-H), 6.56 (d, 2H, J=16.0 Hz,

R-CH=CH-R), 3.80 (s, 6H, OCH$_3$), 2.62 (m, 4H, CH$_2$), 1.74 (m, 4H, CH$_2$). ^{13}C-NMR (DMSO-d_6): δ 171.6, 168.3, 151.8, 144.0, 141.5, 133.9, 123.8, 122.1, 120.2, 112.5, 56.6, 33.5, 24.4. IR (KBr, cm^{-1}): 2586 (OH, COOH), 1766 (C=O, ester), 1677 (C=O, COOH), 1625 and 1600 (C=C). T$_m$: 243-245 ºC. ESI-MS *m/z* 497 *z-1*.

SinA (adipic) diacid (6.4b). Yield: 97% (beige powder). ^{1}H-NMR (500 MHz, DMSO-d_6): δ H 13.00 (s, 2H, COOH), 7.61 (d, 2H, *J*=15.9 Hz, R-CH=CH-R), 7.17 (s, 4 H, Ar-H), 6.68 (d, 2H, *J*=15.9 Hz, R-CH=CH-R), 3.85 (s, 12H, OCH$_3$), 2.68 (m, 4H, CH$_2$), 1.82 (m, 4H, CH$_2$). ^{13}C-NMR (DMSO-d_6): δ 171.2, 168.2, 152.6, 144.5, 133.3, 130.1, 120.4, 105.9, 56.8, 33.4, 24.5. IR (KBr, cm^{-1}): 2586 (OH, COOH), 1763 (C=O, ester), 1692 (C=O, COOH), 1630 and 1597 (C=C). T$_m$: 230-232 ºC. ESI-MS *m/z* 557 *z-1*.

6.2.5.4. HC (adipic) poly(anhydride-ester)

The polymer (**6.5**) was prepared using a modified version of a previously described procedure[26] (Figure 6.3). Diacid **6.4** (1 eq) was dissolved in 20 mL anhydrous DCM under argon. After adding triethylamine (NEt$_3$, 4.4 eq), the reaction mixture was cooled to 0 °C. Triphosgene (0.33 eq) dissolved in 10 mL anhydrous DCM was added dropwise (20 mL/h). The reaction was allowed to stir at 0 °C until CO$_2$ evolution ceased (ca. 6 h). The reaction mixture was poured over chilled diethyl ether (400 mL), and the precipitate was isolated via vacuum filtration. The residue was dissolved in anhydrous DCM, washed with acidic water (1 x 250 mL), dried over MgSO$_4$, concentrated, and precipitated with

an excess of chilled diethyl ether (500 mL). The ether was removed via vacuum filtration, and the polymer was dried *in vacuo* at room temperature.

FA (adipic) poly(anhydride-ester) (6.5a). Yield: 61 % (white solid). ^{1}H-NMR (500 MHz, DMSO-d_6): δ 7.84 (2H, 2H, J=16 Hz, R-CH=CH-R), 7.60 (2H, Ar-H), 7.38 (2H, Ar-H), 7.18 (Ar-H), 6.83 (2H, J=16 Hz, R-CH=CH-R), 3.81 (6H, CH$_3$), 2.64 (4H, CH$_2$), 1.73 (4H, CH$_2$). ^{13}C-NMR (DMSO-d_6): δ 171.5, 163.4, 151.9, 148.7, 142.5, 133.3, 124.0, 123.2, 117.8, 113.2, 56.8, 33.5, 24.4. IR (KBr, cm^{-1}): 1800-1720 (C=O, anhydride and ester region), 1630 and 1600 (C=C). M_w = 21,700 Da, PDI = 1.7. T_g = 82 °C. T_d = 332 °C.

SinA (adipic) poly(anhydride-ester) (6.5a). Yield: 82 % (yellow solid). ^{1}H-NMR (500 MHz, DMSO-d_6): δ 7.85 (2H, J=16.0 Hz, R-CH=CH-R), 7.29 (4H, Ar-H), 6.96 (2H, J=16.0 Hz, R-CH=CH-R), 3.80 (12H, CH$_3$), 2.62 (4H, CH$_2$), 1.75 (4H, CH$_2$). ^{13}C-NMR (DMSO-d_6): δ 171.1, 163.5, 152.8, 149.2, 132.6, 131.1, 117.9, 106.7, 56.9, 33.4, 24.5. IR (KBr, cm^{-1}): 1760, 1730 (C=O, anhydride), 1760 (C=O, ester), 1630 and 1600 (C=C). M_w = 38,500 Da, PDI = 1.7. T_g = 101 °C. T_d = 340 °C.

6.2.6. *In vitro* HC release from polymer

The release of **6.1** from polymer (**6.5**) was evaluated by *in vitro* degradation in phosphate buffered saline (PBS). Polymer discs (n = 3) were prepared by pressing ground polymer (45 ± 5 mg) into 8 mm diameter x 1 mm thick discs in an IR pellet die (International Crystal Laboratories, Garfield, NJ) with a bench top hydraulic press (Carver model M, Wabash, IN). Pressure of

10,000 psi was applied for 5 min at room temperature. This methodology was preferred, as it minimized interferences from external effects (e.g., formulation additives) on polymer degradation. The PBS pH was adjusted to 7.40 using 1 N sodium hydroxide. All pH measurements were performed using an Accumet® AR15 pH meter (Fisher Scientific, Fair Lawn, NJ).

To measure hydrolytic degradation, the polymer (**6.5**) discs were placed in 20 mL Wheaton glass scintillation vials with 10 mL of PBS and incubated at 37 ºC with agitation at 60 rpm using a controlled environment incubator-shaker (New Brunswick Scientific Co., Edison, NJ). The degradation media was collected every 2 days until day 12 and then collected every 4 days until day 30. Media was replaced by fresh PBS (10 mL) at each time point and the spent media was analyzed over 30 days by high performance liquid chromatography (HPLC). The degradation products were analyzed and quantified via HPLC using an XTerra® RP18 5 µm 4.6x150 mm column (Waters, Milford, MA) on a Waters 2695 Separations Module equipped with a Waters 2487 Dual λ Absorbance Detector. All samples were filtered using 0.22 µm poly(vinylidine fluoride) syringe filters and subsequently injected (20 µL) using an autosampler. The mobile phase was comprised of 50 mM KH_2PO_4 with 1 % formic acid in HPLC grade water at pH 2.5 (70 %) and acetonitrile (30 %) run at 1 mL/min flow rate at ambient temperature. Absorbance was monitored at λ = 335 and 340 nm for **6.1a** and **6.1b**, respectively. Amounts were calculated from a calibration curve of each known HC standard solutions.

6.2.7.   Radical scavenging (antioxidant) activity[27]

To assess HC antioxidant activity in degradation media, a 2,2-diphenyl-1-picrylhydrazyl (DPPH) radical scavenging assay was employed. This activity was evaluated by adding sample (0.1 mL) to a 0.024 mg/mL DPPH solution in methanol (3.9 mL). Day-10 and day-20 polymer degradation media samples (0.1 mL) from the polymer (see *In vitro* HC release from polymer section) were incubated with the 0.024 mg/mL DPPH solution (3.9 mL) at room temperature. After 1 h, solutions were analyzed via UV/vis with a Perkin-Elmer Lambda XLS spectrophotometer (Waltham, MA) (λ = 517 nm).   A free HC solution was freshly prepared at specific concentrations corresponding to HPLC data gathered on days 10 and 20.   These samples were each analyzed identically to the aforementioned degradation media samples.   DPPH % radical reduction was calculated by: $[(Abs_{t0} - Abs_t)/Abs_{t0}]$ x 100, where Abs_{t0} is the initial absorbance and Abs_t is the absorbance after a period of time, namely 1 h. Absorbance values from adding PBS (0.1 mL) to the DPPH solution (3.9 mL) was used as Abs_{t0}. All radical scavenging assays were performed in triplicate. Student's t-tests were used to determine the significant difference of the antioxidant activity between free HC and HC degradation media (significantly different if $p < 0.05$).

6.2.8.   *In vitro* cytotoxicity assay

The cytotoxicity studies were performed by Dr. Jeremy Griffin, Ph.D. graduate in Biomedical Engineering (Rutgers University, Piscataway, NJ) supervised by Professor Uhrich.

Evaluation of the polymer cell compatibility was performed by culturing NCTC clone 929 (strain L) mouse areolar fibroblasts in media containing the dissolved polymer.   These L929 fibroblasts are a standard cell type for cytocompatibility testing as recommended by ASTM.[28]   The polymer was dissolved in dimethyl sulfoxide (DMSO; 10 mg/mL) as a stock solution and serially diluted with cell culture media to two concentrations (0.01 mg/mL and 0.10 mg/mL), based on standard cytotoxicity protocols.[29-32]   Cell culture media consisted of Dulbecco's Modified Eagle's Medium, 10 % v/v fetal bovine serum, 1 % L-glutamate, and 1 % penicillin/streptomycin.   The polymer-containing media was distributed into a 96-well plate and seeded at 2,000 cells per well (n = 3) as the initial concentration.   The media with dissolved polymer was compared to two controls: DMSO-containing media and media alone.

Cellular morphology was observed and documented at 100X original magnification (Olympus, IX81, Center Valley, PA) at 48, 72, and 96 h post seeding.   Cell viability was determined by using a CellTiter 96®AQueous One Solution Cell Proliferation Assay (Promega, Madison, WI).   The MTS tetrazolium compound   [3-(4,5-dimethylthiazol-2-yl)-5-(3-carboxymethoxyphenyl)-2-(4-7   sulfo-phenyl)-2H-tetrazolium, inner salt; MTS)] is bioreduced by cells into a colored formazan product that is soluble in the tissue culture medium.   Following the appropriate incubation time, 20 µL of the MTS reagent was added to 100 µL of culture medium and further incubated for 4 h.   The absorbance was then recorded with a microplate reader (Model 680; Bio-Rad, Hercules, CA) at λ = 490

nm. Cell numbers were calculated based upon a standard curve created 24 h after original cell seeding.

Cell studies were performed in triplicate, and statistical analysis was performed with SPSS software (version 15.0 for Windows; Chicago, IL). ANOVA followed by pairwise comparison with Scheffe's post hoc test allowed for pair-wise comparison of the polymer to the DMSO media control.

6.2.9.   *In vitro* antibacterial assays

The antibacterial studies were performed by Dr. Wen-Hsuan Wu, Ph.D. graduate in Food Science (Rutgers University, Piscataway, NJ) supervised by Professor Di Rong.

A supplemental study to the antioxidant assays was performed to ensure that full activity was maintained after polymer synthesis and processing. To further assess FA and SinA bioactivity, the antibacterial activity was evaluated by hydrolyzing the polymer (**5**) (ca. 150 mg) with 1 N sodium hydroxide (2 mL) with PBS (10 mL) and incubated at 37 ºC with 60 rpm agitation using a controlled environment incubator-shaker. After complete polymer degradation, solutions were acidified to pH 2 using concentrated HCl, then HC and adipic acid extracted with ethyl acetate (3 x 40 mL). The organic layer was collected, dried over $MgSO_4$, and the solvent removed *in vacuo* to yield a powder of free HC (82 % calculated from ^{1}H NMR) and adipic acid (18 % calculated from ^{1}H NMR), labeled "extracted powders".

The antibacterial activity of the extracted powders and free HC was screened in liquid Brain Heart Infusion (BHI) broth in 96-well plates. Free HC (600 mg/mL), extracted powders (740 mg/mL from **6.5**, corresponding to 600 mg/mL HC), and adipic acid (132 mg/mL, calculated according to amount per extracted powder) were each dissolved in sterile DMSO to prepare stock solutions. *Escherichia coli* (*E. coli*) O157:H7 ATCC 43895, *Salmonella enteric* serovar Newport, and *Listeria monocytogenes* Scott A were each cultured in 5 mL BHI broth at 37 °C for at least 18 hours. Inoculum was prepared by making serial tenfold dilutions in fresh BHI broth to approximately 10^5 CFU/mL and plated on BHI agar to confirm the cell numbers. Samples were diluted in BHI broth from their DMSO stock solution to prepare solutions containing a final HC concentration of 3 mg/mL (these specific concentrations were chosen to observe antibacterial activity). A 100 µL aliquot of each sample (free HC and extracted powder from **6.5**) were mixed with 100 µL of inoculums in a 96-well plate in triplicate. Untreated cells were used as a positive control. The plate was incubated at 37 °C in a Dynex 96-well plate reader MRX with Revelation software to monitor optical density (OD) at λ = 630 nm over 24 hours. Control studies verified that free and extracted acids alone, DMSO alone, and BHI broth alone did not absorb at this wavelength and were not contaminated.

A 3.66 mg/mL extracted powder (containing 3 mg/mL HC and 0.66 mg/mL adipic acid) solution, 3 mg/mL HC solution, and 0.66 mg/mL adipic acid solution were used for testing bacteria. These studies were performed in triplicate, while the complete assay was performed twice to ensure reproducibility. Student's t-

tests were used to determine the significant difference of the antibacterial activity between free HC and extracted powder (significantly different if $p < 0.05$).

6.3.   Results and Discussion

6.3.1.   Polymer synthesis and characterization

To overcome FA and SinA limitations regarding its poor physicochemical stability, each bioactive was chemically incorporated into a polymer backbone as outlined in Figure 6.3.   A one-pot Knoevenagel condensation reaction was utilized by reacting *t*-butanol with Meldrum's acid to form a malonic acid monoester, which was immediately reacted with vanillin in the presence of pyridine and piperidine as catalysts to yield the *t*-butyl HC compound (**6.2**).

To synthesize **6.4**, various reaction conditions were explored by changing temperature, base, and solvent to directly couple the acyl chloride to the HC phenol; however, these conditions resulted in impure products that could not be further purified.   For sole reaction at the phenol, various groups were used to protect the carboxylate group, where the *t*-butyl groups yielded pure material without compromising the integrity of the HC structure during protection and deprotection.   Ultimately, diacid (**6.4**) was formed after coupling compound **6.2** to adipoyl chloride in DMF containing NaH and removing the *t*-butyl ester with TFA. The diacid (**6.4**) was isolated and the structure confirmed by ^{1}H and ^{13}C NMR and FTIR spectra.   DSC and MS were used for melting point and molecular weight determination, respectively.
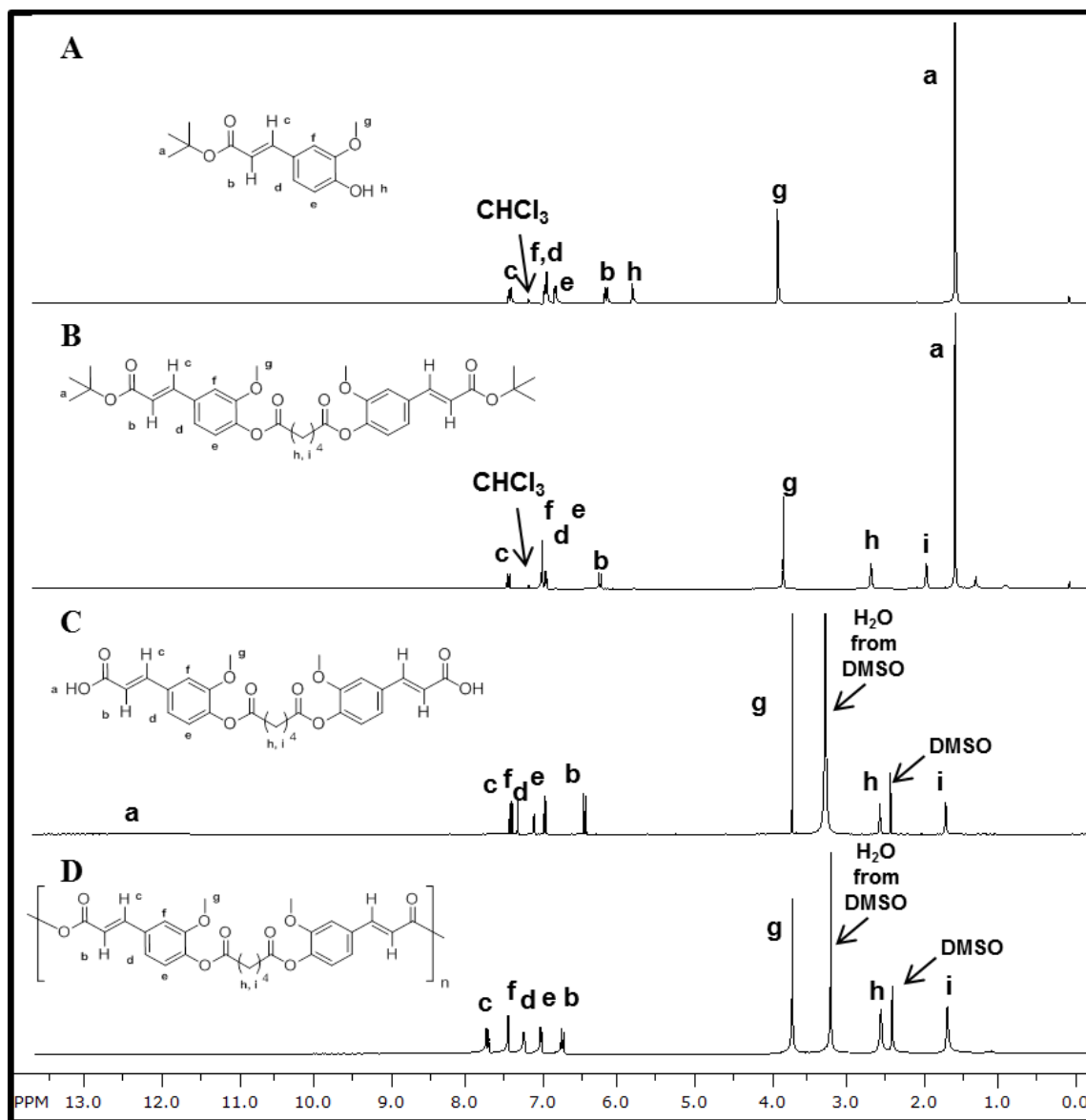
Figure 6.4. ^{1}H NMR spectra of FA-containing polymer and each intermediate step. *t*-Butyl FA, **6.2a** (A), *t*-butyl FA-containing diacid intermediate, **6.3a** (B), FA-containing diacid, **6.4a** (C), and FA-containing polymer, **6.5a** (D) are illustrated above
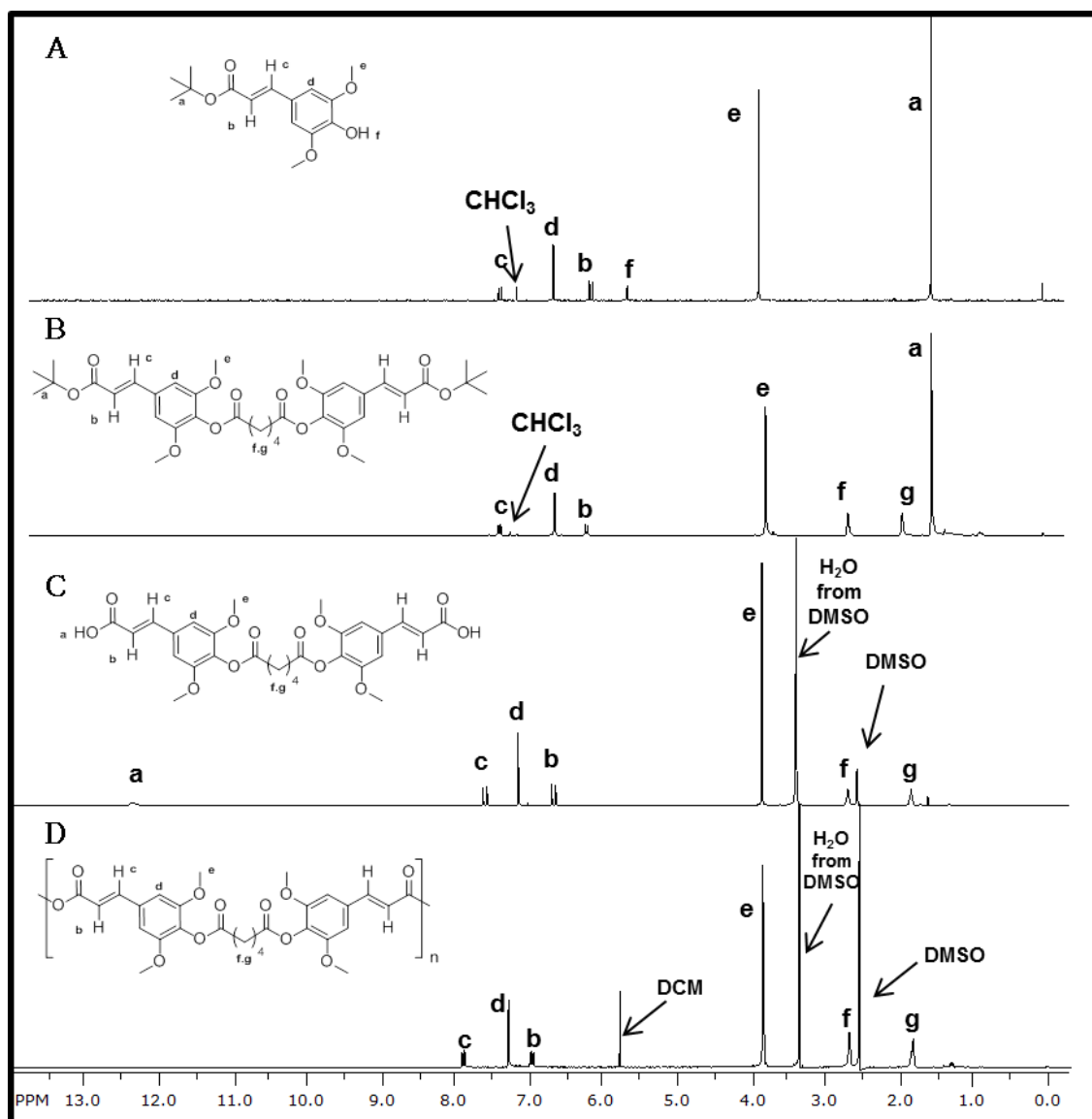
Figure 6.5. ^{1}H NMR spectra of *t*-butyl SinA, **6.2b** (A), *t*-butyl SinA-containing diacid intermediate, **6.3b** (B), SinA-containing diacid, **6.4b** (C), and SinA-containing polymer, **6.5b** (D)

^{1}H NMR spectra confirmed all polymer intermediates and polymer structures shown in Figures 6.4 and 6.5. FA and SinA resulted in successful syntheses; for simplicity, FA is used as an example for descriptive purposes.

Coupling constants between 15.8 and 16 Hz demonstrated that the double bonds are in the *trans* (*E*) configuration, with signals appearing at 7.84 and 6.83 ppm for **6.5** (Figure 6.4D). As depicted in Figure 6.4B, the appearance of signals at 2.67 and 1.92 ppm and the disappearance of the phenol signal (6.06 ppm for **6.2**) indicated successful acyl chloride coupling to FA in a 1:2 ratio (acyl chloride:FA). The disappearance of signals at 1.54 ppm (Figure 6.4C) illustrates the complete removal of the protecting *t*-butyl groups. The FTIR spectrum of **6.4** (Figure 6.6B) indicates coupling of the acyl chloride via ester bond formation (1766 cm^{-1}) and presence of carboxylic acid bands (at 2586 and 1677 cm^{-1} illustrating the alcohol and carbonyl groups of the acid). Spectra for SinA-based systems are depicted in Figure 6.5 and Figure 6.7.
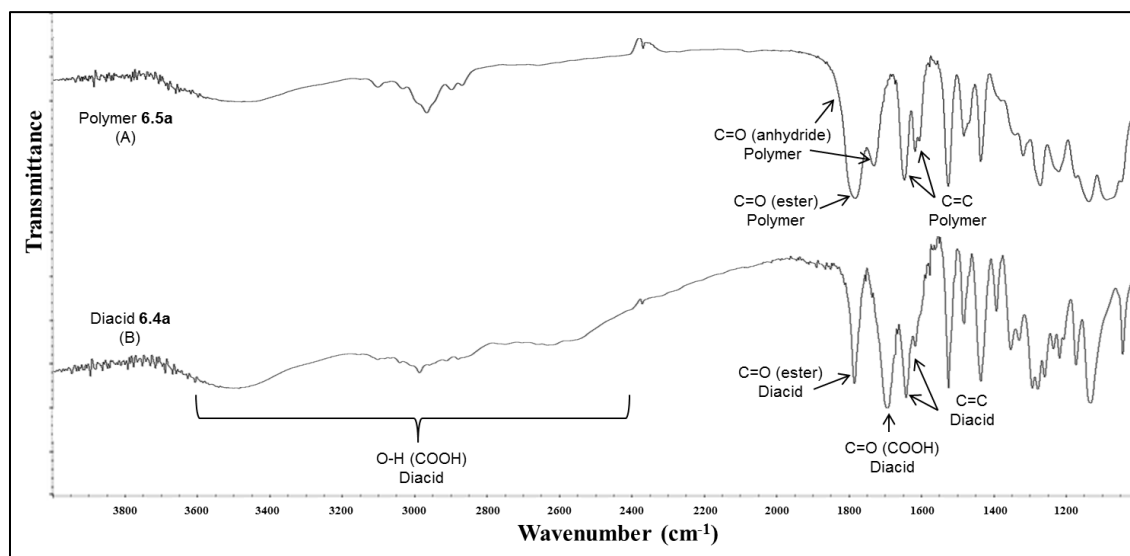
Figure 6.6. FTIR spectra of FA-containing polymer **6.5a** (A, top) and diacid **6.4a** (B, bottom)
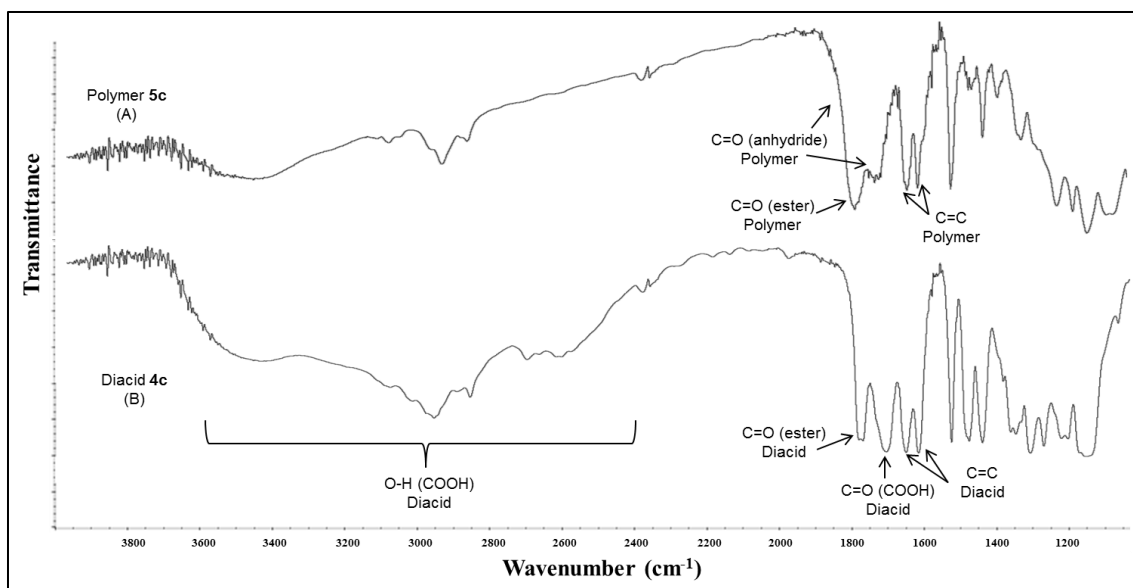
Figure 6.7. FTIR spectra of SinA-containing polymer **6.5b** (A, top) and diacid **6.4b** (B, bottom)

Due to thermal instability of FA and SinA, each diacid **6.4** was used directly for low-temperature solution polymerization using triphosgene as the coupling agent in the presence of triethylamine to form the poly(anhydride-ester) (**6.5**). The HC structure within the polymer was preserved after polymerization as indicated by the ^{1}H NMR spectra (Figures 6.3D and 6.4D) and FTIR spectra (Figure 5A and 6A), illustrating the disappearance of the diacid carboxylic acid peaks, the presence of the anhydride carbonyls and ester preservation between 1800 and 1720 cm^{-1}, and preservation of the double bonds (1600 and 1630 cm^{-1}). As depicted in Table 6.1, the polymers exhibited a M_w ranging from 21,700 to 38,500 Da and relatively narrow polydispersity indices after isolation. Thermal properties of the polymers are favorable as they degrade above 332 °C and exhibit T_g values well above physiological temperature (Table 6.1). The

successful FA and SinA chemical incorporation into a poly(anhydride-ester) backbone allows for high drug loading, where > 80 % of the polymer is the HC, significantly improving upon other researchers' methods.[13-17]

Table 6.1. Properties of HC-based poly(anhydride-esters), **6.5**

	Drug Loading (%)	M_W (Da)	PDI	T_d (°C)	T_g (°C)
Polymer **6.5a**	81	21,700	1.7	332	82
Polymer **6.5b**	80	38,500	1.7	340	101

6.3.2. *In vitro* HC release from polymer

The polymer's *in vitro* degradation (Figure 6.8) was measured by the appearance of FA or SinA in degradation media via HPLC to elucidate release rates from **6.5 (a-b)** to yield **6.1 (a-b)** and biocompatible adipic acid (not detected by HPLC), as depicted in Figure 6.9B and 6.9C. This degradation is integral to improving HC stability and delivery, as the HC release is controlled via anhydride and ester bond hydrolysis. To ascertain whether the polymer would ultimately hydrolyze and release the covalently attached bioactive, *in vitro* degradation was monitored over 30 days using polymer discs.

Previous studies have indicated more rapid anhydride bond hydrolysis than that of ester bonds.[33] Within this study, however, the relative hydrolysis rate was not apparent in the studies performed as diacid (**6.4**) absorbance (retention time of 8.07 min and 7.04 min, for **6.4a** and **6.4b**, respectively (Figure 6.9B,

6.8C)), was minimal at the specified wavelength for HPLC studies. Moreover, the diacid exhibits limited solubility in PBS relative to the HC.

Although diacid was likely present due to anhydride bond hydrolysis, minimal amounts were detected under the conditions studied. FA and SinA detection with a 3.71 min and 3.31 min retention times, respectively, (Figure 6.9B and 6.8C) indicated further hydrolysis of ester bonds. The polymer released 6.2 % FA and 11.1 % SinA (release rates: 0.21 and 0.97 % HC release per day, respectively) over 30 days, as depicted in Figure 6.9A. It is important to note that no decomposition peaks were observed, suggesting the HC compound remains active. However, decomposition peaks were observed at days 16-30 for polymer **6.5b** samples. This observation was likely the cause for the plateau observed in the release curve; noticeably less SinA was released and the degradation media yellowed. After 30 days, thinner substrate were observed from the initial 8 mm diameter x 1 mm thick discs suggesting that complete degradation for these polymers is > 30 days.

$R_1 = OCH_3$ $R_2 = H$ **a**
$R_1 = OCH_3$ $R_2 = OCH_3$ **b**
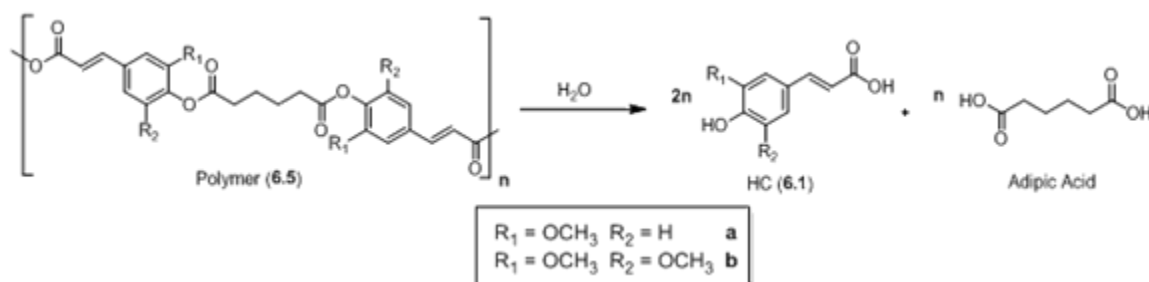
Figure 6.8. Proposed hydrolytic degradation scheme of HC-containing polymers (**6.5**) to yield diacid (**6.4**) and HC (**6.1**)
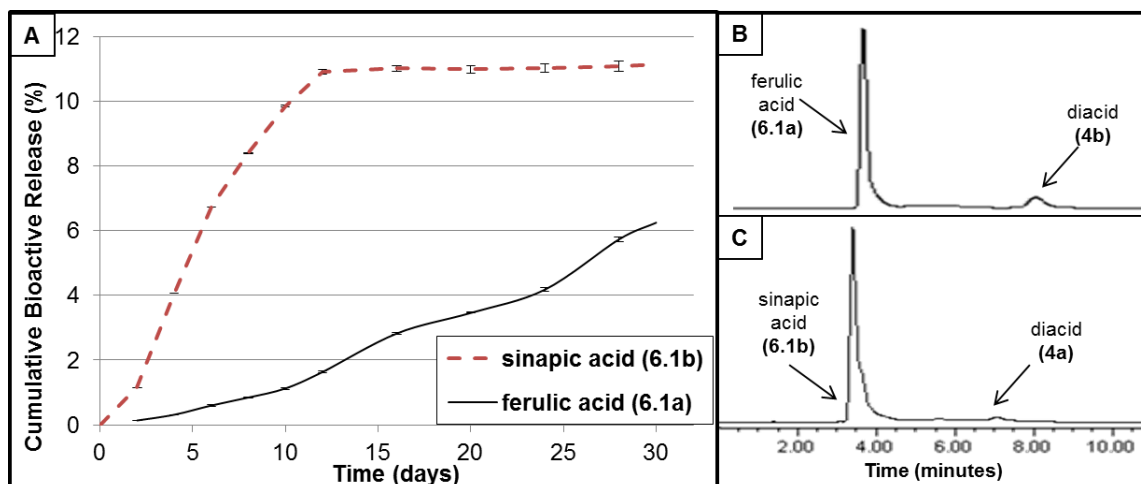
Figure 6.9. *In vitro* HC (**6.1a** and **6.1b**) release from HC-containing poly(anhydride-esters) (**6.5**) (HC ± standard deviation) (A). HPLC chromatographs demonstrating appropriate peaks for FA (**6.1a**) and diacid (**6.4a**) (B) and SinA (**6.1b**) and diacid (**6.4b**) (C) for day 10 samples

As previous poly(anhydride-ester) studies suggest polymer degradation to be pH-dependent,[29] the release medium pH for each sample was monitored to ensure acidic degradation products did not alter the pH. The media pH throughout degradation studies became more acidic, yet only deviated from the initial 7.40 reading by -0.19 ± 0.13 and -0.24 ± 0.05 from **6.5a** and **6.5b**, respectively. Due to these low values, it is expected that the slightly acidic media did not affect release rates.

6.3.3. Radical scavenging (antioxidant) activity

To establish whether polymer processing had an effect on antioxidant activity of released FA, a DPPH radical scavenging assay was employed. DPPH is widely used to assess the ability of antioxidants to scavenge or quench free

radicals or donate a hydrogen atom, causing a color change from violet to pale yellow and a reduction in absorbance.[27, 34, 35] The degradation media antioxidant activity from days 10 (containing all products released from days 8-10) and 20 (containing all products released from days 16-20) were analyzed. These samples were compared to the corresponding free FA and free SinA (**6.1a** and **6.1b**) using freshly prepared solutions with concentrations equal to HPLC data on day 10 (18 ± 1 and 26 ± 1 µg/mL, respectively) and day 20 (52 ± 1 and 0.1 ± 0 µg/mL, respectively) (Figure 9). Comparable concentrations were chosen because the quenching percentage is dependent on the antioxidant concentration.[34]

Student's t-tests comparing degradation media to the free FA solution and free SinA solution were performed ($p < 0.05$). The observed antioxidant activity showed no statistical differences between degradation media and free HC solution for day 10, whereas day 20 degradation media demonstrated significantly higher radical reduction than FA alone, indicating increased quenching (denoted by asterisk in Figure 6.10). In both cases, increased antioxidant activity of degradation media relative to free HC was observed. This result may be due to potential diacid antioxidant activity, as it has the ability to scavenge the free radial similarly to free FA and SinA. Adipic acid (which exhibits minimal antioxidant activity)[36] was present in the degradation media and may have contributed to this increase as well. Further studies must be performed to elucidate the diacid antioxidant activity. From these results, the

polymer degradation products sustain antioxidant activity over time and have not been affected by the synthetic approach utilized.
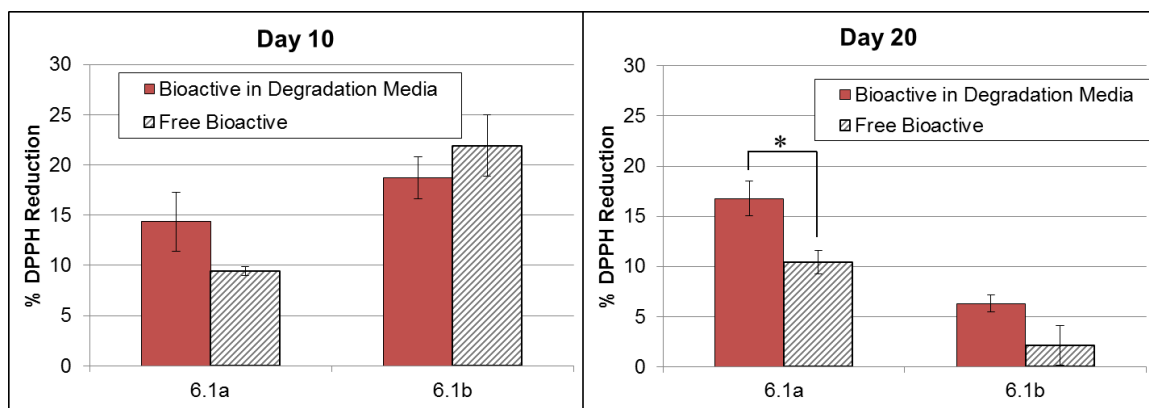
Figure 6.10. DPPH reduction results for bioactive, either FA (**6.1a**) or SinA (**6.1b**) in degradation media and free bioactive for day 10 and day 20 of the release study; statistical difference indicated by * ($p < 0.05$)

6.3.4.   *In vitro* cytotoxicity assay

Assessing the polymer toxicity potential is important if this polymer is to be used for *in vivo* applications. Cytotoxicity of **6.5** was evaluated by culturing fibroblast cells in polymer-containing media at 0.01 and 0.10 mg/mL, as these concentrations are well above those seen *in vitro* and can be used to determine dose dependent toxicity. Studies were performed over a 96 h time period, in which cell proliferation and morphology were observed. For both polymer concentrations (Figure 6.11), pair-wise comparison with Scheffe's post hoc test indicated no significant statistical difference between the polymer and the DMSO media control at the 48, 72, and 96 h time points ($p < 0.05$).
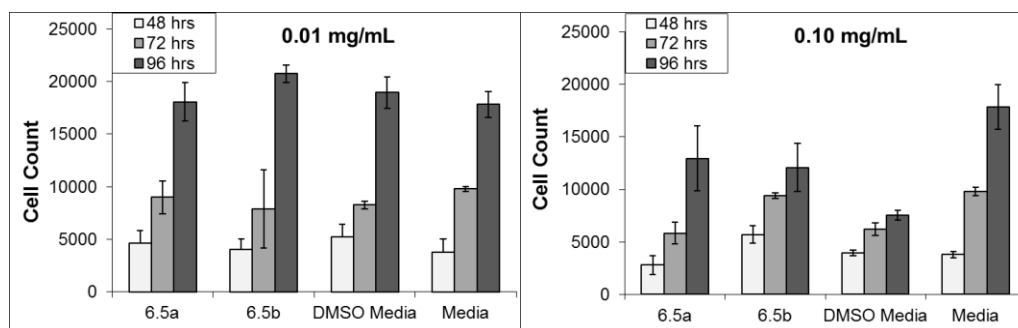
Figure 6.11. Cell viability/proliferation after 48, 72, and 96 h in culture media with the polymer at concentration of 0.01 mg polymer/mL media (A) and 0.10 mg polymer/mL media (B)

For all conditions, the cell morphology images demonstrate the typical proliferation expected of healthy fibroblasts. After 96 h of culture, proliferating viable cells were visible with stellate morphology and extending filopodia. No visible differences were observed in fibroblast morphology for the polymer at the two concentrations and three time points; therefore, under these specific concentrations and conditions, **6.5** can be considered noncytotoxic.

6.3.5.   *In vitro* antibacterial assays

To further assess whether the polymer processing affected the chemically incorporated bioactive and remained active, antibacterial tests were performed against Gram-negative and Gram-positive bacteria. Degradation media from the *in vitro* release studies yielded FA and SinA concentrations too low for antibacterial activity to be observed. Therefore, the polymer was completely hydrolyzed, and a fixed concentration was prepared from the extracted degradation products and compared to free HC activity. Samples dissolved in

DMSO without added bacteria were first examined to ensure contamination did not occur with the solutions; negligible increase of OD_{630nm} indicated no bacteria growth and thus no contamination.

A fixed HC concentration (3 mg/mL) was selected to compare the bacteria susceptibility to free and extracted HC. The extracted powders from **6.5** included both HC (82 %) and adipic acid (18 %); free adipic acid was therefore analyzed for antibacterial activity at the concentrations present in extracted powders (0.66 mg/mL). DMSO concentrations were kept lower than 0.5 % to minimize its inhibitory effect.
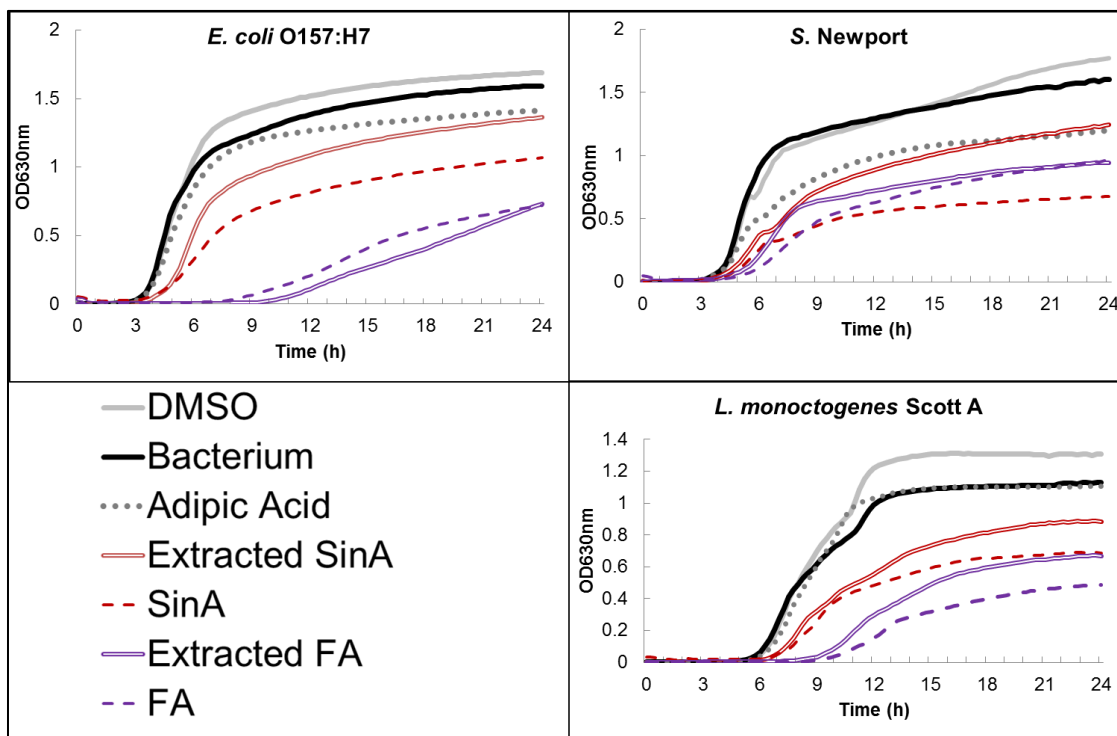
Figure 6.12. Growth curve of treated cells at OD 630nm. *E. coli* O157:H7, *S. Newport*, and *L. monocytogenes* Scott A with DMSO at 0.5 %. Data is presented as an average of triplicate OD measurements from two independent tests.

As depicted in Figure 6.12, free FA, free SinA, and both extracted powders from **6.5** demonstrated antibacterial activity against all three bacteria. Although minimal, adipic acid also demonstrated inhibitory activity. The observed activity showed no statistical differences between free HC and the extracted powder. This assay suggests that both HCs retain their antibacterial activity, further demonstrating that the polymer degradation products did not decompose and have not been affected by the synthetic methods utilized. These results also suggest that the polymer may also be useful as preservative agents in formulations due to its antibacterial activity, but additional studies must be performed.

6.4. Conclusion

By incorporating FA and SinA each into a polymer backbone, the physicochemical stability is improved as the HC is protected from premature degradation. The polymer was found to be hydrolytically degradable, where the degradation products exhibited comparable antioxidant and antibacterial activity to that of free FA and free SinA. The demonstrated controlled release of the chemically incorporated HC with no detectable decomposition suggests that the frequency of antioxidant/photoprotective agent applications can be reduced. The polymers were deemed noncytotoxic in mouse fibroblast cultures at 0.01 and 0.10 mg/mL concentrations, demonstrating the potential for use *in vivo*. The polymer design allows for opportunities to develop tunable HC release profiles; future studies will focus on increasing the bioactive release rate by changing the

acyl chloride in polymer synthesis or formulating the polymer into microspheres to further improve their use for skin care formulations and to perform skin permeation experiments.

6.5. References

1. Ouimet MA, Griffin J, Carbone-Howell AL, Wu WH, Stebbins ND, Di R, Uhrich KE, *Biomacromolecules* **2013**, *14*, 854–61.

2. Svobodova A, Psotova J, Walterova D, *Biomedical Papers* **2003**, *147*, 137-45.

3. El-Seedi HR, El-Said AMA, Khalifa SAM, Göransson U, Bohlin L, Borg-Karlson A-K, Verpoorte R, *J Agr Food Chem* **2012**, *60*, 10877-95.

4. Nuutila A, Kammiovirta K, Oksman-Caldentey K, *Food Chem* **2002**, *76*.

5. Ou S, Kwok K, *J Sci Food Agric* **2004**, *84*, 1261-9.

6. Puupponen-Pimia R, Nohynek L, Meier C, Kahkonen M, Heinonen M, Hopia A, Oksman-Caldentey K, *J Appl Microbiol* **2001**, *90*.

7. Gonzaga ER, *Am J Clin Dermatol* **2009**, *10 Suppl 1*, 19-24.

8. Pannala A, Razaq R, Halliwell B, Singh S, Rice-Evans CA, *Free Radical Bio Med* **1998**, *24*, 594-606.

9. Wang Q, Gao X, Gong H, Lin X, Saint-Leger D, Senee J, *J Cosmet Sci* **2011**, *62*, 483-503.

10. Fiddler W, Parker WE, Wasserman AE, Doerr RC, *J Agr Food Chem* **1967**, *15*, 757-61.

11. Rizzi GP, Boekley LJ, *Journal of Agricultural and Food Chemistry* **1992**, *40*, 1666-70.

12. Li F-Q, Hu J-H, Deng J-X, Su H, Xu S, Liu J-Y, *Int J Pharm* **2006**, *324*, 152-7.

13. Biswick T, Park D-H, Shul Y-G, Choy J-H, *J Phys Chem Solids* **2010**, *71*, 647-9.

14. Biswick T, Park D-H, Shul Y-G, Hwang S-J, Choy J-H, *J Nanosci Nanotechno* **2011**, *11*, 413-6.

15. Karpkird T, Wanichweacharungruang S, *J Photoch Photobio A* **2010**, *212*, 56-61.

16. Hu X, Chen X, Cheng H, Jing X, *J Polym Sci, Part A: Polym Chem* **2009**, *47*, 161-9.

17. Nagata M, Hizakae S, *Macromol Biosci* **2003**, *3*, 412-9.

18. Wattamwar PP, Biswal D, Cochran DB, Lyvers AC, Eitel RE, Anderson KW, Hilt JZ, Dziubla TD, *Acta Biomater* **2012**, *8*, 2529-37.

19. Wattamwar PP, Hardas SS, Butterfield DA, Anderson KW, Dziubla TD, *J Biomed Mater Res Part A* **2011**, *99A*, 184-91.

20. Wattamwar PP, Mo Y, Wan R, Palli R, Zhang Q, Dziubla TD, *Adv Funct Mater* **2010**, *20*, 147-54.

21. Kaneko T, Matsusaki M, Hang TT, Akashi M, *Macromol Rapid Commun* **2004**, *25*, 673-7.

22. Morozowich NL, Nichol JL, Allcock HR, *Chemistry of Materials* **2012**, *24*, 3500-9.

23. Morozowich NL, Nichol JL, Mondschein RJ, Allcock HR, *Polymer Chemistry* **2012**, *3*, 778-86.

24. Uhrich KE, Cannizzaro SM, Langer RS, Shakesheff KM, *Chem Rev* **1999**, *99*, 3181-98.

25. Hu WX, Xia CN, Wang GH, Zhou W, *J Chem Res-S* **2006**, 586-8.

26. Schmeltzer R, Johnson M, Griffin J, Uhrich K, *J Biomat Sci Polym Ed* **2008**, *19*, 1295-306.

27. Scherer R, Godoy H, *Food Chem* **2009**, *112*, 654-8.

28. Duncan E, Lemons J, Mayesh J, Saha P, Saha S, Scranton M. In New products and standards in biomaterials science. New York: Elsevier Academic Press; 2004.

29. Schmeltzer RC, Schmalenberg KE, Uhrich KE, *Biomacromolecules* **2005**, *6*, 359-67.

30. Carbone AL, Song M, Uhrich KE, *Biomacromolecules* **2008**, *9*, 1604-12.

31. Fischer D, Li YX, Ahlemeyer B, Krieglstein J, Kissel T, *Biomaterials* **2003**, *24*, 1121-31.

32. Standardization IOf, International C, Canada SCo. In Biological Evaluation of Medical Devices. Part 5, Tests for in Vitro Cytotoxicity: CSA International; 2001.

33. Erdmann L, Uhrich KE, *Biomaterials* **2000**, *21*, 1941-6.

34. Brand-Williams W, Cuvelier ME, Berset C, *LWT-Food Sci Technol* **1995**, *28*, 25-30.

35. Molyneux P, *Songklanakarin Journal of Science and Technology* **2004**, *26*, 211-9.

36. Papadopoulos K, Triantis T, Dimotikali D, Nikokavouras J, *Anal Chim Acta* **2001**, *433*, 263-8.

CHAPTER 7: FERULIC ACID-CONTAINING POLYMERS WITH GLYCOL FUNCTIONALITY FOR TAILORING PHYSICOCHEMICAL PROPERTIES AND RELEASE PROFILES

7.1. Introduction

Currently, significant evidence demonstrates the role of antioxidants in protecting cells from free radical species.[1] Free radicals have been identified as major sources of oxidative stress in cells leading to DNA damage.[1] This increased oxidative stress has been implicated in various deleterious conditions including cardiovascular diseases, neurodegenerative diseases, and cancer,[2] while also contributing to the physiology of ageing.[3] The human body combats this oxidative stress by employing antioxidants made in the body or acquired from diet and/or supplements.[4, 5] These antioxidants, however, are usually at insufficient levels to overcome the damage from oxidative stress accumulation. Therefore, much effort is focused on developing topical antioxidants with photoprotective and therapeutic efficacy.
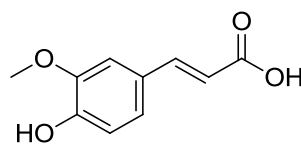
ferulic acid, **7.1**

Figure 7.1. Chemical structure of the bioactive, ferulic acid

Ferulic acid (Figure 7.1) is a hydroxycinnamic acid and potent ubiquitous plant antioxidant due to its phenolic and extended side chain conjugation, which forms a resonance-stabilized phenolic radical.[6] Ferulic acid has been studied as an ultra-violet absorber for enhanced skin protection against photodamage and approved as a sunscreen in Japan.[7] While ferulic acid can be quite useful, its limited elimination half-life (less than 2 hours)[8] and stability issues (degradation over time) lower its efficacy in current formulations.[9] Ferulic acid delivery can thus be improved by incorporation into a biodegradable polymer backbone,[10] enabling controlled bioactive release and preventing the active functional groups from degradation,[9, 10] as discussed in Chapter 6. In this previously designed polymer, ferulic acid was stabilized (i.e., degradation and discoloration did not occur) and antioxidant activity was comparable to that of the free bioactive, indicating ferulic acid maintained its bioactivity over time.[10]

Although this polymer demonstrated that ferulic acid could be stabilized via covalent incorporation into a polymer backbone, limited amounts of ferulic acid were released upon polymer degradation over the timeframe studied. A means to increase polymer degradation rates is to incorporate ethylene glycol functionalities into the polymer via copolymerization with poly(ethylene glycol) (PEG)[11-13] or to incorporate ethylene glycol groups within the monomer unit.[14, 15] In this work, ethylene glycol groups were employed as the linker molecule between two ferulic acid molecules allowing for increased hydrophilicity and modified polymer physicochemical properties.

Based on trends established from previous ethylene glycol incorporation research, [14, 15] we developed ferulic acid-containing biodegradable polymers with ethylene glycol as a linker molecule. Through incorporating glycol groups into the polymer backbone, we hypothesized increased degradation rates due to enhanced hydrophilic behavior. The synthesis, characterization, and drug release profiles of the glycol-modified polymers are discussed.

7.2. Experimental

7.2.1. Materials

1 N HCl, poly(vinylidine fluoride) and polytetrafluoroethylene syringe filters, and Wheaton glass scintillation vials were purchased from Fisher Scientific (Fair Lawn, NJ). All other reagents, solvents, and fine chemicals were purchased from Aldrich (Milwaukee, WI) and used as received.

7.2.2. ^{1}H and ^{13}C NMR and FTIR spectroscopies

^{1}H and ^{13}C NMR spectra were recorded on a Varian 400 MHz or 500 MHz spectrometer using deuterated chloroform (CDCl$_3$) with trimethylsilane (TMS) as internal reference or deuterated dimethyl sulfoxide (DMSO-d_6) as solvent and internal reference. FTIR spectra were obtained using a Thermo Nicolet/Avatar 360 spectrometer, samples (1 wt %) ground and pressed with KBr into a disc. Each spectrum was an average of 32 scans.

7.2.3.　　　Molecular weight

Polymer precursors were analyzed via mass spectrometry to determine molecular weights. A Finnigan LCQ-DUO equipped with Xcalibur software and an adjustable atmospheric pressure ionization electrospray ion source (API-ESI Ion Source) was used with a pressure of 0.8×10^{-5} and 150 °C API temperature. Samples dissolved in methanol (< 10 µg/mL) were injected with a glass syringe. GPC was used to determine polymer weight-averaged molecular weight and polydispersity using a Perkin-Elmer liquid chromatography system consisting of a Series 200 refractive index detector, a Series 200 LC pump, and an ISS 200 autosampler. Automation of the samples and processing of the data was performed using a Dell OptiPlex GX110 computer running Perkin-Elmer TurboChrom 4 software with a Perkin-Elmer Nelson 900 Series Interface and 600 Series Link. Polymer samples were prepared for autoinjection by dissolving in dichloromethane (DCM, 10 mg/mL) and filtering through 0.45 µm polytetrafluoroethylene syringe filters. Samples were resolved on a Jordi divinylbenzene mixed-bed GPC column (7.8 x 300 mm, Alltech Associates, Deerfield, IL) at 25 °C, with DCM as the mobile phase at a flow rate of 1.0 mL/min. Molecular weights were calibrated relative to broad polydispersity polystyrene standards (Polymer Source Inc., Dorval, Canada).

7.2.4.　　　Thermal properties

DSC measurements were carried out on TA Instrument Q200 to determine melting (T_m) and glass transition (T_g) temperatures. Measurements on samples

(4-6 mg) heated under nitrogen atmosphere from $-10\ °C$ to $200\ °C$ at a heating rate of $10\ °C/min$ and cooled to $-10\ °C$ at a rate of $10\ °C/min$ with a two-cycle minimum were performed. TA Instruments Universal Analysis 2000 software, version 4.5A was used to analyze the data. T_m values were measured at the onset of melting and T_g values were calculated as half Cp extrapolated. TGA was utilized for determining decomposition temperatures (T_d) using a Perkin-Elmer Pyris 1 system with TAC 7/DX instrument controller and Perkin-Elmer Pyris software for data collection. Samples (5-10 mg) were heated under nitrogen atmosphere from $25\ °C$ to $400\ °C$ at a heating rate of $10\ °C/min$. Decomposition temperatures were measured at the onset of thermal decomposition.
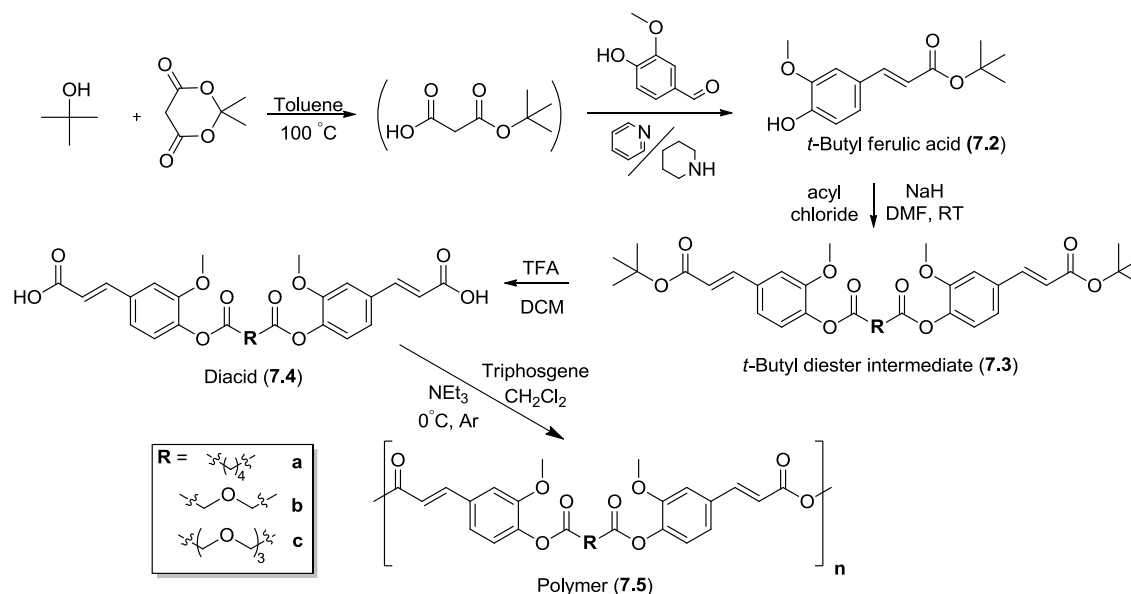
Figure 7.2. Synthesis of ferulic acid-containing poly(anhydride-esters) (**7.5**) and ferulic acid-containing polymer precursors including diacids (**7.4**) and t-butyl intermediates (**7.3**) with varying linkers (**a**[10], **b**, **c**)

7.2.5.   *t*-Butyl ferulic acid synthesis (7.2)

This compound was prepared according to previously published methods (Figure 7.2, **7.2**).[10, 16]

7.2.6.   t-Butyl ferulic acid-containing diester synthesis (7.3)

t-Butyl ferulic acid (**7.2**) (2 eq) was dissolved in anhydrous dimethylformamide (DMF) to which sodium hydride (NaH, 2.2 eq) was added slowly. After 30 minutes, acyl chloride (1 eq) dissolved in 10 mL DMF was added drop-wise at 20 mL/hr. Reaction progress was monitored by thin layer chromatography (5:1 hexane:ethyl acetate as eluent). Once completed, the reaction mixture was diluted with ethyl acetate (250 mL) and washed with deionized water (2 x 100 mL). The organic layer was collected, dried over MgSO$_4$, and the solvents removed *in vacuo*. This reaction mixture was purified on silica gel via flash chromatography using 5:1 hexane:ethyl acetate as eluent.

7.2.6.1.   *t*-Butyl ferulic acid-containing (diglycolic) diester (7.3b)

Diglycolyl chloride (1 eq) was used as the acyl chloride to prepare **7.3b**. Yield: 82 % (white powder). ^{1}H-NMR (400 MHz, CDCl$_3$): δ 7.56 (d, 2H, *J*=16.0 Hz, R-CH=CH-R), 7.10 (s, 2H, Ar-H), 7.09 (d, 2H, Ar-H), 7.08 (d, 2H, Ar-H), 6.34 (d, 2H, *J*=16.0 Hz, R-CH=CH-R), 4.62 (s, 4H, CH$_2$), 3.86 (s, 6H, OCH$_3$), 1.54 (s, 18H, 3CH$_3$). ^{13}C-NMR (CDCl$_3$): δ 167.9, 166.3, 151.3, 142.8, 140.7, 134.3, 123.2, 121.4, 120.9, 111.3, 80.9, 68.1, 56.2, 28.4. T$_m$: 222-223 ºC.

7.2.6.2.　　*t*-Butyl ferulic acid-containing (tetraglycolic) diester (7.3c)

To prepare the acyl chloride, 3,6,9-trioxaundecanedioic acid, termed tetraglycolic acid, (1 eq) was reacted neat in thionyl chloride (8 eq) and heated to reflux for 24 hours to yield a yellow liquid, termed "tetraglycolyl dichloride." Tetraglycolyl dichloride (1 eq) was used directly as the acyl chloride to prepare **7.3c**. Yield: 78 % (beige powder). ^{1}H-NMR (400 MHz, CDCl$_3$): δ 7.55 (d, 2H, *J*=16.0 Hz, R-CH=CH-R), 7.10 (s, 2H, Ar-H), 7.08 (d, 2H, Ar-H), 7.06 (d, 2H, Ar-H), 6.32 (d, 2H, *J*=16.0 Hz, R-CH=CH-R), 4.45 (s, 4H, CH$_2$), 3.84 (s, 6H, OCH$_3$), 3.78 (t, 4H, CH$_2$), 3.76 (t, 4H, CH$_2$), 1.54 (s, 18H, 3CH$_3$). ^{13}C-NMR (CDCl$_3$): δ 168.6, 166.3, 151.4, 142.9, 141.2, 134.1, 123.2, 121.3, 120.8, 111.3, 80.9, 71.2, 70.9, 68.6, 56.1, 28.4. T$_m$: 239-242 ºC.

7.2.7.　　Ferulic acid-containing diacid synthesis (7.4)

To prepare diacid (**7.4**), compound **7.3** (1 eq) was dissolved in anhydrous DCM to which trifluoroacetic acid (TFA) (40 eq) was added and stirred over-night at room temperature. Solvent was removed *in vacuo* and the residue was triturated with DI water (300 mL), isolated via vacuum filtration, and dried *in vacuo* for 24 hours.

7.2.7.1.　　Ferulic acid-containing (diglycolic) diacid (7.4b)

Yield: 84 % (white powder). ^{1}H-NMR (500 MHz, DMSO-*d$_6$*): δ 12.43 (s, 2H, COOH), 7.58 (d, 2H, *J*=16.0 Hz, R-CH=CH-R), 7.51 (s, 2 H, Ar-H), 7.29 (d, 2H, Ar-H), 7.20 (d, 2H, Ar-H), 6.60 (d, 2H, *J*=16.0 Hz, R-CH=CH-R), 4.60 (s, 4H,

CH$_2$), 3.84 (s, 6H, OCH$_3$). ^{13}C-NMR (DMSO-d_6): δ 171.6, 168.3, 151.8, 144.0, 141.5, 133.9, 123.8, 122.1, 120.2, 112.5, 56.6, 33.5, 24.4. IR (KBr, cm^{-1}): 3000-2500 (OH, COOH), 1752 (C=O, ester), 1696 (C=O, COOH), 1633 and 1600 (C=C). T$_m$: 241-244 ⁰C. ESI-MS *m/z*: 485 *z-1*.

7.2.7.2.   Ferulic acid-containing (tetraglycolic) diacid (7.4c)

Yield: 98 % (white crystals). ^{1}H-NMR (500 MHz, DMSO-d_6): δ 12.40 (s, 2H, COOH), 7.51 (d, 2H, *J*=16.0 Hz, R-CH=CH-R), 7.41 (s, 2 H, Ar-H), 7.18 (d, 2H, Ar-H), 7.08 (d, 2H, Ar-H), 6.52 (d, 2H, *J*=16.0 Hz, R-CH=CH-R), 4.35 (s, 4H, CH$_2$), 3.74 (s, 6H, OCH$_3$), 3.62 (t, 4H, CH$_2$), 3.54 (t, 4H, CH$_2$). ^{13}C-NMR (DMSO-d_6): δ 169.0, 168.3, 151.7, 144.0, 140.9, 134.2, 123.8, 122.1, 120.4, 112.7, 70.8, 70.3, 68.1, 56.8. IR (KBr, cm^{-1}): 2920 (OH, COOH), 1780 (C=O, ester), 1690 (C=O, COOH), 1630 and 1600 (C=C). T$_m$: 86-89 ⁰C. ESI-MS *m/z*: 597 [*z* + Na]

7.2.8.   Ferulic acid-containing polymer synthesis (7.5)

Polymer (**7.5**) was prepared using a modified version of a previously described procedure (Figure 7.2).[17]   Diacid 4 (1 eq) was dissolved in 20 mL anhydrous DCM under argon. After adding triethylamine (NEt$_3$, 4.4 eq), the reaction mixture was cooled to 0 °C. Triphosgene (0.33 eq) dissolved in 10 mL anhydrous DCM was added drop-wise (20 mL/h). The reaction was allowed to stir at 0 °C until CO$_2$ evolution ceased (ca. 6 h). The reaction mixture was poured over chilled diethyl ether (400 mL) and the precipitate was isolated via vacuum filtration. The residue was dissolved in anhydrous DCM, washed with

acidic water (1 x 250 mL), dried over $MgSO_4$, concentrated, and precipitated with an excess of chilled diethyl ether (500 mL). Ether was filtered off via vacuum filtration and polymer dried *in vacuo* at room temperature.

7.2.8.1. Ferulic acid-containing (diglycolic) polymer (7.5b)

Yield: 84 % (white powder). ^{1}H-NMR (500 MHz, DMSO-d_6): 7.93 (d, 2H, *J*=16.0 Hz, R-CH=CH-R), 7.66 (s, 2 H, Ar-H), 7.45 (d, 2H, Ar-H), 7.28 (d, 2H, Ar-H), 6.94 (d, 2H, *J*=16.0 Hz, R-CH=CH-R), 4.63 (s, 4H, CH_2), 3.86 (s, 6H, OCH_3). ^{13}C-NMR (DMSO-d_6): δ 168.3, 163.4, 151.8, 148.7, 141.8, 133.6, 124.0, 123.2, 118.0, 113.4, 67.9, 56.9. IR (KBr, cm^{-1}): 1780-1710 (C=O, anhydride and ester region), 1630 and 1600 (C=C). M_w = 18,300 Da, PDI = 1.3. T_g = 108 °C. T_d = 338 °C.

7.2.8.2. Ferulic acid-containing (tetraglycolic) polymer (7.5c)

Yield: 90 % (light beige powder). ^{1}H-NMR (500 MHz, DMSO-d_6): 7.87 (b, 2H, *J*=16.0 Hz, R-CH=CH-R), 7.58 (b, 2 H, Ar-H), 7.38 (b, 2H, Ar-H), 7.20 (b, 2H, Ar-H), 6.86 (b, 2H, *J*=16.0 Hz, R-CH=CH-R), 4.42 (b, 4H, CH_2), 3.81 (b, 6H, OCH_3), 3.66 (b, 4H, CH_2), 3.48 (b, 4H, CH_2). ^{13}C-NMR (DMSO-d_6): δ 168.9, 163.3, 151.8, 148.6, 141.8, 133.4, 124.0, 123.1, 117.9, 113.2, 70.8, 70.3, 68.1, 59.8. IR (KBr, cm^{-1}): 1800-1710 (C=O, anhydride and ester region), 1630 and 1600 (C=C). M_w = 15,400 Da, PDI = 1.4. T_g = 49 °C. T_d = 251 °C.

7.2.9.   Relative diacid hydrophilicity

A polymeric reverse-phase C_{18} (RP18) column was used to measure the diacid hydrophilicity.[18, 19] Studies were performed on an XTerra® RP18 5 μm 4.6x150 mm column (Waters, Milford, MA) on a Waters 2695 Separations Module equipped with a Waters 2487 Dual λ Absorbance Detector using a mobile phase consisting of 50 mM KH_2PO_4 with 1 % formic acid in DI water at pH 2.5 (65 %) and acetonitrile (35 %) run at 1 mL/min flow rate at ambient temperature using λ = 255 and 275 nm for reference samples and λ = 320 nm for diacid samples. HPLC was performed after all samples were filtered using 0.22 μm poly(vinylidine fluoride) syringe filters and subsequently injected (20 μL) using an autosampler. Samples were prepared in phosphate buffered saline (PBS). The phase preference is expressed by capacity factor k', where k' can be calculated using Equation 7.1, and t_R and t_0 are the retention times of the sample and solvent, respectively.

$$k' = (t_R - t_0) / t_0 \qquad \text{Equation 7.1}$$

$$log\ P_{o,w} = slope * log\ k' + y\text{-}intercept \qquad \text{Equation 7.2}$$

Toluene, thymol, anisole, and benzyl alcohol were used as reference samples and their retention times obtained. A calibration curve was generated using published log $P_{o,w}$ values[19] for the reference samples plotted on the y – axis

and calculated log k' values for the x – axis. This curve was used to find the extrapolated log P diacid values of the regression line using equation 7.2.

7.2.10.   Contact angle measurements for polymer

Static contact angles were measured by dropping deionized water onto pressed polymer discs using a Ramé-Hart Standard Goniometer Model Number 250-00 156 (Mountain Lakes, NJ) outfitted with a Dell Dimension 3000 computer with DROPimage Advanced software. Six data points were obtained per sample.

7.2.11.   *In vitro* ferulic acid release

Polymer degradation was measured as a function of ferulic acid release. Triplicate samples of polymer discs were prepared by pressing ground polymer (50 ± 5 mg) into 8 mm diameter x 1 mm thick discs in an IR pellet die (International Crystal Laboratories, Garfield, NJ) with a bench-top hydraulic press (Carver model M, Wabash, IN). Pressure of 10,000 psi was applied for 10 min at room temperature. This methodology was preferred as it minimized interferences from external effects (e.g., formulation additives) on polymer degradation. The PBS pH was adjusted to 7.40 using 1 N sodium hydroxide. All pH measurements were performed using an Accumet® AR15 pH meter (Fisher Scientific, Fair Lawn, NJ).

Ferulic acid release was monitored by placing polymer discs into 20 mL Wheaton glass scintillation vials with 10 mL of PBS and incubated at 37 ºC with agitation at 60 rpm using a controlled environment incubator-shaker (New

Brunswick Scientific Co., Edison, NJ). Media was collected every 24 hours for 20 days and replaced with fresh PBS (10 mL). Spent media was analyzed via high-performance liquid chromatography (HPLC). The degradation products were analyzed and quantified via HPLC using an XTerra® RP18 5 µm 4.6x150 mm column (Waters, Milford, MA) on a Waters 2695 Separations Module equipped with a Waters 2487 Dual λ Absorbance Detector. All samples were filtered using 0.22 µm poly(vinylidine fluoride) syringe filters and subsequently injected (20 µL) using an autosampler. The mobile phase was comprised of 50 mM KH_2PO_4 with 1 % formic acid in DI water at pH 2.5 (65 %) and acetonitrile (35 %) run at 1 mL/min flow rate at ambient temperature. Absorbance was monitored at λ = 320 nm. Amounts were calculated from known concentrations of standard ferulic acid solutions.

7.2.12.   Antioxidant activity

The antioxidant activity of polymer degradation products were compared to free ferulic acid using a 2,2-diphenyl-1-picrylhydrazyl (DPPH) radical scavenging assay. Antioxidant activity was evaluated by adding sample (0.1 mL) to a 0.024 mg/mL DPPH solution in methanol (3.9 mL). Day-10 samples (0.1 mL) from the each polymer degradation media were mixed with the 0.024 mg/mL DPPH solution (3.9 mL) at room temperature. After 1 hour, solutions were analyzed via UV/vis with a Perkin-Elmer Lambda XLS spectrophotometer (Waltham, MA) (λ = 517 nm). Fresh ferulic acid solutions prepared at specific concentrations corresponding to day-10 HPLC data were each identically

analyzed to the degradation media samples. DPPH % radical reduction was calculated by: $[(Abs_{t0} - Abs_t)/Abs_{t0}] \times 100$, where Abs_{t0} is the initial absorbance and Abs_t is the absorbance after 1 hour. Absorbance values from adding PBS (0.1 mL) to the DPPH solution (3.9 mL) was used as Abs_{t0}. All radical scavenging assays were performed in triplicate. Student's t-tests were performed to determine significant differences between free ferulic acid and degradation media antioxidant activity ($p < 0.05$).

7.3.   Results and Discussion

7.3.1.   Synthesis and characterization

Polymers were successfully prepared by chemically incorporating ferulic acid into the backbone via ester and anhydride bonds. The commercial availability of diglycolyl chloride simplified **7.3b** synthesis. Although tetraglycolyl chloride was not commercially available, tetraglycolic acid, which was commercially available, was chlorinated using thionyl chloride to obtain a dichlorinated molecule. The acyl chlorides (both tetraglycolic and diglycolic) were then separately reacted with *t*-butyl ferulic acid to yield **7.3**, (Figure 7.2) whose structure was confirmed using ^{1}H NMR spectroscopy (Figures 7.3A and 7.4A). The ferulic acid-containing diesters (**7.3**) were subsequently deprotected using TFA, as denoted by the *t*-butyl group disappearance at 1.54 ppm (Figures 7.3B and 7.4B). The synthesized diacid (**7.4**) underwent solution polymerization using triphosgene as

a coupling agent to yield polymer (Figures 7.3C and 7.4C) and structural integrity confirmed.

Table 7.1. Polymer characterizations including drug loading percentage, M_W, PDI, T_g, T_d, and contact angle measurements

	Drug loading (%)	M_w (Da)	PDI	T_g (°C)	T_d (°C)	Contact angle (degrees)
7.5a[10]	81	21,700	1.7	82	332	52
7.5b	79	18,300	1.3	108	338	34
7.5c	67	15,400	1.4	49	251	17
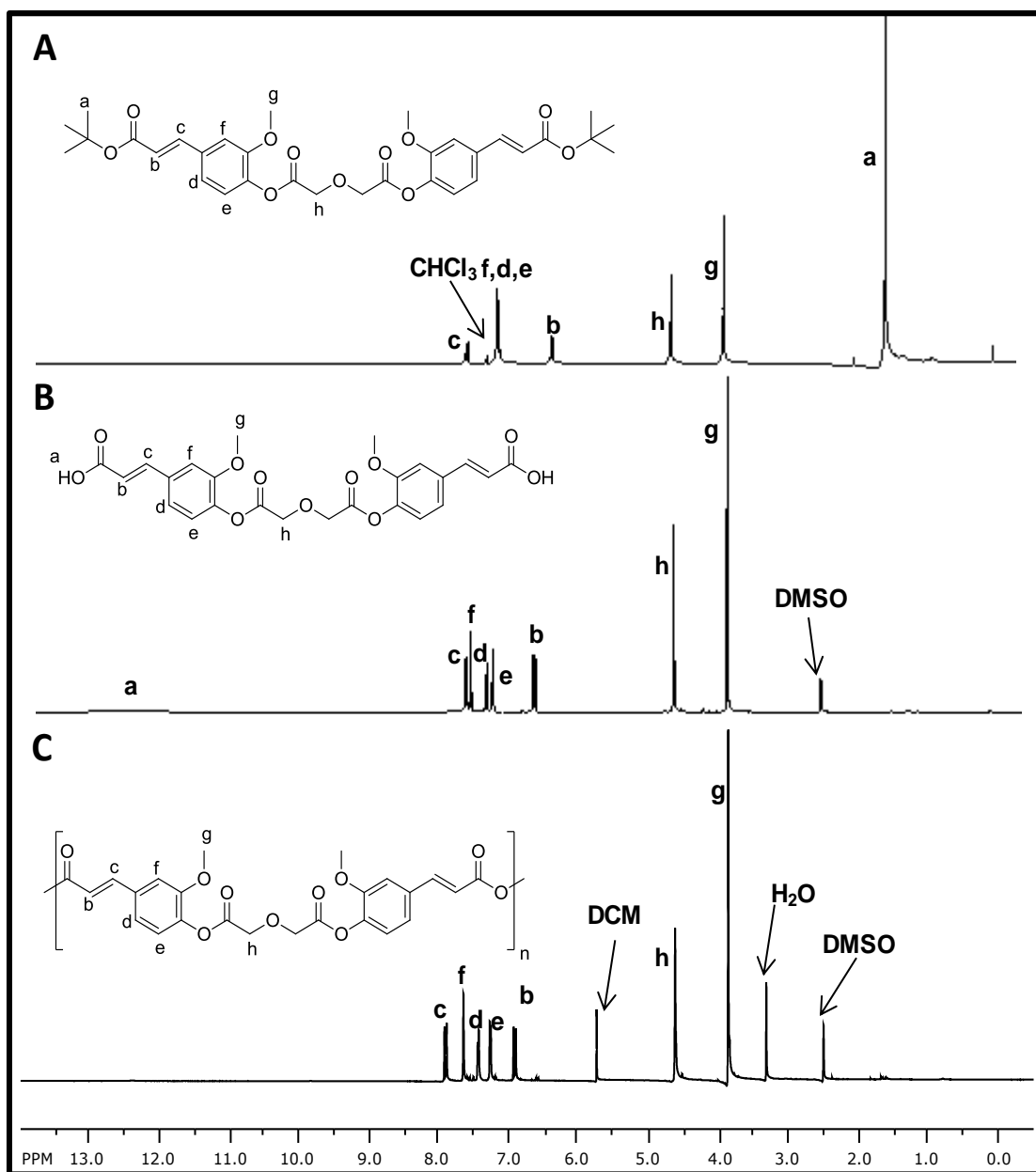
Figure 7.3. ¹H NMR spectra of ferulic acid (diglycolic) polymer and each intermediate step. *t*-Butyl ferulic acid (diglycolic) diester **7.3b** (A), ferulic acid (diglycolic) diacid **7.4b** (B), and ferulic acid (diglycolic) polymer, **7.5b** (C) spectra are illustrated above
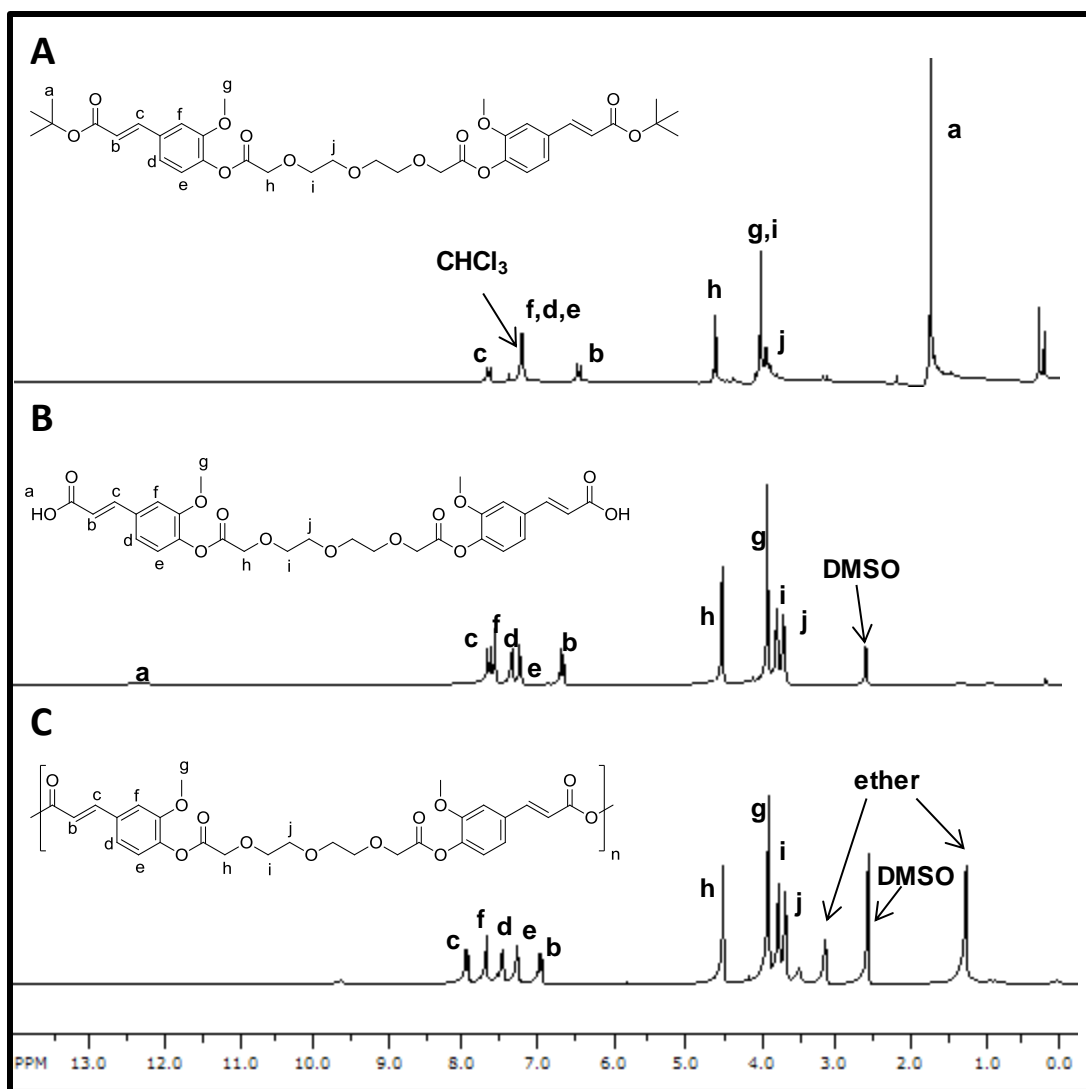
Figure 7.4. ^{1}H NMR spectra of ferulic acid (tetraglycolic) polymer and each intermediate step. *t*-Butyl ferulic acid (tetraglycolic) diester **7.3c** (A), ferulic acid (tetraglycolic) diacid **7.4c** (B), and ferulic acid (tetraglycolic) polymer, **7.5c** (C) spectra are illustrated above

Polymers were obtained with M_W values ranging from 15,800 – 21,700 Da with 1.3 – 1.7 PDI values. Ferulic acid loading was influenced by the different linker molecules; as linker mass increased, the relative amount of ferulic acid

chemically incorporated in the polymer backbone decreased giving a **7.5a** > **7.5b** > **7.5c** drug loading trend. Glass transition (T_g) and decomposition (T_d) temperatures decreased with increasing linker chain length, following the trend **7.5b** > **7.5a** > **7.5c**, due to the polymers' enhanced flexibility with increasing linker chain lengths. For example, **7.5c**, having the greatest linker chain length, was the most flexible polymer and exhibited the lowest T_g value (T_g = 44 ºC). Similarly, **7.5a**, having an intermediate chain length, exhibited a T_g value (T_g = 80 ºC) higher than that of **7.5c** (T_g = 44 ºC) but lower than that of **7.5b** (T_g = 108 ºC).

7.3.2. Relative diacid hydrophilicity

Measuring the diacid (**7.4**) water solubility and relative hydrophilicity proved difficult as diacid quickly degraded into ferulic acid. Therefore, an HPLC-based log P extrapolation method was used. After the diacid retention times were obtained using HPLC (Table 7.2), capacity factor (k') values could be calculated by Equation 7.1 and used to extrapolate the diacids' (**7.4a-c**) log P values. The log P value indicates how a compound partitions between two immiscible phases such as octanol and water; a higher log P value signifies a compound that is more soluble in octanol and correlating to a decreased hydrophilicity. The calculated log P values in Table 7.2 demonstrate a trend where **7.4a** < **7.4b** < **7.4c**, suggesting that hydrophilicity increases as the number of heteroatoms within the linker molecule increases.

Table 7.2. Calculated log P values for diacid molecules (**7.4**)

Sample	Retention time (min)	Calculated log P values
7.4a	19.2	2.2
7.4b	15.4	2.0
7.4c	12.9	1.8

7.3.3.   Contact angle measurements

To evaluate relative hydrophilicity as a factor that may influence ferulic acid release rates, static contact angles were measured by dropping deionized water onto a pressed polymer disc surface.   The polymers were found to be relatively hydrophobic with contact angles ranging from 52 – 17 degrees (Table 1). As oxygen content increased, relative hydrophilicity increased as indicated by the decrease in contact angle, which is in accordance with other published glycol-containing polyanhydrides.[11]   During measurements, the water droplet on the pressed polymer **5c** disc gradually expanded, whereas the water droplets on **7.5a** and **7.5b** discs remained stagnant, further indicating increased hydrophilicity as oxygen content increased.   Relative hydrophilicity may influence the degradation rate and subsequent bioactive release, as water penetration into the polymeric matrix is an important factor in degradation of polyanhydrides.[20, 21] Polymer **7.5a** exhibited the lowest contact angle value and thus was expected to exhibit the fasted release rates relative to polymers **7.5b** and **7.5c**.

7.3.4. *In vitro* ferulic acid release

Polymer degradation was measured by quantifying ferulic acid (**7.1**) in degradation media as **7.1** appearance indicates both anhydride and ester bond hydrolysis. Discs were used to enable uniform polymer degradation conditions without additional formulation steps, which may alter polymer degradation and thus **7.1** release. Relative hydrolysis rates of the hydrolytically labile bonds were not apparent as diacid absorbance (R_t = 15.35 and 12.92 min for **7.4b** and **7.4c**, respectively) was minimal at the observed wavelengths. Detection of **7.1** (R_t = 2.98 min) indicated complete ester and anhydride bond hydrolysis with no decomposition peaks observed.

As observed in Figure 7.5, by day 14, cumulative ferulic acid release reached 100 %, 76 %, and 3 % release for polymers **7.5c**, **7.5b**, and **7.5a**, respectively. Ferulic acid release was minimal for **7.5a**, given that **7.5a** was the most hydrophobic polymer tested. This polymer also exhibited a 10-day lag period of minimal-to-no ferulic acid release. Polymer **7.5b** exhibited a linear release profile throughout its 20-day release profile, which is a typical zero-order release profile for polyanhydrides. Incorporating more than one glycol functionality into the polymer backbone resulted in a logistic, or S-shaped curve for polymer **7.5c**, which was similar to other oxygen-containing polymers.[15] Additionally, an initial state of swelling was visually observed for **7.5c** that was not apparent for **7.5a** or **7.5b**. This observed increased water content results in an increase in volume,[22] and likely stemmed from the ethylene glycol groups' ability to hydrogen bond and attract water.
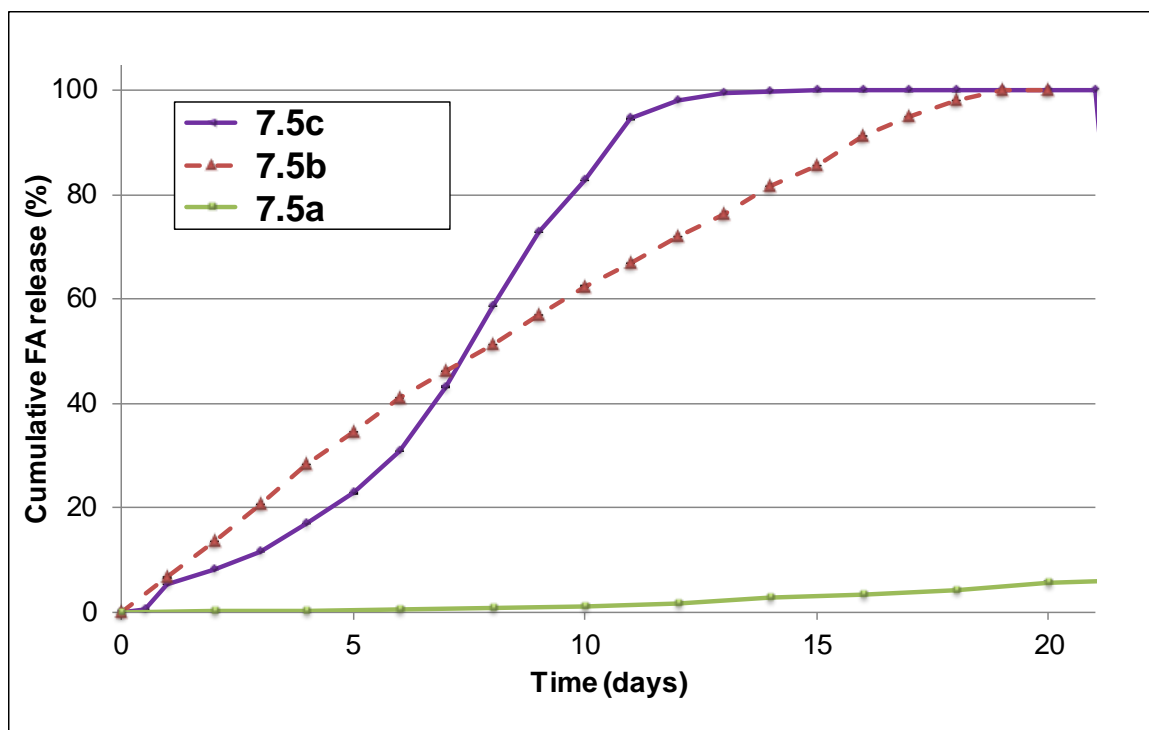
Figure 7.5. *In vitro* ferulic acid release from thee different polymers, each in triplicate (average ± standard deviation)

The degradation media pH was monitored throughout the *in vitro* release tests, to ensure pH alterations did not impact release rates. During polymer degradation, pH was consistently less than the initial pH = 7.4 (Figure 7.6) due to acidic degradation products. The noticeable decrease observed for **7.5c**, can be due to the extensive bulk erosion presumably taking place for **7.5c**, as confirmed by the loss of structural integrity on days 6 and 7.
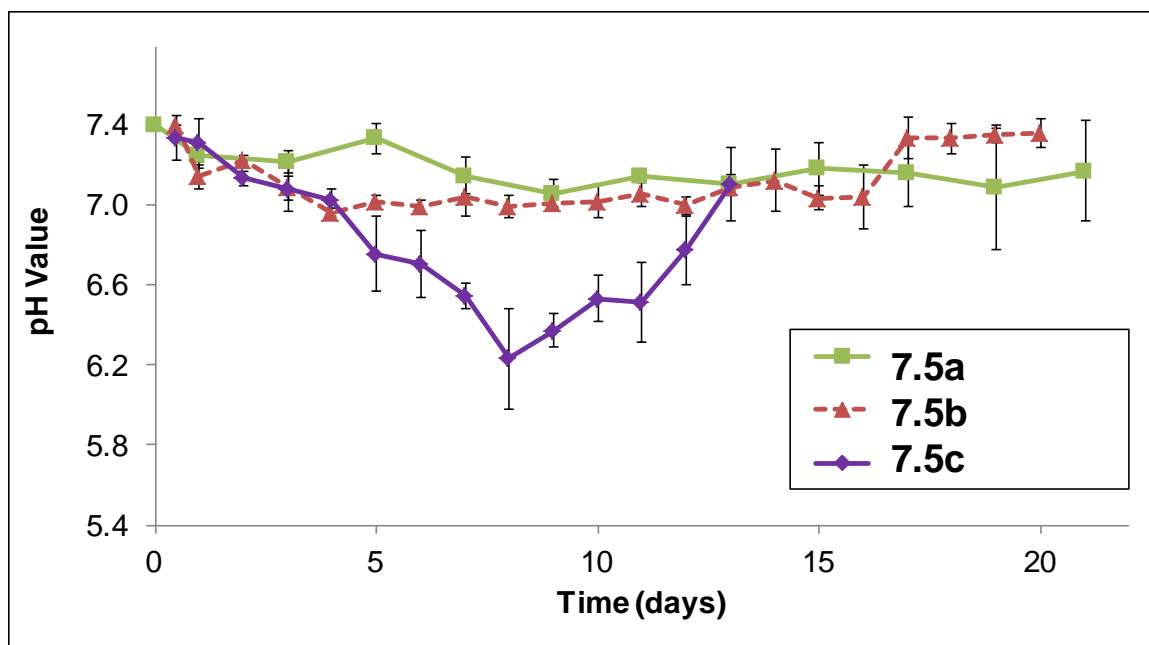
Figure 7.6. Change of degradation media pH over time during *in vitro* studies (average ± standard deviation)

Initial slower ferulic acid release observed for polymer **7.5c** is presumably due to water uptake and subsequent bulk polymer degradation. Swelling continues until a critical osmotic pressure was attained within the disc, at which point the degradation products were released. Once the degradation products were released from the disc, a larger internal surface area was available for erosion to occur, thus leading to an increased release rate (Figure 7.5). Overall differences in release rates (measured by slope of line) were attributed to increased polymer hydrophilicity resulting from the addition of glycol functionalities into the polymer backbone; release rates increased with **7.5c** > **7.5b** > **7.5a** (8.02, 5.16, 0.29 % FA release per day for **7.5c**, **7.5b**, and **7.5a**, respectively).

7.3.5.   Antioxidant assay

A radical quenching assay was used to determine polymer degradation media antioxidant activity to ensure synthetic methods and release conditions did not alter ferulic acid activity. The DPPH reduction percentage was expected to increase with increasing antioxidant concentration. Each polymer's day 10 degradation media (containing all products released) was analyzed for antioxidant activity. These samples were compared to the corresponding free ferulic acid (**7.1**) using freshly prepared solutions with concentrations equal to HPLC data on day 10 (0.018, 0.206, and 0.293 mg/mL for **7.5a, 7.5b**, and **7.5c**, respectively), (Figure 7.8). Comparable concentrations were chosen because the quenching percentage is dependent on the antioxidant concentration.[23]
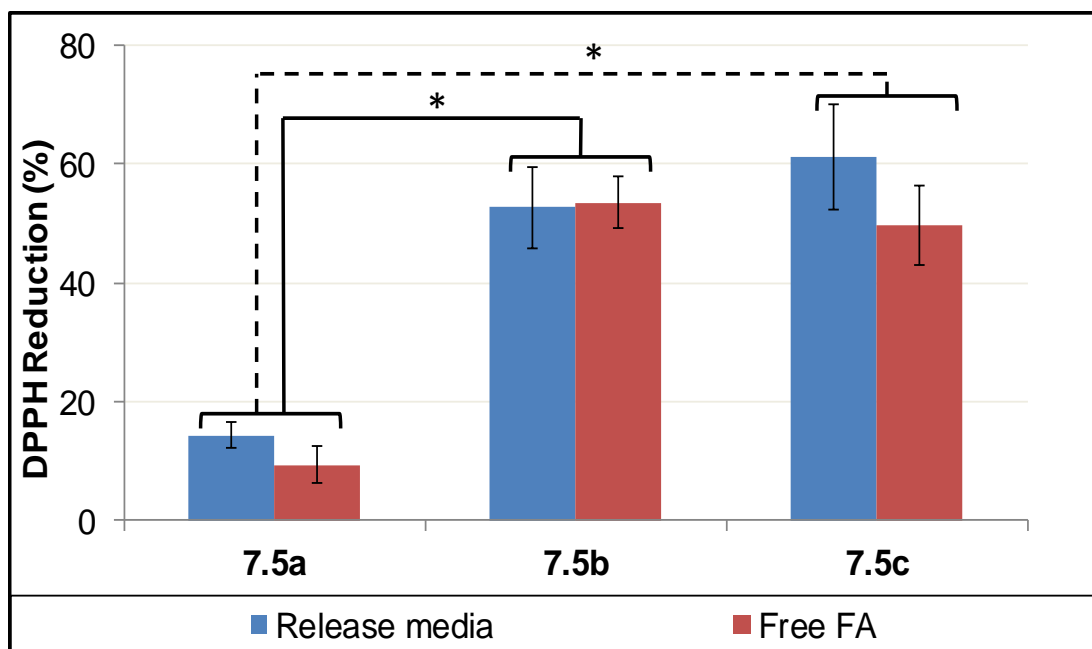
Figure 7.7. DPPH reduction results for ferulic acid as compared to the degradation media for day 10 of the release study (average ± standard deviation); statistical difference indicated by * ($p < 0.05$)

The observed antioxidant activity showed no statistical differences between degradation media and free ferulic acid solution for all day 10 samples. Statistical differences were observed for **7.5a** ferulic acid alone as well as degradation media samples compared to both **7.5b** and **7.5c** as denoted by the asterisks in Figure 7.7. From these results, the polymer degradation products sustain antioxidant activity over time and have not been affected by the synthetic approach utilized. Additionally, antioxidant activity increased as glycol functionality increased.

## 7.4.	Conclusion

Compounds with antioxidant activity (e.g., ferulic acid) exhibit beneficial therapeutic properties to combat oxidative stress, but need improved delivery systems. Such drug delivery systems are finding significant and diverse applications ranging from biomaterials to consumer products. Our approach is to incorporate glycol groups into the main chain of the polymer via chemical incorporation to tune the drug release rate and alter polymer properties. Systematically modifying polymer hydrophilicity not only enables a controlled ferulic acid release, but also alters polymer physicochemical properties. These biodegradable polymers can be beneficial for short-term drug delivery systems with an emphasis on ethylene glycol functionalities to tailor antioxidant-based polymer physicochemical properties and release profiles.

## 7.5.	References

1.	Orrenius S, Gogvadze V, Zhivotovsky B, *Annu Rev Pharmacol Toxicol* **2007**, *47*, 143-83.

2.	Vokurkova M, Xu S, Touyz RM, *Future Cardiol* **2007**, *3*, 53-63.

3.	Kregel KC, Zhang HJ, *AJP: Regulatory, Integrative and Comparative Physiology* **2006**, *292*, R18-R36.

4.	Podda M, Grundmann-Kollmann M, *Clin Exp Dermatol* **2001**, *26*, 578-82.

5.	Kohen R, Gati I, *Toxicology* **2000**, *148*, 149-57.

6.	Graf E, *Free Radical Bio Med* **1992**, *13*, 435-48.

7.	MHW Ministry of Health and Welfare, Notification No.331 of 2000, Standards for Cosmetics, (2000).

8. Li F-Q, Hu J-H, Deng J-X, Su H, Xu S, Liu J-Y, *Int J Pharm* **2006**, *324*, 152-7.

9. Wang Q, Gao X, Gong H, Lin X, Saint-Leger D, Senee J, *J Cosmet Sci* **2011**, *62*, 483-503.

10. Ouimet MA, Griffin J, Carbone-Howell AL, Wu WH, Stebbins ND, Di R, Uhrich KE, *Biomacromolecules* **2013**, *14*, 854–61.

11. Hou S, McCauley LK, Ma PX, *Macromol Biosci* **2007**, *7*, 620-8.

12. Jiang HL, Zhu KJ, *Polym Int* **1999**, *48*, 47-52.

13. Cai Q, Zhu KJ, Zhang J, *Drug Delivery* **2005**, *12*, 97-102.

14. Torres MP, Vogel BM, Narasimhan B, Mallapragada SK, *J Biomed Mater Res Part A* **2006**, *76A*, 102-10.

15. Vogel BM, Mallapragada SK, *Biomaterials* **2005**, *26*, 721-8.

16. Hu WX, Xia CN, Wang GH, Zhou W, *J Chem Res-S* **2006**, 586-8.

17. Schmeltzer RC, Johnson M, Griffin J, Uhrich K, *J Biomater Sci Polym Ed* **2008**, *19*, 1295-306.

18. Meng QC, Zou H, Johansson JS, Eckenhoff RG, *Anal Biochem* **2001**, *292*, 102-6.

19. OECD Nuclear Energy Agency., Organisation for Economic Co-operation and Development. Partition coefficient (1-octanol/water), High Performance Liquid Chromatography (HPLC) Method. Paris: Organisation for Economic Co-Operation and Development; 2004. Available from: http://www.myilibrary.com?id=60669.

20. Göpferich A, Tessmar J, *Adv Drug Deliv Rev* **2002**, *54*, 911-31.

21. Gopferich A, *Biomaterials* **1996**, *17*, 103-14.

22. Siegel RA, Rathbone MJ. Overview of Controlled Release Mechanisms. In: Siegel RA, Rathbone MJ, Siepmann J, editors. Fundamentals and Applications of Controlled Release Drug Delivery. New York: Springer; 2012. pp. 19-43.

23. Brand-Williams W, Cuvelier ME, Berset C, *LWT-Food Sci Technol* **1995**, *28*, 25-30.

CHAPTER 8:   MISCELLANEOUS PROJECTS

Described in this chapter is a series of short research projects explored in combination with the main research goals. The data pertaining to these projects are outlined and provides the fundamentals for future experiments. Included are research collaborations where a less significant role was played, but much value was gained.

8.1.   Incorporation of Unsaturated Linker Molecules into Bioactive-based Polymers

Linker molecules with unsaturated, double bonds could be beneficial for further chemical modification or conjugation as well as photoreactivity (i.e., crosslinking).[1-3] This methodology of using unsaturated linker molecules can be adapted and used for bioactive-based polymers that do not have an inherent double bond (e.g., hydroxycinnamic acids (HCs)). Furthermore, if used as a linker within the HC systems (Chapters 5 and 6), it can be used as a crosslinking site (in addition to the double bond in the HC backbone) to alter thermal and mechanical properties,[4] through polymer chain crosslinking via the carbon-carbon double bonds upon UV irradiation.[5, 6] This approach can be achieved by using acyl chlorides such as itaconyl chloride or fumaryl chlorides.[7, 8] It is also expected that unreacted fumaric acid would not lead to toxicity issues as it is a naturally occurring compound in the body.[8]

8.1.1. Experimental

8.1.1.1. Synthesis of salicylic acid (fumaric) diacid

As depicted in Figure 8.1., salicylic acid (2 eq) was dissolved in THF, to which pyridine (4.4 eq) was added to give a clear, transparent solution. Fumaryl chloride (1 eq), dissolved in THF was added dropwise at 20 mL/hr. Upon addition, the reaction mixture turned an opaque, dark purple and reaction progress monitored by TLC. After starting material consumption (2 h), the reaction mixture was quenched over water and acidified to pH 2 using concentrated HCl. The formed purple precipitate was isolated via vacuum filtration. The crude product was dissolved in acetone, precipitated over hexanes, and isolated via vacuum filtration. Yield: 83 % (purple powder). ^{1}H NMR (400 MHz, DMSO-d_6): δ 13.20 (s, 2H, COOH), 8.01 (d, 2H, Ar-H), 7.70 (t, 2H, Ar-H), 7.46 (t, 2H, Ar-H), 7.36 (d, 2H, Ar-H), 7.19 (s, 2H, J=16.0 Hz, R-CH=CH-R). IR (KBr, cm^{-1}): 1740 (C=O, ester), 1700 (C=O, COOH), 1600 (C=C). T_m: 189-192 °C. T_d: 202 °C.
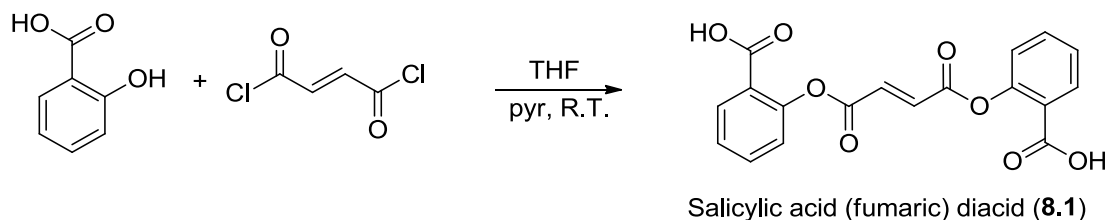

Salicylic acid (fumaric) diacid (**8.1**)

Figure 8.1. Synthetic scheme of salicylic acid (fumaric) diacid, **8.1**

8.1.1.2.   Diacid: Qualitative solubility test

Diacid was dissolved in 10 mL of each solvent listed in Table 8.1.1. If the diacid was insoluble, serial dilutions to the shown concentrations then followed. If dissolution occurred between two end points, a new solution was made at the previous concentration and the solvent was added dropwise until an accurate concentration was reached.

8.1.1.3.   *In vitro* salicylic acid (fumaric) diacid release study

Salicylic acid release from diacid (**8.1**) was evaluated by *in vitro* degradation in phosphate buffered saline (PBS). Diacid discs (n = 3) were prepared by pressing ground diacid (100 ± 5 mg) into 13 mm diameter x 1 mm thick discs in an IR pellet die (International Crystal Laboratories, Garfield, NJ) with a bench top hydraulic press (Carver model M, Wabash, IN). Pressure of 10,000 psi was applied for 5 min at room temperature. The PBS pH was adjusted to 7.40 using 1 N sodium hydroxide. All pH measurements were performed using an Accumet® AR15 pH meter (Fisher Scientific, Fair Lawn, NJ).

To measure hydrolytic degradation, the diacid (**8.1**) discs were placed in 20 mL Wheaton glass scintillation vials with 10 mL of PBS and incubated at 37 ºC with agitation at 60 rpm using a controlled environment incubator-shaker (New Brunswick Scientific Co., Edison, NJ). The degradation media was collected at predetermined time points and media was replaced by fresh PBS (10 mL) over 15 days. The spent media was analyzed by ultra violet spectrophotometry using a Perkin Elmer Lambda XLS spectrophotometer to monitor salicylic acid release.

Measurements were obtained at λ = 303 nm, the maximum absorbance that did not overlap with other diacid degradation products. Data were calculated against a calibration curve from standard salicylic acid solutions in PBS. All sets of experiments were performed in triplicate, carried out until drug release was no longer detected, and normalized to 100 %.

8.1.1.4.   Synthesis of salicylic acid (fumaric) polymer

As depicted in Figure 8.2, polymer was obtained by first dissolving salicylic acid (fumaric) diacid (1 eq) in anhydrous DCM under argon where triethylamine (4.4 eq) was then added and reaction cooled in an ice bath. Triphosgene (1.1 eq) dissolved in anhydrous DCM was added dropwise at 20 mL/hr. The reaction was stirred for 4 h, monitored by CO_2 evolution. The reaction mixture was then poured over chilled ethyl ether and a purple-grey precipitate formed and isolate via vacuum filtration. The crude product was washed with acidic water in the Buchner funnel. The collected solid was placed in a desiccator under vacuum (<2 mm Hg) and dried overnight. Yield: 83 % (purple powder). ^{1}H NMR (400 MHz, DMSO-d_6): δ 13.20 (s, 2H, COOH), 8.01 (d, 2H, Ar-H), 7.70 (t, 2H, Ar-H), 7.46 (t, 2H, Ar-H), 7.36 (d, 2H, Ar-H), 7.19 (s, 2H, J=16.0 Hz, R-CH=CH-R). IR (KBr, cm^{-1}): 1791, 1750 (C=O, anhydride), 1747 (C=O, ester), 1608 (C=C). T_g: 77 ºC; T_d: 202 ºC; M_W: 8500 Da; PDI: 2.7.

Salicylic acid (fumaric) diacid (**8.1**)   Salicylic acid (fumaric) polymer (**8.2**)
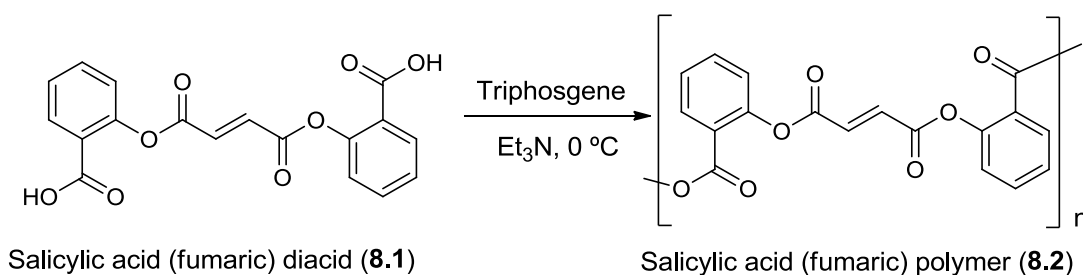
Figure 8.2. Synthetic scheme of salicylic acid (fumaric) polymer, **8.2**, undergoing solution polymerization

8.1.1.5.   Polymer: Qualitative solubility test

Polymer was originally dissolved in 10 mL of each solvent listed in Table 8.1.   If the polymer was insoluble, serial dilutions to the shown concentrations then followed.   If dissolution occurred between two end points, a new solution was made at the previous concentration and the solvent was added dropwise until an accurate concentration was reached.

8.1.2.   Results and Discussion

8.1.2.1.   Synthesis and characterization

Salicylic   acid-based   diacids   and   polymers   do   not   have   inherent unsaturated bonds to undergo chemical modification and/or crosslinking.   To prepare degradable polymers with an unsaturated bond, an acyl chloride with a fumaryl moiety was introduced.   Diacid was synthesized by first coupling salicylic acid to fumaryl chloride in the presence of pyridine (Figure 8.3, top).   The phenol is preferential to the formed acyl pyridinium ion and therefore, pyridine acts as a

catalyst to both quench the formed HCl and activate the acyl chloride. The diacid (**8.4**) was isolated, purified, and the structure confirmed by ^{1}H NMR and FTIR spectra.
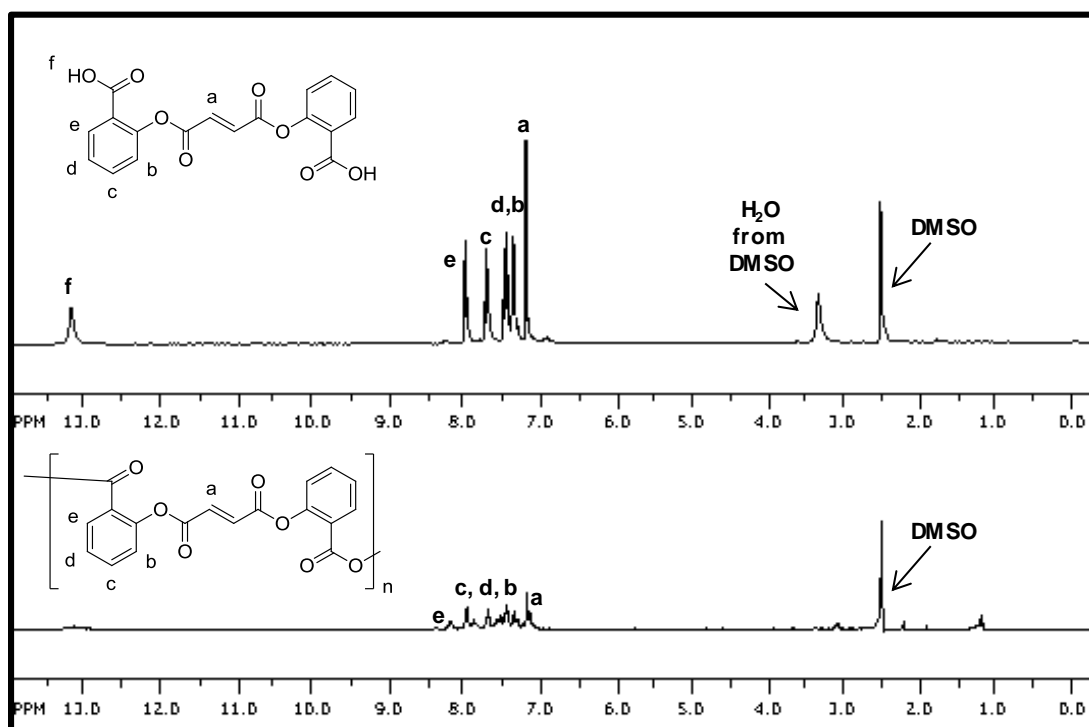
Figure 8.3. ^{1}H NMR spectra of salicylic acid (fumaric) diacid (top) and polymer (bottom) are illustrated above.

Solution polymerization was used to prepare polymer due to potential issues with double bond reactivity. DSC and TGA were used to determine melting point and decomposition temperatures, respectively. Solution polymerization methods outlined herein yielded a mixed product; both diacid and new chemical shifts (i.e., potentially polymer) were observed via ^{1}H NMR (Figure 8.3, bottom). Although a glass transition temperature was found and no melting

temperature was observed (indicating potential diacid presence), future studies will need to be performed to ensure pure polymer product is obtained.

8.1.2.2. Polymer and diacid qualitative solubility

Qualitative solubility tests for both the diacid (Table 8.1) and polymer were performed. These tests provide insight to the types of solvents one may use for further formulations. Additionally, solubility tests can assist with determining solvents for various reactions. Elucidating water solubility is an important factor for drug release studies as this may enable salicylic acid to be the only component found in the degradation media.

Table 8.1. Qualitative solubility test of salicylic acid (fumaric) diacid (**8.1**) where -/- is insoluble, +/- is partially soluble, and +/+ is soluble

		1 mg/mL	0.5 mg/mL	0.1 mg/mL
hexane	**color**	clear	clear	clear
	solubility	-/-	-/-	-/-
chloroform	**color**	clear	cloudy light blue	light navy
	solubility	-/-	+/-	+/+
ethanol	**color**	deep purple		
	solubility	+/+		
water	**color**	faded purple	cloudy purple	light purple
	solubility	+/-	+/-	+/+
tetrahydrofuran	**color**	dark navy		
	solubility	+/+		
dimethylformamide	**color**	dark purple		
	solubility	+/+		

Table 8.2. Qualitative solubility test of salicylic acid (fumaric) polymer (**8.2**) where -/- is insoluble, +/- is partially soluble, and +/+ is soluble

		1 mg/mL	0.5 mg/mL	0.1 mg/mL
hexane	**color**	cloudy grey w/ clumps	cloudy grey w/ clumps	cloudy grey w/ clumps
	solubility	+/-	+/-	+/-
chloroform	**color**	black		
	solubility	+/+		
ethanol	**color**	dark, cloudy small particles	no particles, dark	dark, cloudy small particles
	solubility	+/-	+/+	+/+
water	**color**	clumps, dark, cloudy	dark, cloudy	light, cloudy, particles
	solubility	+/-	+/-	+/-
tetrahydrofuran	**color**	black	black	
	solubility	+/-	+/+	
dimethylformamide	**color**	black		
	solubility	+/+		

8.1.2.3.   *In vitro* salicylic acid (fumaric) diacid release study

The diacid's *in vitro* degradation was monitored by the appearance of salicylic acid in degradation media via UV spectrophotometry. To ascertain whether the diacid would eventually hydrolyze into the active salicylic acid prior to preparing polymer and performing polymer release studies, a release curve was generated for diacid hydrolysis (Figure 8.4) Salicylic acid was released over a 15 day time frame. From day 4 to 5, and day 10 to 11, a drug release plateau was observed; this is likely due to saturation points reached over the weekend. Although sink conditions were not kept throughout the study, overall proof of

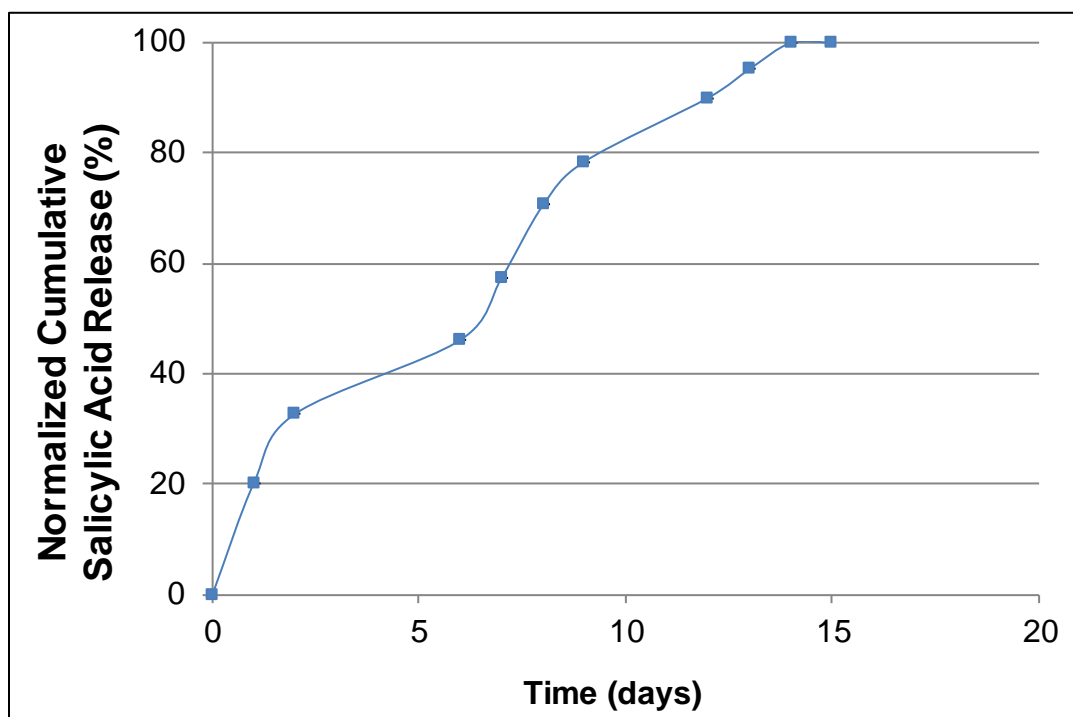concept was obtained from this initial test and more detailed studies should follow.


Figure 8.4. *In vitro* salicylic acid (fumaric) diacid release profile

These studies demonstrated the successful incorporation of an unsaturated linker molecule into the diacid was performed. The polymer, although prepared, must be purified and its synthesis optimized. This work provides the basis for utilizing unsaturated, double bonds as a site for further chemical modification.

8.2.   **Amfenac-loaded Microspheres**

Amfenac is a non-steroidal anti-inflammatory drug (NSAID) clinically used as treatment for inflammatory ailments such as rheumatoid arthritis, ocular diseases, and trauma-induced inflammation.[9]   Based on their ability to reduce prostaglandin production, NSAIDs have been explored as efficacious drugs to treat the aforementioned inflammation.[9, 10]   Current topical NSAID administration (i.e., eye drops) is ineffective as rapid drug clearance occurs[11] and penetration to the eye's posterior region is inefficient.[11, 12]   Preparing a controlled amfenac releasing delivery system by chemically incorporating amfenac into a polymer backbone would be beneficial.
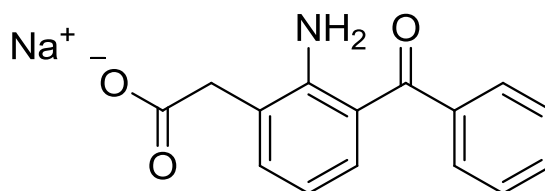
sodium amfenac, 8.3

Figure 8.5. Structure of sodium amfenac molecule, **8.3**, which is encapsulated in salicylic acid (adipic) polymer microspheres

However, efforts to prepare an amfenac-based polymer were unsuccessful as amfenac would degrade into an inactive, lactam during polymer and polymer precursor synthesis.[13]   Therefore, a salicylic acid (adipic) polymer (Figure 8.6, and also in Chapter 3, **3.2**) was used to physically encapsulate the bioactive, sodium amfenac (**8.3**) using a water-in-oil-in-water emulsion

technique.[14]   These amfenac-loaded microspheres render an injectable, dual anti-inflammatory drug delivery system.
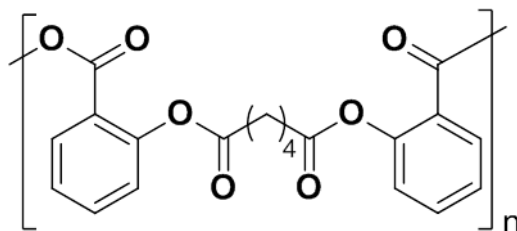

Figure 8.6. Structure of salicylic acid-based polymer with an adipic linker used for microsphere preparation

8.2.1.   Experimental

8.2.1.1.   Microsphere formulation

Sodium amfenac-loaded microspheres were prepared from a salicylic acid (adipic)-based polymer using a water-in-oil-in-water double emulsion solvent evaporation technique. Sodium amfenac (10 mg) was dissolved in 100 µL of DI water and added dropwise to 200 mg of polymer dissolved in 2 mL of dichloromethane. This mixture was homogenized for 1.5 minutes at 4000 rpm. The resulting emulsion was added dropwise to 100 mL of 1% (w/v) poly (vinyl alcohol) (80 % hydrolyzed, 30-70 kDa) and homogenized for 4 min at 2000 rpm. The mixture was stirred for 2 h at 500 rpm at room temperature to evaporate the organic solvent. Microspheres were precipitated by centrifugation at 3000 rpm for 10 min. After centrifugation, the microspheres were washed several times

with acidic water (pH 7.0) to remove non-encapsulated sodium amfenac and any excess PVA. Samples were freeze-dried overnight, and stored at -20°C.

8.2.1.2.   Microsphere morphology

Microsphere morphology was determined using SEM. Images for each set of microspheres were obtained using an AMRAY-1830I microscope (AMRAY Inc.) after coating the samples with Au/Pd using a sputter coater (SCD 004, Blazers Union Limited). SEM images of each polymer microsphere sample were then analyzed using NIH ImageJ software.

8.2.2.   Results and Discussion

Amfenac-loaded microspheres were successfully formulated using a conventional oil-in-water method. Samples exhibited spherical and smooth morphology with sizes ranging from 2-50 μm. A representative image of the microspheres is shown in Figure 8.7.
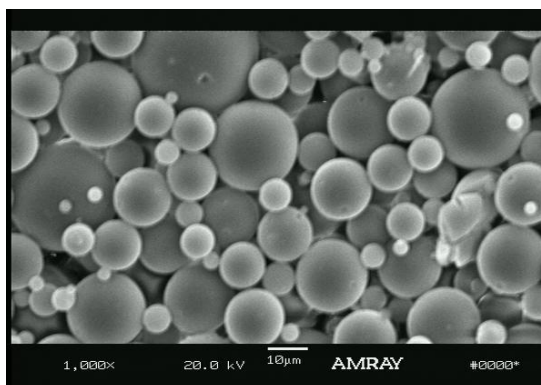

Figure 8.7. Scanning electron microscopy image of sodium amfenac-loaded microspheres

Bioactive release studies to determine salicylic acid and sodium amfenac release were carried out by Kevin Memoli, Department of Chemistry and Chemical Biology, Rutgers University, Piscataway, NJ) to ascertain the dual release of salicylic acid and sodium amfenac.[13]   Release profiles demonstrate more rapid drug release at a higher pH (7.4) compared to more acidic conditions (pH 4.0).   Amfenac release was more rapid than microsphere degradation (measured by salicylic acid release) indicating that amfenac may be not only be encapsulated, but also located at the microsphere surface.   For example, on day 14 at pH 7.4, 100 % amfenac was released, whereas ~50 % salicylic acid was released.   The results also indicate that although not all amfenac was loaded inside the microspheres, release was extended over a 2 week timeframe compared to a burst release expected from non-encapsulated drug.   To extend the amfenac release profile, nepamfenac (a less soluble, amide analog of amfenac) can be encapsulated.

8.3.   Spray Coating Polymers for Microbial Prevention

For traditional food packaging, bioactives (e.g., antimicrobials, preservatives, antioxidants) are physically incorporated into a polymer "carrier". In this section, a polymer used as both the carrier and bioactive is described. The bioactive is only released when the polymer is in contact with water. Additional bioactive molecules can be "loaded" into the polymer to give a dual or triple release system.   These polymers, as compared to small molecules, have

enhanced processing and can be easily manipulated into a variety of geometries for different products such as food wraps for packaging purposes. They have also been proven effective for prevention of biofilm formation on both Gram negative and Gram positive bacteria including *E. coli, S. enterica, P. aeruginosa, S. epidermis, and S. aureus*. In this study, the polymers were evaluated as spray coatings for biofilm prevention.

8.3.1. Experimental

8.3.1.1. Polymer coating preparation

Salicylic acid (adipic) polymer (8.6) was dissolved in chloroform and sprayed onto the surface of Glad ClingWrap and low density polyethylene (LDPE) squares to create a smooth light brown/clear coating (Figure 8.8). These samples were then given to Dr. Chikindas' laboratory in the Food Science Department at Rutgers University.
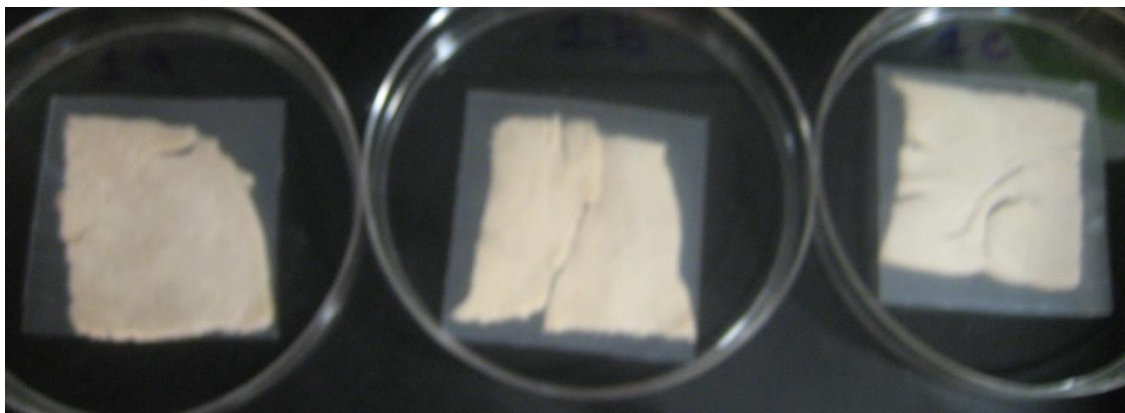
Figure 8.8. Representative image of spray coated films with polymer covering kosher turkey meat

8.3.1.2.   Microbial studies

Studies were performed by Jason (Food Science Department, Rutgers University, Piscataway, NJ) supervised by Dr. Chikindas

Empire turkey breast was purchased from a local supermarket on the day of the experiment and was refrigerated at 6° C until it was used. For the experiment, 75 g of turkey was ascetically transferred into a sterile stomacher bag containing 75 ml of Tryptic Soy Broth. The bag was agitated at ambient temperature for 30 min at 140 rpm to transfer bacterial cells from the meat's surface into the broth. Subsequently, 100 µL of this cell suspension in broth was surface-plated on each of the Plate Count Agar Petri plates that were used for the testing. The film (15x50 mm) tested for the antimicrobial activity was then gently applied to the agar's surface. The antimicrobial activity was evaluated by averaging the inhibition zone along the long edges of the film rectangle. Blank LDPE film and Glad ClingWrap were used as a negative control, while the spot

on a lawn test using 10 µL of 1.0 % and 0.1 % of lauric arginate (the broad spectrum antimicrobial manufactured by Vedeqsa, Barcelona, Spain) was used as a positive control. Each sample was tested in triplicates and the controls were done in duplicates.

8.3.2. Results and Discussion

8.3.2.1. Antimicrobial assay

Film containing 5-16.5 % of the antimicrobial did not induce any visible inhibition zone, much like the negative controls. In contrast, lauric arginate produced clear circular inhibition zones (15-18 mm) with the defined edges. Mild inhibition zone (1-3 mm) with blurry edges was noticed around the spray-coated film.

Table 8.3. Summary of inhibition zones observed from the various substrates

Trial	lauric arginate (1.0%)	lauric arginate (0.1%)	film with polymer
1	18 mm	15 mm	1 mm
2	18 mm	18 mm	2.5 mm
3			3 mm

Interestingly, there was no visible bacterial growth on the agar surface covered by the spray-coated film, suggesting that the film has a potential to extend the shelf life of foods. All other samples tested in this study, much like the negative controls, did not affect the bacterial growth underneath the film.

8.4. Salicylic Acid-based Polymers for Diabetic Bone Regeneration

Performed in collaboration with Roselin Rosario-Meléndez and Connie Fish (Rutgers University, Piscataway, NJ under the supervision of Dr. Uhrich) as well as Dana Graves and Keisuke Wada (University of Pennsylvania School of Dental Medicine, Philadelphia, PA)

Diabetes is characterized by increased chronic inflammation, which can impair wound healing and lead to bone resorption. Localized drug release to reduce inflammation may enhance bone repair for diabetic patients where increased infection susceptibility and enhanced inflammation occur. Previous studies demonstrated controlled release of salicylic acid from a salicylic acid-based polymer may be beneficial for bone regeneration for non-diabetic *in vivo* studies and is dose dependent.[15-17] Investigated in this study was the controlled, localized salicylic acid release effect on bone regeneration in diabetic rats.

Figure 8.9. Sample paste placed into a critical size defect in a rat mandible

8.4.1. Experimental

8.4.1.1. Bone graft/polymer sample formulation and preparation

Polymers were synthesized according to previously published methods.[18] Samples were prepared by adding freeze-dried mineralized bone allograft obtained from LifeNet Health® (Virginia Beach, VA) to polymer powder in a 1:1 weight ratio. Two drops of mineral oil (Sigma Aldrich) were added and contents physically mixed together (Figure 8.10). Samples were then transferred to Eppendorf tubes (for animal studies) or Wheaton glass scintillation vials (for *in vitro* release studies) and subjected to ultra-violet (UV) radiation for 900 seconds in a UV Spectrolinker XL-1500 UV crosslinker chamber (Spectronics Corporation, Westbury, NY) at λ = 254 nm and 5,500-6,500 $\mu W/cm^2$ intensity for sterilization.
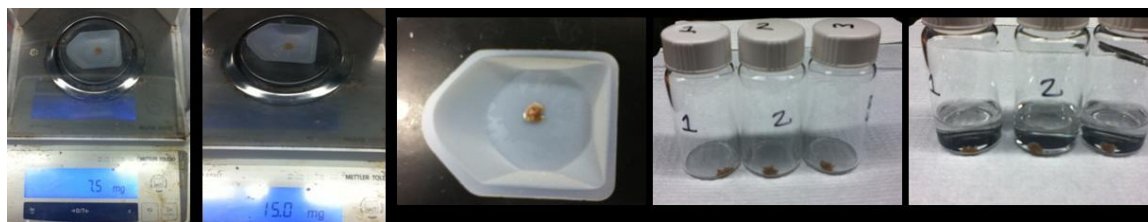
Figure 8.10. Sample preparation included weighing polymer, bone graft, and addition of mineral oil (2 drops)

8.4.1.2. *In vitro* bone graft/polymer salicylic acid release studies

Salicylic acid release was evaluated *in vitro* using phosphate buffered saline (PBS). Samples were prepared according to the aforementioned sample preparation section. The PBS pH was adjusted to 7.4 using 1 N sodium

hydroxide. All pH measurements were performed using an Accumet® AR15 pH meter (Fisher Scientific, Fair Lawn, NJ). To measure drug release, sterilized samples were placed in 20 mL Wheaton glass scintillation vials with 10 mL of PBS and incubated at 37 ºC with agitation at 60 rpm using a controlled environment incubator-shaker (New Brunswick Scientific Co., Edison, NJ) to mimic physiological conditions. The buffer solution was replaced with fresh solution (10 mL) every 24 hours and analyzed over 21 days. Spent media was analyzed by UV spectrophotometry using a Perkin Elmer Lambda XLS spectrophotometer (Waltham, MA) to specifically monitor salicylic acid release. Measurements were obtained at $\lambda = 303$ nm, the maximum absorbance of SA; control studies were performed to ensure other degradation products did not absorb at this wavelength. Data were calculated against a calibration curve of absorbance values from standard solutions of known drug concentrations in PBS.

8.4.2.   Results and Discussion

The formulation described in this section investigates the addition of bone graft and mineral oil to the polymer, both of which may have an effect on salicylic acid release from the polymer. *In vitro* studies were performed in PBS over 21 days using this new formulation and analyzed by UV spectrophotometry to ascertain the release profile. The normalized, cumulative salicylic acid release curve (Figure 8.11) demonstrates salicylic acid is released after day 2 following a lag period of no drug release. Near zero order release was observed from days

3-13, which is common for polyanhydrides due to their surface-eroding behavior.[19, 20] These results demonstrate that this novel formulation sustained salicylic acid release over 16 days.
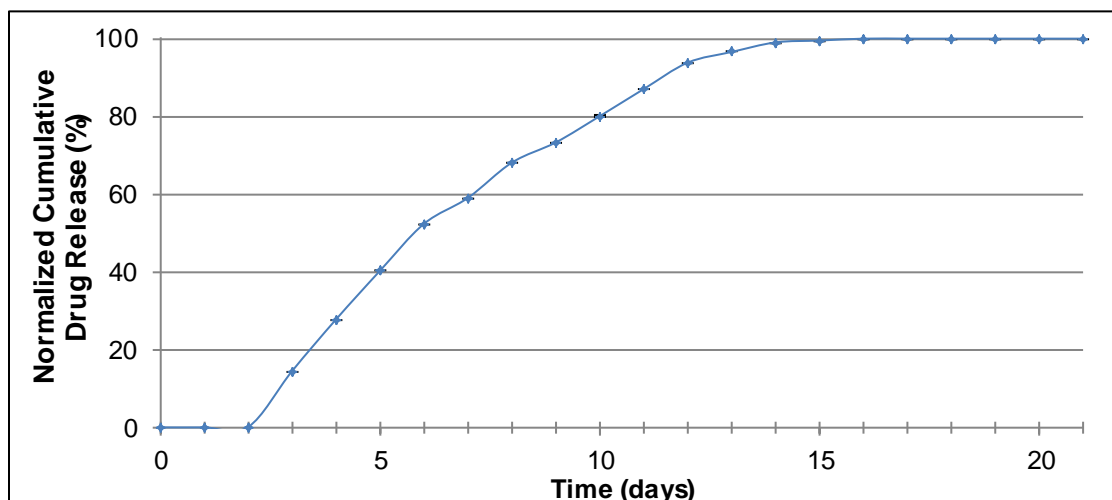

Figure 8.11. *In vitro* salicylic acid release from formulated samples (drug ± standard deviation) over 21 days

Preliminary *in vivo* studies showed that bone fill increased significantly at 4 and 12 weeks in bone graft/salicylic acid-based polymer-treated diabetic rats compared to diabetic rats with bone graft alone. This study demonstrated the potential for the novel material's use for enhancing bone regeneration in diabetic patients.

8.5.   **Utilizing an Artificial Digestive System**

Performed with William Baker, undergraduate visiting student from Clemson University, Clemson, SC.

Background information was collected to provide an understanding and motivation for using an artificial digestive system as much research has been performed to enable the release of therapeutic drugs into the lower regions of the gastrointestinal (GI) tract as drug delivery to the large and small intestines has been difficult due to the stomach's acidic environment. It is imperative for therapeutics to reach the small intestine and colon for the treatment of various inflammatory diseases including arthritis,[21] cancer,[22, 23] diabetes (type 2),[24] and Inflammatory Bowel Disease (IBD).[25] Through the use of biodegradable polymers, new methods have been developed to provide more efficient drug delivery to organs distal to the stomach in the GI tract.

The polymers described throughout this dissertation can be viable options to treat chronic inflammatory diseases, by controlling the drug amount released over time. Additionally, the ability to pass through the stomach without releasing the bioactive will also negate the previously mentioned side effects.

Recently, researchers have a found a way to better mimic GI conditions inside the human body.[26] In 2007, a Netherlands company, TNO Nutrition and Food Research, successfully developed an *in vitro* GI tract simulator creating the opportunity for a more detailed study of how the GI tract environment breaks down and absorbs foods and drugs. TIM-1 simulates the environment of GI tract from the stomach through the ileum. This simulator has the capability to monitor

enzyme release, pH, addition of cofactors, and transit times for each step of digestion, along with removal of the products of digestion.[27] This release of enzymes, rate of peristalsis, flow of pancreatic and gastric juices, and temperature within the system are all controlled via use of a computer system.[28] These parameters can even be altered to reflect the digestive process in different aged individuals. It is the combination of timing, mixing, and movement that sets the TIM-1 apart from previous attempts to mirror the GI tract. Aliquots are efficiently collected and analyzed at different time points without removing the samples from its physiological environment.

A dynamic artificial GI simulator can be used to investigate the drug release profile from the aforementioned degradable polymers through the digestive system. The drug absorption can be determined through analyses of GI tract aliquots to determine the use of bioactive-based polymers as a potential therapeutic for the treatment of inflammatory diseases.

8.6.   Synthesis of Liquid Crystal Salicylic Acid-based Polymers

Salicylic acid-based polymers exhibit relatively low thermal stability and brittle mechanical properties,[18, 29] which their use in applications where higher thermal properties and more elasticity are necessary. Liquid crystal polymers are known to form highly ordered regions that result in enhanced mechanical strength and increased thermal stability.[30] *p*-Hydroxybenzoic acid is known as a building block for liquid crystal polymers.[31] To impart liquid crystalline properties on the salicylic acid-based poly(anhydride-esters), copolymers with [30] *p*-

hydroxybenzoic acid-based polymers were synthesized using melt-condensation and solution polymerization methods. Chemical and thermal properties for the copolymers were compared to the homopolymers to optimize thermal and mechanical properties.

8.6.1.　　　　Experimental

Salicylic acid polymer was made with an adipic linker (SAA), using methods described in Chapter 2. As depicted in Figure 8.12, *p*-hydroxybenzoic acid polymer (PHB) was prepared by made with an adipic linker by first dissolving *p*-hydroxybenzoic acid (2 eq) in THF, to which pyridine (4.4 eq) was added to give a clear, transparent solution. Adipoyl chloride (1 eq), dissolved in THF was added dropwise at 20 mL/hr. Upon addition, the reaction mixture turned a white and was no longer transparent and reaction progress monitored by TLC. After starting material consumption (2 h), the reaction mixture was quenched over water and acidified to pH 2 using concentrated HCl. The formed precipitate was isolated via vacuum filtration. The crude product was dissolved in acetone, precipitated over hexanes, and isolated via vacuum filtration.
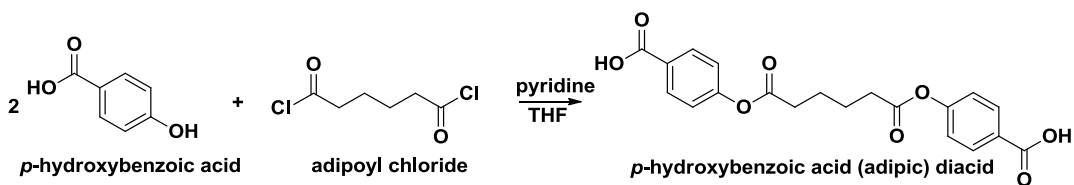
Figure 8.12. Synthesis of p-hydroxybenzoic acid (adipic) diacid
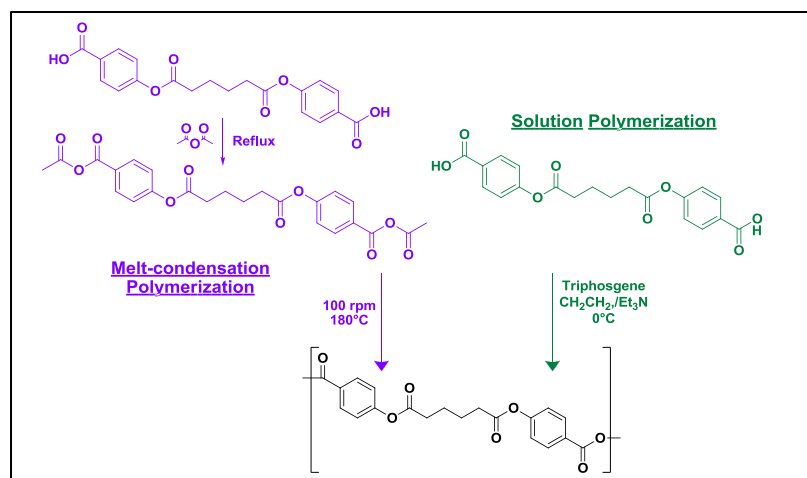
Figure 8.13. PHB homopolymer prepared via melt and solution polymerization methods

Each diacid (1 eq) (to prepare the homopolymer) or SAA diacid (0.5 eq) and PHB diacid (0.5 eq) added together were polymerized via melt-condensation polymerization (Figure 8.13, left) by first acetylating the diacid or mixture using an excess of acetic anhydride and heating to 180 ºC with stirring at 100 rpm under vacuum until no change in viscosity was observed. Product was dissolved in a minimal amount of dichloromethane and precipitated over diethyl ether. Ether was decanted and precipitate dried overnight *in vacuo*.

To prepare homopolymer and copolymer via solution polymerization methods (Figure 8.14), diacid (1 eq) or SAA diacid (0.5 eq) and PHB diacid (0.5 eq) was dissolved in anhydrous DCM under argon. After adding triethylamine (NEt$_3$, 4.4 eq), the reaction mixture was cooled to 0 °C. Triphosgene (0.33 eq) dissolved in 10 mL anhydrous DCM was added dropwise (20 mL/h). The reaction was allowed to stir at 0 °C until CO$_2$ evolution ceased (ca. 6 h). The reaction mixture was precipitated over chilled diethyl ether (400 mL), and the

precipitate was isolated via vacuum filtration. The residue was dissolved in anhydrous DCM, washed with acidic water (1 x 250 mL), dried over MgSO$_4$, concentrated, and precipitated with an excess of chilled diethyl ether (500 mL). The ether was filtered off via vacuum filtration, and the polymer was dried *in vacuo* at room temperature.

Figure 8.14. SAA:PHB copolymer synthesis via melt and solution polymerization methods

Molecular weights (M$_w$) were measured using gel permeation chromatography. Glass transition temperatures (T$_g$) and melting points (T$_m$) were measured using differential scanning calorimetry. Decomposition temperatures (T$_d$) were measured using thermal gravimetric analysis. Young's Modulus was measured using dynamic mechanical analysis in compression mode. Polarized optical microscopy was used to visualize liquid crystal properties with a microscope and polarizer and analyzer lenses (performed by Dr. Jeremy Griffin).

8.6.2.   Results and Discussion

To overcome the relatively low thermal and mechanical stability, salicylic acid-based polymers were copolymerized with PHB. Physical, thermal, and mechanical properties of SAA homopolymers, PHB homopolymers, and SAA:PHB copolymers prepared by melt-condensation (melt) and solution polymerization (solution) methods were analyzed (Table 8.4). SAA, PHB, and 1:1 copolymers of SAA:PHB were successfully synthesized using melt condensation and solution polymerization methods and obtained in good to moderate yields.

Table 8.4. Polymer properties for homopolymers and copolymers

	SAA (melt)	SAA (solution)	PHB (melt)	PHB (solution)	SAA:PHB (melt)	SAA:PHB (solution)
Yield (%)	73	72	68	60	72	65
T_g (°C)	38 °C	40 °C	54 °C	55 °C	51 °C	40 °C
T_M (°C)	-	-	128 °C	162 °C	-	-
T_d (°C)	253 °C	283 °C	252 °C	270 °C	257 °C	255 °C
M_W (Da)	18,300 Da	27,800 Da	19,600 Da	45,000 Da	10,000 Da	49,500 Da
Young's Modulus	1170 kPa	-	140 kPa	146 kPa	-	-

The T_g of SAA:PHB was increased as compared to the homopolymers, broadening the scope of applications. A decreased Young's Modulus of the PHB homopolymer was observed as compared to the SAA homopolymer thus indicated the PHB homopolymers have more elasticity. Copolymer mechanical tests must still be performed. Optical microscopy images of SAA:PHB indicate the presence of amorphous and liquid crystal region, indicating the copolymerization may have imparted liquid crystalline behavior unto the SAA polymers.
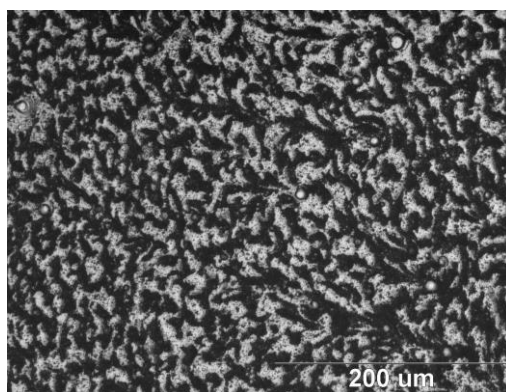
Figure 8.15. Polarized optical microscopy image of a SAA:PHB (solution) copolymer showing amorphous regions (dark) and crystal regions (light).

Polymer degradation studies on the copolymers should be performed as future work to investigate the effect on SA release. Also, if used for biological purposes, biocompatibility tests must be performed.

8.7.   Ferulic Acid Polymer Microspheres

As discussed in Chapter 7, oxidative stress causes DNA damage leading to many debilitating diseases. A ferulic acid-based polymer that degrades within three weeks was designed and synthesized. As the polymer degrades in the presence of water, ferulic acid is released. Ferulic acid is a potent antioxidant with radical scavenging and photoprotective properties useful to combat oxidative stress and therefore used in cosmetics as a topical antioxidant in anti-aging remedies and sunscreens.

ferulic acid (diglycolic) polymer
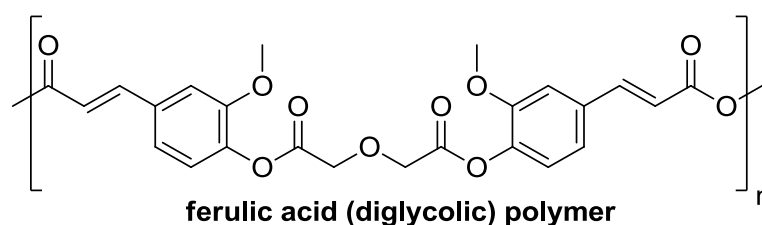
Figure 8.16. Ferulic acid-containing polymer with a diglycolic linker labeled ferulic acid (diglycolic) polymer

Several delivery systems employed in cosmetics and personal care that utilize entrapment or adsorption technologies include emulsions, vesicles such as liposomes and hollow microparticles (empty with no drug), and suspensions.[32] One of the most common methods to topically deliver bioactives is through suspensions and emulsions.[33] Micromulsions can be utilized to directly entrap actives, fragrances, or flavors as bulk emulsions have been primary formulations in the cosmetic industry.[34] These microspheres are advantageous over using a disc (as described in Chapters 6 and 7) in that the surface area is greatly

increased, thus accelerating bioactive release. Furthermore, these microspheres can act as carriers to encapsulate other bioactive molecules for dual release and potential synergistic activity.

8.7.1. Experimental

8.7.1.1. Microsphere preparation

Ferulic acid (FA)-containing polymer using a diglycolic linker synthesized according to Chapter 7 were formulated into microspheres using an oil-in-water single emulsion solvent evaporation technique.[35] In general, FA-containing polymer (0.50 g) was dissolved in dichloromethane (3 mL) and added drop-wise to 1% aqueous poly(vinyl alcohol) (PVA) solution (80 mL) at room temperature. The emulsion was homogenized for 2 min using an IKA Ultra-Turrax T8 homogenizer at approximately 10,000 rpm. The homogenized solution was left stirring for 2 h to allow microsphere formation by solvent evaporation. Microspheres were transferred to sterile 50 mL polypropylene conical tubes, washed with acidic water (pH 1) to remove residual PVA, centrifuged at 3,000 rpm for 10 min and supernatant decanted. This process was repeated 5 times. Microspheres were frozen by placing the conical tubes in a dry ice/acetone bath and lyophilized for 24 h at -40 °C and 133×10^{-3} mBar (LABCONO Freeze Dry System/Freezon 4.5).

8.7.1.2.   Size and morphology

Size and morphology of the microspheres were determined using SEM. Images for each set of microspheres were obtained using an AMRAY-1830I microscope (AMRAY Inc.) after coating the samples with Au/Pd using a sputter coater (SCD 004, Blazers Union Limited).   SEM images of each polymer microsphere sample were then analyzed using NIH ImageJ software. Distributions of particle diameter were obtained by evaluating > 50 particles per sample.

8.7.1.3.   Molecular weight

Polymer precursors were analyzed via mass spectrometry to determine molecular weights. A Finnigan LCQ-DUO equipped with Xcalibur software and an adjustable atmospheric pressure ionization electrospray ion source (API-ESI Ion Source) was used with a pressure of 0.8×10^{-5} and 150 °C API temperature. Samples dissolved in methanol (< 10 µg/mL) were injected with a glass syringe. GPC was used to determine polymer weight-averaged molecular weight and polydispersity using a Perkin-Elmer liquid chromatography system consisting of a Series 200 refractive index detector, a Series 200 LC pump, and an ISS 200 autosampler.   Automation of the samples and processing of the data was performed using a Dell OptiPlex GX110 computer running Perkin-Elmer TurboChrom 4 software with a Perkin-Elmer Nelson 900 Series Interface and 600 Series Link. Polymer samples were prepared for autoinjection by dissolving in dichloromethane (DCM, 10 mg/mL) and filtering through 0.45 µm

polytetrafluoroethylene syringe filters. Samples were resolved on a Jordi divinylbenzene mixed-bed GPC column (7.8 x 300 mm, Alltech Associates, Deerfield, IL) at 25 °C, with DCM as the mobile phase at a flow rate of 1.0 mL/min. Molecular weights were calibrated relative to broad polystyrene standards (Polymer Source Inc., Dorval, Canada).

8.7.1.4. Thermal properties

DSC measurements were carried out on TA Instrument Q200 to determine melting (T_m) and glass transition (T_g) temperatures. Measurements on samples (4-6 mg) heated under nitrogen atmosphere from −10 °C to 200 °C at a heating rate of 10 °C/min and cooled to −10 °C at a rate of 10 °C/min with a two-cycle minimum were performed. TA Instruments Universal Analysis 2000 software, version 4.5A was used to analyze the data. Glass transition temperatures were calculated as half Cp extrapolated. TGA was utilized for determining decomposition temperatures (T_d) using a Perkin-Elmer Pyris 1 system with TAC 7/DX instrument controller and Perkin-Elmer Pyris software for data collection. Samples (5-10 mg) were heated under nitrogen atmosphere from 25 °C to 400 °C at a heating rate of 10 °C/min. Decomposition temperatures were measured at the onset of thermal decomposition.

8.7.1.5. *In vitro* ferulic acid release

FA release from polymer microspheres was studied at 37 °C in phosphate buffered saline (PBS) at pH 7.4 with agitation (60 rpm) to mimic physiological

conditions. Triplicate samples of microspheres (20.0 mg) were suspended in 20 mL of PBS. After 12 hours, and every 24 hours after day 1, samples were centrifuged at 3,000 rpm for 5 minutes (Hettich Zentrifugen EBA12) to separate the microspheres. Aliquots of the supernatant (15 mL) were collected and replaced with fresh PBS (15 mL). Spent media was analyzed via high-performance liquid chromatography (HPLC). The degradation products were analyzed and quantified via HPLC using an XTerra® RP18 5 µm 4.6x150 mm column (Waters, Milford, MA) on a Waters 2695 Separations Module equipped with a Waters 2487 Dual λ Absorbance Detector. All samples were filtered using 0.22 µm poly(vinylidine fluoride) syringe filters and subsequently injected (20 µL) using an autosampler. The mobile phase was comprised of 50 mM KH_2PO_4 with 1 % formic acid in DI water at pH 2.5 (65 %) and acetonitrile (35 %) run at 1 mL/min flow rate at ambient temperature. Absorbance was monitored at $\lambda = 320$ nm. Amounts were calculated from known concentrations of standard FA solutions.

8.7.2.   Results and Discussion

The microsphere M_w and T_g were determined and compared to the values obtained for the unprocessed polymers (Table 8.5). A slight M_w decrease and increase in PDI compared to the unprocessed polymer was observed as expected due to the water exposure during formulation. The changes in T_g values decreased post formulation, but maintained above 37 ^{o}C, which ensure their shape will remain if used *in vivo*.

Table 8.5. Molecular weight, M_W (polymer and microspheres), glass transition temperature, Tg (polymer and microspheres), and % yield (microspheres).

	M_w (Da) Polymer (PDI)	M_w (Da) Microspheres	T_g (°C) polymer	T_g (°C) microspheres	% Yield microspheres
Polymer	18,300 (1.3)	15,500 (1.5)	108	80	83

Microspheres 2-27 μm in diameter were obtained in 83 % yield without aggregation and are represented in Figure 8.17. Smooth microsphere surfaces are important for uniform bioactive release. Future studies will entail decreasing size distribution. Additionally, homogenization speed and polymer concentration are two parameters to optimize microsphere size.
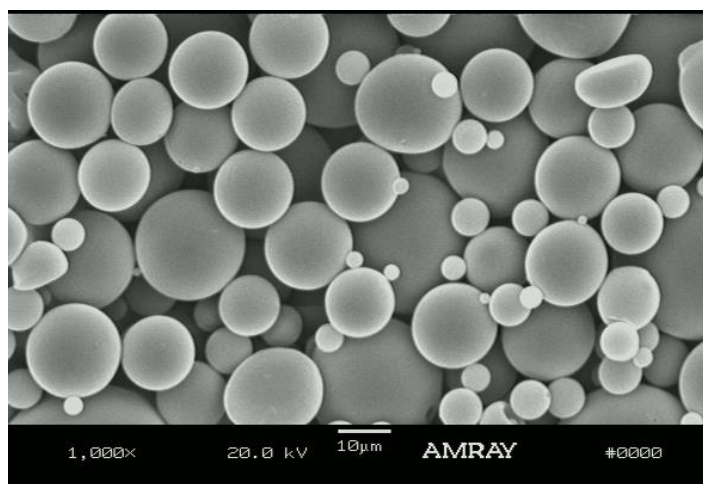
Figure 8.17. Representative scanning electron microscopy images of microspheres prepared from the FA-containing polymer

The polymer microsphere's *in vitro* degradation was measured by the appearance of ferulic acid release in degradation media via HPLC. FA detection with a 3.71 minute retention time (Figure 3B) indicated complete of anhydride and ester bond hydrolysis. The polymer microspheres released 100 % ferulic acid over 10 days compared to polymer discs, which took 20 days for total release.
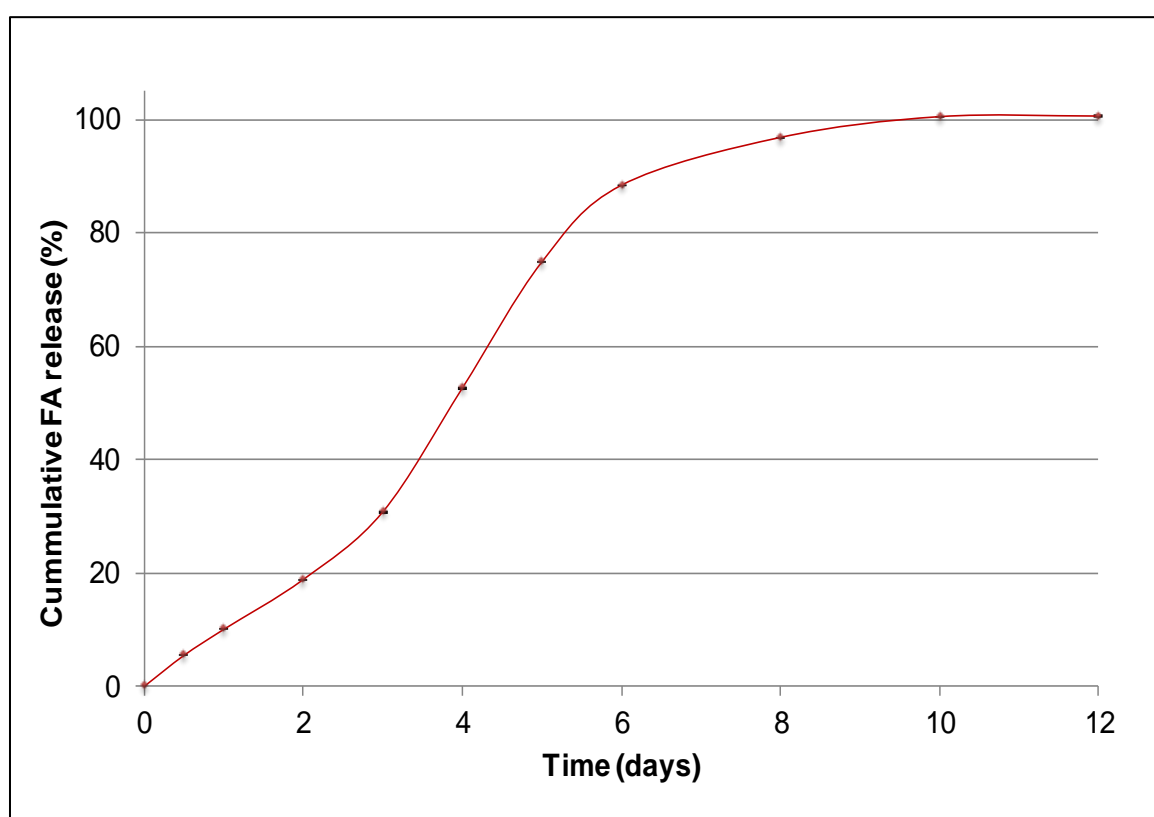
Figure 8.18. In vitro ferulic acid release from polymer microspheres (FA ± standard deviation)

8.8. Skin Diffusion Studies

Skin models were used to evaluate salicylic acid-based polymer and degradation products movement across the skin membrane elucidated their performance for topical applications. To investigate the efficiency of these polymers to degrade into salicylic acid and transport salicylic acid through skin, diffusion studies were performed. With diffusion performance highly correlated to human skin, a Strat-M[TM] synthetic membrane was used for *in vitro* transdermal diffusion testing in place of human skin, as a model.[36]
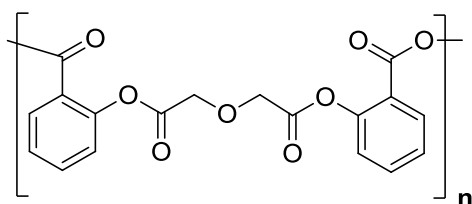
Figure 8.19. Salicylic acid (diglycolic) polymer was formulated with DMSO and propylene glycol for Franz diffusion studies

8.8.1. Experimental

Salicylic acid (diglycolic) polymer was formulated by dissolving 54 mg polymer in 0.1 mL DMSO. A 0.05 mL aliquot of this solution was added to 0.95 mL propylene glycol and then vortexed. The suspension was cloudy, but much more homogenous than polymer in propylene glycol. This 2 % w/v solution (200 µL) was added atop the Strat-M[TM] membrane in the donor compartment. PBS

(4.9 mL) was added to the receiver compartment. Every 2 h for 8 h and at 24 h, degradation media was removed (0.3 mL) from the receiver compartment and replaced with fresh PBS.

Figure 8.20. Photograph of Franz diffusion cells using the Strat-M^{TM} membrane

To quantify salicylic acid release, HPLC was used. The degradation products were analyzed and quantified via HPLC using an XTerra® RP18 5 µm 4.6x150 mm column (Waters, Milford, MA) on a Waters 2695 Separations Module equipped with a Waters 2487 Dual λ Absorbance Detector. All samples were filtered using 0.22 µm poly(vinylidine fluoride) syringe filters and subsequently injected (20 µL) using an autosampler. The mobile phase was comprised of 50 mM KH_2PO_4 with 1 % formic acid in HPLC grade water at pH 2.5 (75 %) and acetonitrile (25 %) run at 1 mL/min flow rate at ambient temperature. Absorbance was monitored at λ = 290 nm and amounts calculated against a predetermined calibration curve.
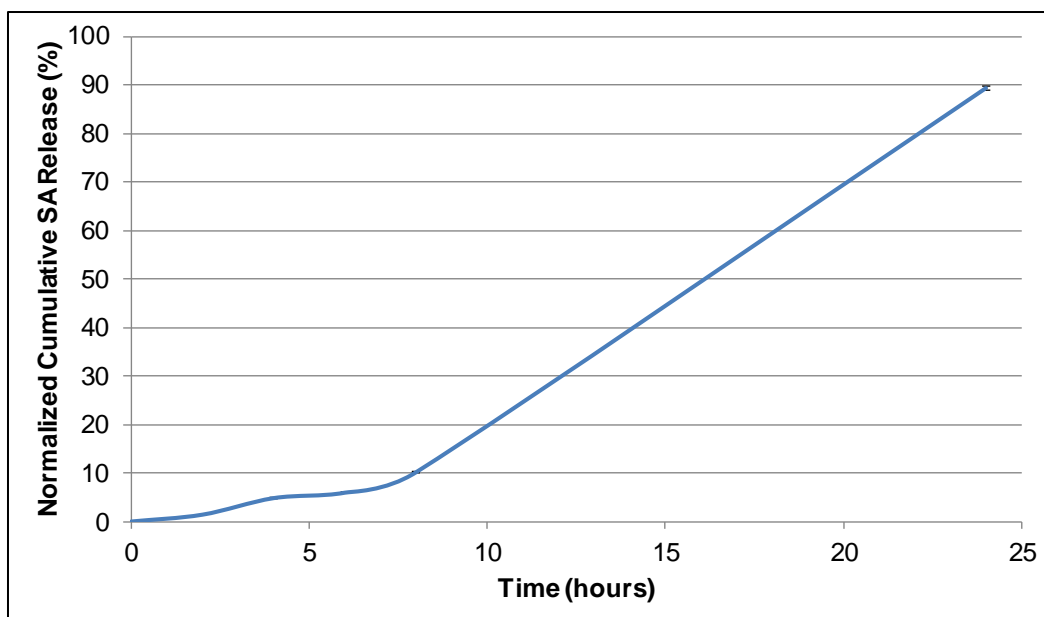
Figure 8.21. Salicylic acid release curve from Franz diffusion studies (SA ± standard deviation)

8.8.2.　　　Results and Discussion

Studies showed minimal salicylic acid released in the given formulation within the first 8 h. At the 24 hour time point, almost 90% salicylic acid was released. Lack of water available to hydrolyze the anhydride and ester bonds are presumably the cause for the delayed salicylic acid release. Future studies should include varying the formulation by adding water (potentially 50% propylene glycol, 50 % water).   Additionally, keratinocyte testing to elucidate cytoxicity, inflammation, and irritation should also be performed.   Once this information is known, human cadaver skin can be used with florescence microscopy to determine the location within various skin depths that salicylic acid may reside throughout the study.

8.9. References

1. Baroli B, *Journal of Chemical Technology & Biotechnology* **2006**, *81*, 491-9.

2. Timmer MD, Jo S, Wang C, Ambrose CG, Mikos AG, *Macromolecules* **2002**, *35*, 4373-9.

3. Davis KA, Anseth KS, *Crit Rev Ther Drug Carrier Syst* **2002**, *19*, 385-423.

4. Muggli DS, Burkoth AK, Anseth KS, *J Biomed Mater Res* **1999**, *46*, 271-8.

5. Subramanian K, Krishnasamy V, Nanjundan S, Rami Reddy AV, *Euro Polym J* **2000**, *36*, 2343-50.

6. Hu X, Chen X, Cheng H, Jing X, *J Polym Sci, Part A: Polym Chem* **2009**, *47*, 161-9.

7. Grijpma DW, Hou Q, Feijen J, *Biomaterials* **2005**, *26*, 2795-802.

8. Shin H, Temenoff JS, Mikos AG, *Biomacromolecules* **2003**, *4*, 552-60.

9. Walters T, Raizman M, Ernest P, Gayton J, Lehmann R, *Journal of Cataract & Refractive Surgery* **2007**, *33*, 1539-45.

10. Kim SJ, Flach AJ, Jampol LM, *Surv Ophthalmol* **2010**, *55*, 108-33.

11. de Smet MD, Taylor SR, Bodaghi B, Miserocchi E, Murray PI, Pleyer U, Zierhut M, et al., *Prog Retin Eye Res* **2011**, *30*, 452-70.

12. Gamache DA, Graff G, Brady MT, Spellman JM, Yanni JM, *Inflammation* **2000**, *24*, 357-70.

13. Memoli KA. Rutgers University-Graduate School-New Brunswick, 2012.

14. Zheng W, *Int J Pharm* **2009**, *374*, 90-5.

15. Erdmann L, Macedo B, Uhrich KE, *Biomaterials* **2000**, *21*, 2507-12.

16. Harten RD, Svach DJ, Schmeltzer R, Uhrich KE, *J Biomed Mater Res Part A* **2005**, *72*, 354-62.

17. Reynolds MA, Prudencio A, Aichelmann-Reidy ME, Woodward K, Uhrich KE, *Curr Drug Deliv* **2007**, *4*, 233-9.

18.   Prudencio A, Schmeltzer RC, Uhrich KE, *Macromolecules* **2005**, *38*, 6895-901.

19.   Whitaker-Brothers K, Uhrich K, *J Biomed Mater Res Part A* **2006**, *76A*, 470-9.

20.   Göpferich A, Tessmar J, *Adv Drug Deliv Rev* **2002**, *54*, 911-31.

21.   Yamazaki R, Kusunoki N, Matsuzaki T, Hashimoto S, Kawai S, *J Pharm Pharmacol* **2002**, *54*, 1675-9.

22.   Spitz GA, Furtado CM, Sola-Penna M, Zancan P, *Biochem Pharmacol* **2009**, *77*, 46-53.

23.   Perugini RA, McDade TP, Vittimberga FJ, Jr., Duffy AJ, Callery MP, *J Gastrointest Surg* **2000**, *4*, 24-32.

24.   Rumore MM, Kim KS, *Ann Pharmacother* **2010**, *44*, 1207-21.

25.   Engel MA, Neurath MF, *J Gastroenterol* **2010**, *45*, 571-83.

26.   Mitea C, Havenaar R, Drijfhout JW, Edens L, Dekking L, Koning F, *Gut* **2008**, *57*, 25-32.

27.   Blanquet S, Zeijdner E, Beyssac E, Meunier JP, Denis S, Havenaar R, Alric M, *Pharm Res* **2004**, *21*, 585-91.

28.   Chen L, Hebrard G, Beyssac E, Denis S, Subirade M, *J Agric Food Chem* **2010**, *58*, 9861-7.

29.   Erdmann L, Uhrich KE, *Biomaterials* **2000**, *21*, 1941-6.

30.   Ratner BD. In Biomaterials science : an introduction to materials in medicine. 2nd ed. Amsterdam ; Boston: Elsevier Academic Press; 2004.

31.   Jackson WJ, Kuhfuss HF, *J Polym Sci, Part A: Polym Chem* **1996**, *34*, 3031-46.

32.   Gupta S, *HAPPI* **2003**, *January*, 49-59.

33.   Somasundaran P, Chakraborty S, Deo P, Deo N, Somasundaran T. Nanoparticles for Cosmetics and Personal Care Formulations. Skin Delivery Systems: Transdermals, Dermatologicals and Cosmetic Actives. 1st ed. Ames, Ioawa: Blackwell Pub.; 2006. pp. 247-56.

34. Shroot B, Aust D. Current Trends in Dermatologicals and Delivery Systems. Skin Delivery Systems: Transdermals, Dermatologicals and Cosmetic Actives. Ames, Iowa: Blackwell Pub.; 2006. pp. 129-35.

35. Yeagy BA, Prudencio A, Schmeltzer RC, Uhrich KE, Cook TJ, *J Microencapsulation* **2006**, *23*, 643-53.

36. Joshi V, Brewster D, Colonero P. In Vitro Diffusion Studies in Transdermal Research: A Synthetic Membrane Model in Place of Human Skin. Drug Development & Delivery 2012:40-2.

CHAPTER 9:   CONCLUDING REMARKS

Controlled release technologies impact the health and well-being of many people every year. Recently, the use of biodegradable polymers for controlled release systems has expanded opportunities to significantly improve drug delivery. However, there therapeutic use has been limited due to burst drug release and low drug loading. This dissertation described how bioactive bioactive-based polymers with high drug loading capability were designed, synthesized, and fabricated to tune bioactive release profiles and overcome such limitations of biodegradable polymers.

Specifically, salicylic acid-based polymer release profiles, which demonstrate salicylic acid release rates via hydrolytic degradation, were tuned using small molecules as discussed in Chapter 2. Admixture of small molecules into a salicylic acid-based polymer matrix increased initial salicylic acid release, while maintaining sustained salicylic acid release over 30 days. Different release rates were observed depending upon admixture type and percentage added.

Chapters 2 and 3 described the said polymer's fabrication into hydrogels and microspheres to broaden their application scope. The microspheres were formulated using a bulk oil-in-water method that released salicylic acid within 3 days. These microspheres have the potential to be used in consumer good products where rapid salicylic acid release is required. Additionally, the microspheres provide potential as carriers for other bioactive molecules to be delivered as a multi-release system.

The hydrogels were formulated by simply blending salicylic acid-based polymers with poly (vinyl pyrrolidone) (PVP) and using a solvent cast method that prepared miscible blended films. Once hydrated, the films displayed hydrogel-like properties that have the potential as wound dressings as they exhibited porosity with swelling abilities. The salicylic acid-based polymers are brittle in nature when solvent cast; blending this polymer with PVP allowed for flexible, gel-like materials. Additionally, this formulation allowed for salicylic acid release to be extended over a few days, where physically admixed salicylic acid had previously been shown to last in less than 24 hours. Improvements to the blends' mechanical integrity are necessary for use as wound dressings.

Once the salicylic acid-based polymers were used to provide the ground work for synthesis feasibility of bioactive-based polymers, other bioactives were investigated for their chemical incorporation into a polymer backbone. Hydroxycinnamic acids are a class of potent antioxidants ubiquitous in plants. *p*-Coumaric, ferulic, and sinapic acid molecules detailed in Chapters 5 and 6 were each separately incorporated into a polymer backbone. Antioxidant and antimicrobial assays verified that polymer processing did not have a negative effect on the released hydroxycinnamic acids' bioactivity. In Chapter 7, the ferulic acid-based polymer was further tuned by the addition of glycol functionality into the monomer allowed tailoring of the polymer hydrophilicity. The changes in hydrophilicity allowed for physicochemical and drug release rate tunability, demonstrating a method to alter polymer properties.

This work demonstrates the ability to tune polymer properties by changing the bioactive covalently incorporated into the monomer unit, altering the monomer's molecular structure (i.e., adding glycol functionality), adding small molecules to the polymer matrix, and formulating the polymer (i.e., fabrication into microspheres and hydrogels). By molecularly designing these polymers, one has better control over the physiochemical properties and drug release rates, thus broadening the scope for use in controlled release applications.

APPENDIX

A.1.   Copyright permissions

A.1.1.   Sage copyright[1]

A.1.2. Polymer Bulletin / Springer copyright[2]

A.1.3. Biomacromolecules copyright[3]

A.2. References

1. Ouimet MA, Snyder SS, Uhrich KE, *J Bioact Compat Pol* **2012**, *27*, 540-9.

2. Rosario-Meléndez R, Ouimet MA, Uhrich KE, *Polym Bull* **2013**, *70*, 343-51.

3. Ouimet MA, Griffin J, Carbone-Howell AL, Wu WH, Stebbins ND, Di R, Uhrich KE, *Biomacromolecules* **2013**, *14*, 854–61.

CURRICULUM VITAE

M I C H E L L E   A I M E E   O U I M E T

EDUCATION:

2009-2013   Rutgers, The State University of New Jersey
Ph.D. Organic and Polymer Chemistry

2005-2009   Clemson University
B.S. Chemistry, ACS Certified, Magna Cum Laude

POSITIONS HELD:

9/2011– 7/2013   *Graduate Fellow*
Department of Chemistry and Chemical Biology
Rutgers University; Piscataway, NJ
Supervisor: Kathryn E. Uhrich, Ph.D.

5/2013 – 8/2013   *Research, Development, and Quality Intern*
Gum and Candy Ingredient Technology
Mondelēz International (formally Kraft Foods); Whippany, NJ
Supervisor: Navroz Boghani, Ph.D.

9/2010 – 8/2011   *Graduate Assistant*
Department of Chemistry and Chemical Biology
Rutgers University; Piscataway, NJ
Supervisor: Kathryn E. Uhrich, Ph.D.

9/2009 – 8/2010   *Teaching Assistant*
Department of Chemistry and Chemical Biology
Rutgers University; Piscataway, NJ
Supervisor: Kathryn E. Uhrich, Ph.D.

1/2008 – 5/2009   *Undergraduate Researcher*
Department of Animal and Veterinary Sciences
Clemson University, Clemson, SC
Supervisor: Ashby B. Bodine, Ph.D.

1/2009 – 5/2009   *Undergraduate Researcher*
Department of Chemistry
Clemson University, Clemson, SC
Supervisor: Dr. Julia L. Brumaghim

PUBLISHED WORK:

Ouimet, MA; Uhrich, KE "Ferulic acid-containing polymers with glycol functionality for tailoring physicochemical properties and release profiles" *in preparation, 2013.*

Ouimet, MA; Fogaça, R; Snyder, SS; Sathaye, S; Pochan, D; Catalani, LH; Uhrich, KE "Biodegradable Salicylic acid-based Poly(anhydride-ester) and Poly(N-vinyl-2-pyrrolidone) Blends with Hydrogel Properties for Drug Delivery Applications" *in preparation, 2013.*

Ouimet, MA; Stebbins, N; Uhrich, KE "Biodegradable Coumaric Acid-based Poly(anhydride-ester) Synthesis and Subsequent Controlled Release" *Macromolecular Rapid Communications,* **2013**, *accepted.*

Carbone-Howell, A; Ouimet, MA; Uhrich, KE "Biodegradable, bioactive-based poly(anhydride-esters) for personal care and cosmetic applications" in ACS Symposium Series book *Polymers for Personal Care and Cosmetics*, Anjali Patil, Ed., ACS, **2013**, in press.

Fogaça, R; Ouimet, MA; Catalani, LH; Uhrich, KE "Bioactive-based poly(anhydride-esters) and blends for controlled drug delivery, in ACS Symposium Series book *Tailored Polymer Architectures for Pharmaceutical and Biomedical Applications*, Carmen Scholz, Joerg Kressler, Eds., ACS, **2013**, in press.

Ouimet, MA; Griffin, J.; Carbone, A; Wu, W; Stebbins, N; Di, R; Uhrich, KE, "Biodegradable Ferulic Acid-Containing Poly(anhydride-ester): Degradation Products with Controlled Release and Sustained Antioxidant Activity" *Biomacromolecules*, **14**, 854-61 (2013).

Ouimet, MA; Rosario-Meléndez, R.; Uhrich, KE "Optimized Formulation of Salicylate-based Poly(anhydride-ester) Microspheres for Short- to Long-term Salicylic Acid Delivery" *Polym. Bull.,* **70**, 343-351 (2013).

Ouimet, MA; Snyder, S; Uhrich, KE "Tunable drug release profiles from salicylate-based poly(anhydride-ester) matrices using small molecule admixtures" *J. Bioact. Compat. Polym.,* **27** (6) 540-549 (2012).

Uhrich, KE; Ouimet, MA; Howell, A; Fogaça, R; Catalani, L; "Hydrogels" U.S. Pat. Appl. Publ. (2013), US 20130022569 A1 20130124.

Uhrich, KE; Ouimet, MA; Snyder, S; Fiorellini, J; Graves, D, Meléndez, R; Wada, K; "Polyanhydrides with therapeutic degradation products for bone repair in diabetic patients." Patent disclosure filed.